The Stability of Observed Multiple-Planet Systems

Karl W Jansson

Lund Observatory
Lund University

2012-EXA60

Degree project of 60 higher education credits (for a degree of Master)
May 2012

Lund Observatory
Box 43
SE-221 00 Lund
Sweden

The Stability of Observed Multiple-Planet Systems

Karl W Jansson

June 4, 2012

Abstract

According to theories of planet formation, jovian planets are formed on relatively circular, non-inclined, wide orbits. Despite this, many observed jovian planets are found on tight eccentric orbits. This problem could possibly be solved with multiple-planet systems. A planet in a multiple-planet system is not only affected by the host star but also by the other planets. The interactions express themselves in that the planets transfer angular momentum between each other and the eccentricities and inclination of their orbits will oscillate. I have investigated if these planet-planet interactions can perturb a 'circular' system enough to eject one planet and leave the rest of the system more tightly bound with orbits that have higher eccentricities and hence explain the observed exoplanets. I have studied the evolution of both the observed multiple-planet systems and systems I have generated myself both analytically with perturbation theory and numerically with N-body simulations. I have investigated how the stability of those systems depend on different parameters of the systems such as semi-major axes, inclinations and masses. My conclusions are that the stability of a multiple-planet system is a very sensitive function of the initial separations between the planets but also that the time between the first scattering event and disruption of the system (collision or ejection) is independent of the initial separations. I also find that multiple-planet systems are very chaotic in the sense that small changes in initial conditions lead to huge differences in the outcome.

Populärvetenskaplig sammanfattning på svenska

Solen är inte den enda stjärnan med planeter i universum. Sedan 1995, då den första extra-solära planeten upptäcktes, har 770 exoplaneter observerats och fler upptäcks hela tiden. Enligt teorier om hur planeter formas föds gasjättar med cirkulära, vida banor långt från sin stjärna precis som planeterna i solsystemet. Trots detta har många av de observerade exoplaneterna väldigt elliptiska (excentriska) banor som dessutom är aldeles för nära stjärnan. För att lösa det här problemet har det, i litteraturen, föreslagits flera teorier. En är att en andra stjärna flyger förbi planetsystemet och ändrar planeternas banor. En annan är att man har planetsystem med mer än en planet. I ett sådant flerplanetsystem påverkas planeterna inte bara av stjärnan utan av varandra också. De här planet-planetinteraktionerna skulle då kunna ändra planeternas banor så att planeterna kommer närmare varandra. Om två planeter kommer riktigt nära varandra kommer gravitationen mellan dem att ändra deras banorna ännu mer och efter att detta har upprepats ett antal gånger kommer en av dem kastas ut ur planetsystemet. Resultatet av detta skulle vara att de kvarvarande planeterna får banor som är mer excentriska och ligger närmare stjärnan.

Jag har, i det här projektet, undersökt huruvida teorin med flerplanetsystem skulle kunna fungera. Jag har undersökt hur ett flerplanetsystem utvecklas med tiden både med analytiska approximationer och numeriska simuleringar. Mina resultat visar att tiden det tar för två planeter att komma inom ett visst avstånd från varandra är väldigt beroende på det ursprungliga avståndet mellan dem. Mer överaskande är att tiden mellan första gången planeterna kommer riktigt nära varandra och det att en planet blir utkastad är konstant, oberoende av den ursprungliga separationen mellan planeterna. Slutsatsen man kan dra av detta är att efter det att två planeter i ett planetsystem har stött på varandra en gång ser utvecklingen väsentligen likadan ut för alla planetsystem.

Acknowledgements

I first of all want to thank my supervisor Melvyn B. Davies for providing me with such an interesting project and for all inspiration and help he has given me. When I started with the thesis I had the idea that it would be a project slightly larger than my Bachelor's project. Oh so wrong I was. At times my motivation dropped and I thought I got nowhere just in time to have a meeting with Melvyn, who removed some of my question marks, got me super inspired and I was able to dive right back into work again. I think I now have started to realize what science really is: find a mediocre solution to your question only to discover two new questions you could investigate. Melvyn, you and Ross are also the reason I went from studying theoretical physics to astronomy. Thank you so much!

I also want to thank everyone at the Astronomy Department. To me, we are one giant family. I love that if you have a question for someone you can just go to that person's office and knock on the door. I especially want to thank the other Master's students and the PhD students for making it so easy to crawl out of bed every morning, put on my clothes and sleep walk up Sölvegatan to Astro. Hiva, you have been a great office mate and I am sorry for all the times I have interrupted you in your work to discuss mine.

Thanks also goes to my friends at Theoretical Physics without which I would never have come this far. I just say: Go Teoretisk Elit!

Finally I also want to thank my family and then especially my grandmother for all the support they have given me during all my studies.

Contents

1 Introduction to exoplanets

1.1 What is an exoplanet?

A planet is, by definition by the International Astronomical Union, a celestial body that is orbiting a star or a stellar remnant (white dwarf, neutron star or black hole). It has to be massive enough that its self-gravity has made it round. It is not massive enough to start nuclear fusion and it must have cleared its neighborhood from other planetesimals. An exoplanet is a planet which orbits a star that is not the Sun. The first exoplanet orbiting a main-sequence star was detected in 1995 (Mayor & Queloz 1995) on a four day orbit around the Sun-like star 51 Pegasi. To date over 750 exoplanets have been detected and confirmed in the exoplanet database (`exoplanet.eu`, Schneider et al. (2011)).

According to theories of planet formation, jovian planets (gas giants) are formed on relatively circular, non-inclined, wide orbits. Despite this, many observed exoplanets are found on tight eccentric orbits.

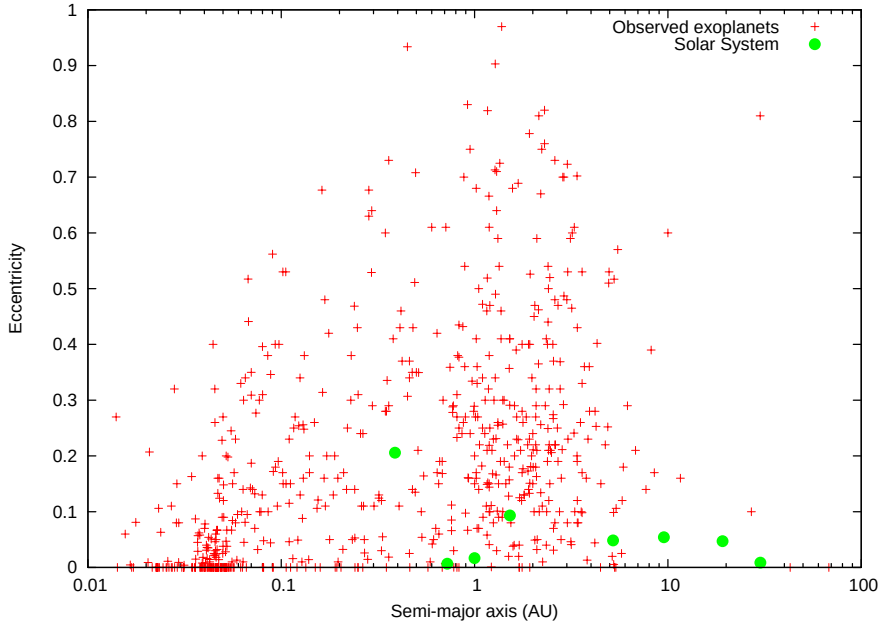

Figure 1.1: Plot of the eccentricity and semi-major axis of all exoplanets (red crosses) in the exoplanet database (`exoplanet.eu`, Schneider et al. (2011)). The green dots are the planets in the Solar System.

In Figure 1.1 we can see that many of the exoplanets have a semi-major axis that is smaller than Jupiter's ($a_{Jup} \sim 5.2$ AU. Many also have eccentricities that is larger than the eccentricity of Jupiter. I compare to Jupiter rather than the other planets in the Solar System since the observed exoplanets have masses that are comparable to Jupiter's mass. It is obviously a problem that the observed exoplanets have tight eccentric orbits both compared to the Solar System and theories of planet formation. My project has been about solving this problem with the help of multiple-planet systems.

1.2 Multiple-planet systems

Some planetary systems contains more than one planet (e.g. the Solar System). In total, over 100 such multiple-planet systems has been observed (`exoplanet.eu`, Schneider et al.

(2011)). I list some of them in Figure 7.1. What is the interesting thing about multiple-planet systems? A planet in a multiple-planet system is not only affected by the host star but also by the other planets. These planet-planet interactions leads to transfer of angular momentum between the planets and can be seen as secular oscillations in the eccentricities and inclinations of the orbits of the planets (see Section 3). Can these oscillations perturb a 'circular' system enough that it becomes unstable and in the end eject a planet leaving the rest of the system more tightly bound with orbits that have higher eccentricities? That could then potentially explain why many of the observed exoplanets are on tight, eccentric orbits.

In Section 3 and Appendix B I analytically derive approximations of the equations for the eccentricity and inclination oscillations for a two-planet system. I also investigate how the oscillations depend on different parameters of the planetary system. I investigate, for example, how the evolution depends on the mass of the planets if you assume you have a system with fixed mass.

Is this the only way to make a system more eccentric or even unstable? In Section 6 I discuss other mechanisms that can destabilize a multiple-planet system. For example, if the host star lies in a stellar cluster, the chance of an encounter with another star is relatively large (a fly-by). Could such an event perturb the system enough? How close does the fly-by have to get to make the system unstable?

I have investigated the stability of both observed multiple-planet systems and systems I have generated myself. To do the investigations I have used the N-body integrator `MERCURY6` (see Section 4.1, Chambers 1999) to simulate the planetary systems. I have taken data for the observed extrasolar planetary systems from 'The Extrasolar Planets Encyclopaedia' (`exoplanet.eu`) where I have chosen planetary systems with more than one planet. I investigate the stability of the observed systems in Section 7.

I am interested in getting a map of the stability of multiple-planet systems as a function of the initial conditions so I have made simulations of systems that are similar to each other. With similar I mean systems with slightly different initial conditions. I numerically investigate the stability as a function of separation between planets and the mass of the planets in Sections 5, 8 and 9.

To summarize: I have looked at both the observed multiple-planet systems and systems that I have generated myself both numerically and analytically. Finally I also want to say that all figures that are included in this thesis I have made myself. For some of them I have got inspiration from others and where that is the case I mention from where that inspiration comes.

2 Planetary systems

2.1 Derivation of the two-body problem

In this section I go through the derivation of the two-body problem for a one-planet system. This is just a short summary and the full derivation can be found in Appendix A. The assumption I do is that the mass of the star, m_c, is much larger than the mass of the planet, m_1. The acceleration of the planet as seen from the star, $\ddot{\boldsymbol{r}}$, can be written as

$$\ddot{\boldsymbol{r}} = -\frac{G(m_c + m_1)}{r^3}\boldsymbol{r} \tag{2.1}$$

To solve this you need to find constants of motion. The first is the angular momentum:

$$\boldsymbol{h} = \boldsymbol{r} \times \dot{\boldsymbol{r}} \tag{2.2}$$

The fact that the angular momentum is constant implies that the motion of the planet lies in one plane. Next you change into polar coordinates (r, θ) in that orbital plane. Now we can get Kepler's second law: The radius vector of a planet covers equal areas in equal times (Eq. (A.9)). In polar coordinates the equation of motion (Eq. (2.1)) becomes

$$\ddot{r} - r\dot{\theta}^2 = -\frac{G(m_c + m_1)}{r^2} \tag{2.3}$$

To make this equation solvable we make another coordinate change, $r = \frac{1}{u}$, and end up with

$$r = \frac{a(1 - e^2)}{1 + e\cos(\theta - \varpi)} \tag{2.4}$$

This is the equation of a conic section (i.e. a circle, an ellipse, a parabola or a hyperbola) with semi-major axis a, eccentricity e, longitude of periapsis ϖ, true anomaly $f = \theta - \varpi$ (see Figure 2.1). We can also get Kepler's third law.

$$T^2 = \frac{4\pi^2}{G(m_c + m_1)}a^3 \tag{2.5}$$

and find that the orbital energy is constant:

$$E = -\frac{G(m_c + m_1)m_1}{2a} \tag{2.6}$$

It is possible to get the position of the planet as a function of time as well. That is however more complicated and is derived in Appendix A.2.

If we want to describe the orbit in three dimensions we need to add two more parameters. The inclination I and the longitude of ascending node Ω (see Figure 2.2). For more information on the orbital parameters see the next section.

2.2 Orbital parameters

A bound, elliptic orbit can be described with six orbital parameters:

- Semi-major axis, a. The semi-major axis determines the size of the orbit, it is one half of the major axis which is the longest diameter of the ellipse/orbit (Figure 2.1).

From the semi-major axis you can get the binding energy of the orbit and vice versa regardless of the other orbital parameters.

- Eccentricity, e. The eccentricity determines how elongated, non-circular the orbit is (Figure 2.1). $e = 0$ for a circular orbit and $0 < e < 1$ for an elliptic orbit. If $e \geq 1$ the orbit is unbound to the star. To get the eccentricity you also need the angular momentum, h, of the orbit as well as the binding energy, E,

$$e = \sqrt{1 - \frac{2Eh^2}{G^2 \left(m_c + m_1\right)^2}} \tag{2.7}$$

- Inclination, I. The inclination is the angle between the normal to the orbit and the normal to the reference plane (Figure 2.2).

- Longitude of ascending node, Ω. The longitude of ascending node is the angle between a reference direction in the reference plane and the ascending node (Figure 2.2). The ascending node is the point where the orbit of the planet crosses the reference plane from south to north.

- Longitude of periapsis, ϖ. The longitude of periapsis is a sum of two angles, $\varpi = \Omega + \omega$ (Figure 2.2). Ω is the longitude of ascending node and ω is the argument of periapsis. The argument of periapsis is defined as the angle between the ascending node and the periapsis of the orbit (the point where the planet is closest to the star).

- True anomaly, f. The true anomaly defines the position of the planet in its orbit. It is the angle between the periapsis and the current position of the planet (Figure 2.1). Sometimes you rather use the mean longitude, λ, as the sixth orbital parameter. The mean longitude is for a Keplerian ellipse an abstract concept and has no geometrical interpretation but also defines the position of the planet in its orbit. It can however be calculated $\lambda = M + \varpi$ where ϖ is the longitude of periapsis and M is the mean anomaly. The mean anomaly is the product between the time, t, since last periapsis passage and the mean motion, n, of the planet. The mean motion is 2π divided by the period of the orbit and can be calculated from the semi-major axis via Kepler's third law, Eq. (2.5):

$$M = nt = \sqrt{\frac{G(m_c + m)}{a^3}}t \tag{2.8}$$

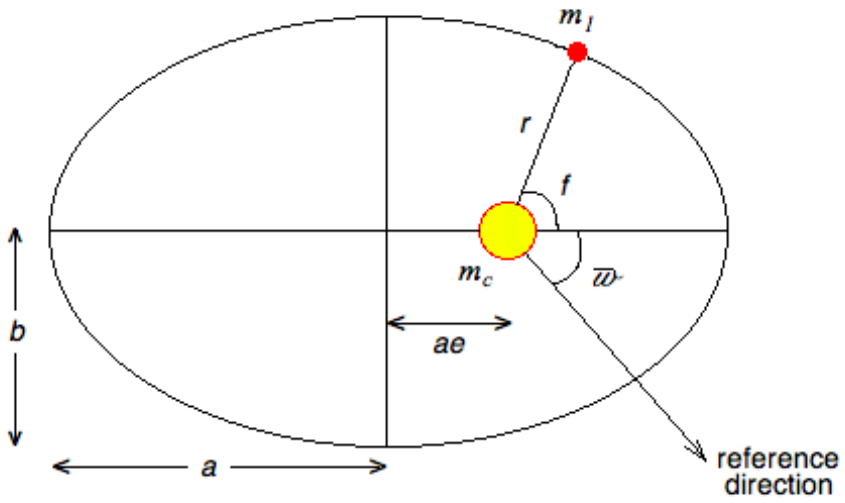

Figure 2.1: An ellipse with semi-major axis a, eccentricity e and longitude of periapsis ϖ together with a planet (m_1) with true anomaly f.

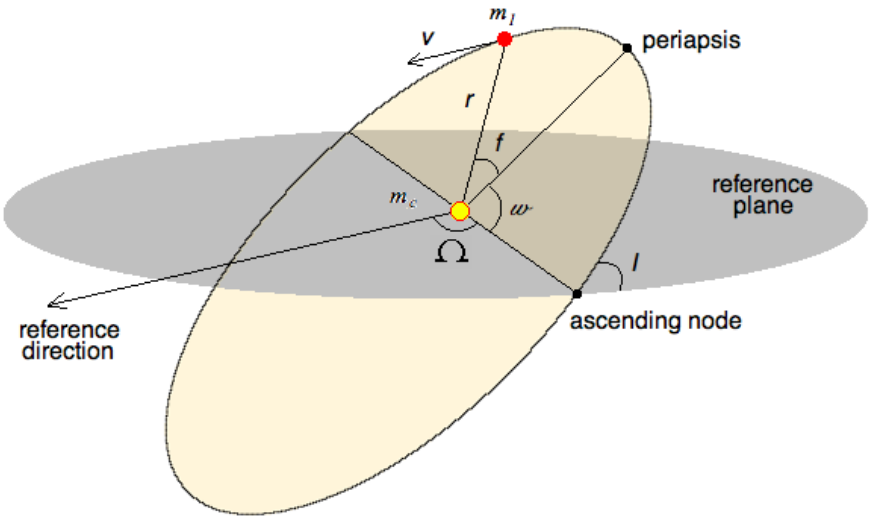

Figure 2.2: Orbit of a planet in three dimensions with respect to an arbitrary reference plane and reference direction in that plane showing the definitions of the inclination I, the longitude of ascending node Ω and the argument of periapsis ω.

2.3 Properties of multiple-planet systems

If a planetary system has more than one planet we can introduce some important quantities.

2.3.1 Mutual inclination, ΔI

The mutual inclination, ΔI, of the orbits of two planets is important when it comes to the interactions between the planets (see Section 3). The mutual inclination is defined

as the angle between the normals (angular momentum vectors) of the two orbits.

$$\cos \Delta I = \hat{\mathbf{h}}_i \cdot \hat{\mathbf{h}}_j = \cos I_i \cos I_j + \cos(\Omega_i - \Omega_j) \sin I_i \sin I_j \tag{2.9}$$

where subscript i is for the inner planet and subscript j is for the outer planet.

2.3.2 Mutual Hill radius, r_{mH}

For stability analysis I express the separations of two planets (difference in semi-major axes, $a_j - a_i$) in mutual Hill radii:

$$r_{mH} = \left(\frac{m_i + m_j}{3m_c} \right)^{1/3} \frac{a_i + a_j}{2} \tag{2.10}$$

where m_c is the mass of the star, subscript i is for the inner planet and subscript j is for the outer planet (e.g. Gladman (1993), Chambers et al. (1996)). From the equation it can be seen that the mutual Hill radius scales as $\left(\frac{m_i+m_j}{3m_c} \right)^{1/3}$ so it can be thought of as some sort of tidal radius.

2.3.3 Mean motion resonance

If the mean motions (periods) of two planets are a simple integer ratio of each other the planets are in mean motion resonance (MMR)

$$\frac{n_i}{n_j} = \frac{T_j}{T_i} = \frac{p}{q} \tag{2.11}$$

where p and q are small integers. MMRs can both stabilize and destabilize a system with multiple bodies. One example where it stabilizes is the Galilean satellites of Jupiter which are in a 4:2:1 MMR. However it is more common that it destabilizes a system because it can make planets or other bodies closer to each other more often. One example of this is the Kirkwood gaps in the asteroid belt which are parts with almost no asteroids. The reason is that at those distances from the Sun the asteroids would be in MMR with Jupiter.

3 Analytic approach for two-planet systems

If you have a planetary system with two planets they will interact not only with the star but with each other as well. If the two planets are on non-coplanar orbits the planet-planet interactions will lead to transfer of angular momentum between the orbits but keeping the total angular momentum constant. This leads to so called secular oscillations in eccentricity and inclination of the orbits of the planets. They are called secular because the timescales for the oscillations are much larger than the orbital timescale. These oscillations take place even if the planets initially are so far away from each other that they don't exchange any energy so the semi-major axes remains constant. If the interaction is strong enough you might, as the eccentricities changes, get crossing orbits. If you have crossing orbits the chance of having strong gravitational encounters increases and such events can lead to collisions and ejections in the system. Equations for these oscillations can be analytically approximated and the full derivation for these approximation can be found in Appendix B.

3.1 Derivation of the secular oscillation equations

Here I summarize the derivation I have made in Appendix B. The first thing you need to do is to assume that the mass of the star is much larger than the mass of the planets $m_1, m_2 \ll m_c$ and you also have to assume that there is no MMR so that the positions of the planets in their orbits is irrelevant. Compared to the two-body problem the second planet adds a perturbation. This can be expressed as a disturbing function in equation of motion:

$$\ddot{\boldsymbol{r}}_1 = \nabla \left(\frac{G(m_c + m_1)}{r_1} + \mathcal{R}_1 \right) \tag{3.1}$$

where the disturbing function $\mathcal{R}_1$ is

$$\mathcal{R}_1 = \frac{Gm_2}{|\boldsymbol{r}_2 - \boldsymbol{r}_1|} - Gm_2 \frac{\boldsymbol{r}_1 \cdot \boldsymbol{r}_2}{r_2^3} \tag{3.2}$$

To get the equation of motion for the second planet you just exchange subscripts (1 to 2 and vice versa). Next you express it in orbital parameters (Murray & Dermott 1999): a, e, I, Ω, ϖ, λ and keep terms to first in order mass, second order in e and I and zeroth order λ (positions are irrelevant, you can think of it as 'rings' of mass). The disturbing function then becomes:

$$\begin{aligned} \mathcal{R}_j = n_j a_j^2 \Bigg[& \frac{1}{2} A_{jj} e_j^2 + A_{jk} e_1 e_2 \cos(\varpi_1 - \varpi_2) \\ & + \frac{1}{2} B_{jj} I_j^2 + B_{jk} I_1 I_2 \cos(\Omega_1 - \Omega_2) \Bigg] \end{aligned} \tag{3.3}$$

where $j = 1, 2$, $k = 2, 1$, $j \neq k$ and

$$A_{jj} = +n_j \frac{1}{4} \frac{m_k}{m_c + m_j} \alpha \bar{\alpha} b_{3/2}^{(1)}(\alpha), \qquad A_{jk} = -n_j \frac{1}{4} \frac{m_k}{m_c + m_j} \alpha \bar{\alpha} b_{3/2}^{(2)}(\alpha) \tag{3.4}$$

$$B_{jj} = -n_j \frac{1}{4} \frac{m_k}{m_c + m_j} \alpha \bar{\alpha} b_{3/2}^{(1)}(\alpha), \qquad B_{jk} = +n_j \frac{1}{4} \frac{m_k}{m_c + m_j} \alpha \bar{\alpha} b_{3/2}^{(1)}(\alpha) \tag{3.5}$$

with $\alpha = \frac{a_1}{a_2}$, $\bar{\alpha} = \alpha$ if $j = 1$ otherwise $\bar{\alpha} = 1$ and $b_x^{(y)}$ are Laplace coefficients (see Eq. (B.6)). You can see that the As and Bs are functions of masses and semi-major axes only. Next you need Lagrange's planetary equations, Eqs. (B.19)–(B.23). We assume that they are independent of positions in the orbits, that there is no energy transfer and keep terms with lowest order in eccentricity and inclination and end up with

$$\dot{e}_j \approx -\frac{1}{n_j a_j^2 e_j}\frac{\partial \mathcal{R}_j}{\partial \varpi_j}, \qquad \dot{\varpi}_j \approx \frac{1}{n_j a_j^2 e_j}\frac{\partial \mathcal{R}_j}{\partial e_j} \tag{3.6}$$

$$\dot{I}_j \approx -\frac{1}{n_j a_j^2 I_j}\frac{\partial \mathcal{R}_j}{\partial \Omega_j}, \qquad \dot{\Omega}_j \approx \frac{1}{n_j a_j^2 I_j}\frac{\partial \mathcal{R}_j}{\partial I_j} \tag{3.7}$$

Next step to solve these equations is to make a variable change to eccentricity and inclination 'vectors'

$$h_j = e_j \sin \varpi_j, \quad k_j = e_j \cos \varpi_j \tag{3.8}$$

$$p_j = I_j \sin \Omega_j, \quad q_j = I_j \cos \Omega_j \tag{3.9}$$

With these variables the disturbing function becomes

$$\begin{aligned}\mathcal{R}_j = n_j a_j^2 \Bigg[&\frac{1}{2}A_{jj}\left(h_j^2 + k_j^2\right) + A_{jk}\left(h_j h_k + k_j k_k\right) \\ &+\frac{1}{2}B_{jj}\left(p_j^2 + q_j^2\right) + B_{jk}\left(p_j p_k + q_j q_k\right)\Bigg]\end{aligned} \tag{3.10}$$

If we differentiate the eccentricity and inclination vectors with respect to time and insert Lagrange's planetary equations, Eqs. (3.6)–(3.7), we end up with

$$\frac{\mathrm{d}h_j}{\mathrm{d}t} = \frac{1}{n_j a_j^2}\frac{\partial \mathcal{R}}{\partial k_j}, \qquad \frac{\mathrm{d}k_j}{\mathrm{d}t} = -\frac{1}{n_j a_j^2}\frac{\partial \mathcal{R}}{\partial h_j} \tag{3.11}$$

$$\frac{\mathrm{d}p_j}{\mathrm{d}t} = \frac{1}{n_j a_j^2}\frac{\partial \mathcal{R}}{\partial q_j}, \qquad \frac{\mathrm{d}q_j}{\mathrm{d}t} = -\frac{1}{n_j a_j^2}\frac{\partial \mathcal{R}}{\partial p_j} \tag{3.12}$$

$$\tag{3.13}$$

Next we differentiate the disturbing function Eq. (3.10) with respect to h_j, k_j, p_j and q_j and insert in above equations to get

$$\dot{h}_j = A_{jj}k_j + A_{jk}k_k, \quad \dot{k}_j = A_{jj}h_j + A_{jk}h_k \tag{3.14}$$

$$\dot{p}_j = B_{jj}q_j + B_{jk}q_k, \quad \dot{q}_j = B_{jj}p_j + B_{jk}p_k \tag{3.15}$$

This can be written in matrix form

$$\dot{\boldsymbol{h}} = \boldsymbol{A}\boldsymbol{k}, \quad \dot{\boldsymbol{k}} = -\boldsymbol{A}\boldsymbol{h} \tag{3.16}$$

$$\dot{\boldsymbol{p}} = \boldsymbol{B}\boldsymbol{q}, \quad \dot{\boldsymbol{q}} = -\boldsymbol{B}\boldsymbol{p} \tag{3.17}$$

Differentiate with respect to time one more time to get

$$\ddot{\boldsymbol{h}} + \boldsymbol{A}^2\boldsymbol{h} = 0, \quad \ddot{\boldsymbol{k}} + \boldsymbol{A}^2\boldsymbol{k} = 0 \tag{3.18}$$

$$\ddot{\boldsymbol{p}} + \boldsymbol{B}^2\boldsymbol{p} = 0, \quad \ddot{\boldsymbol{q}} + \boldsymbol{B}^2\boldsymbol{q} = 0 \tag{3.19}$$

This is an eigenvalue problem with simple harmonic oscillator solutions

$$h_j = \sum_{i=1}^{2} e_{ij} \sin\left(g_i t + \beta_i\right), \quad k_j = \sum_{i=1}^{2} e_{ij} \cos\left(g_i t + \beta_i\right) \tag{3.20}$$

$$p_j = \sum_{i=1}^{2} I_{ij} \sin\left(f_i t + \gamma_i\right), \quad q_j = \sum_{i=1}^{2} I_{ij} \cos\left(f_i t + \gamma_i\right) \tag{3.21}$$

where j denotes which planet it is and i the oscillation mode. The frequencies g_i and f_i are the eigenvalues to $\boldsymbol{A}$ and $\boldsymbol{B}$ respectively. The initial conditions of the two-planet systems determine the amplitudes (e_{ji} and I_{ji} components of eigenvectors) and phases (β_i and γ_i). An example for the Solar system is shown in Section 3.2. This result holds when

i) There is no mean motion resonance.

ii) $\boldsymbol{r}_1 < \boldsymbol{r}_2$, i.e. the orbit of the inner planet stays inside the orbit of the outer planet at all times.

iii) The eccentricities and inclinations are small enough so that a second order approximation is enough.

3.2 Secular oscillations in the Solar System

Jupiter (m_1) and Saturn (m_2) have orbits that are mutually inclined so they will undergo secular oscillations in eccentricity and inclination. The two planets are also relatively massive and close to each other so the amplitudes of the oscillations will be significant. In 1983 the Jupiter and Saturn had the following parameters (Sun, m_c) (Murray & Dermott 1999):

$$\begin{aligned}
m_1/m_c &= 9.54786 \times 10^{-4} & m_2/m_c &= 2.85837 \times 10^{-4} \\
a_1 &= 5.202545 \text{ AU} & a_2 &= 9.554841 \text{ AU} \\
n_1 &= 30.3374^\circ \text{yr}^{-1} & n_2 &= 12.1890^\circ \text{yr}^{-1} \\
e_1 &= 0.0474622 & e_2 &= 0.0575481 \\
\varpi_1 &= 13.983865^\circ & \varpi_2 &= 88.719425^\circ \\
I_1 &= 1.30667^\circ & I_2 &= 2.48795^\circ \\
\Omega_1 &= 100.0381 & \Omega_2 &= 113.1334^\circ
\end{aligned} \tag{3.22}$$

From this we get $\alpha = a_1/a_2 \sim 0.544493$ and from Eq. (B.6) the values of the Laplace coefficients as

$$b^{(1)}_{3/2}(\alpha) \sim 3.17296, \qquad b^{(2)}_{3/2}(\alpha) \sim 2.07110 \tag{3.23}$$

The $\boldsymbol{A}$- and $\boldsymbol{B}$-matrices, Eqs. (3.4)–(3.5), become

$$\boldsymbol{A} = \begin{pmatrix} 0.00203738 & -0.00132987 \\ -0.00328007 & 0.00502513 \end{pmatrix} {}^{\circ}\mathrm{yr}^{-1} \tag{3.24}$$

$$\boldsymbol{B} = \begin{pmatrix} -0.00203738 & 0.00203738 \\ 0.00502513 & -0.00502513 \end{pmatrix} {}^{\circ}\mathrm{yr}^{-1} \tag{3.25}$$

Next we get the frequencies of oscillations, g_i and f_i $(i = 1, 2)$, by solving the characteristic equations for the matrices. This gives

$$g_1 = 9.63435 \times 10^{-4\circ}\mathrm{yr}^{-1}, \qquad g_2 = 6.09908 \times 10^{-3\circ}\mathrm{yr}^{-1} \tag{3.26}$$

$$f_1 = 0, \qquad f_2 = -7.06251 \times 10^{-3\circ}\mathrm{yr}^{-1} \tag{3.27}$$

Now we can get the eigenvectors, $\boldsymbol{x}_1, \boldsymbol{x}_2, \boldsymbol{y}_1, \boldsymbol{y}_2$, of $\boldsymbol{A}$ and $\boldsymbol{B}$.

$$\boldsymbol{A}\boldsymbol{x}_i = g_i \boldsymbol{x}_i, \qquad \boldsymbol{B}\boldsymbol{y}_i = f_i \boldsymbol{y}_i \tag{3.28}$$

which are determined within a scaling constant. As mentioned before $\boldsymbol{x}_i$ and $\boldsymbol{y}_i$ has, when correctly scaled, components e_{ji} and I_{ji}. Say $\bar{e}_{ji}$ and $\bar{I}_{ji}$ are unscaled components and let S_i and T_i be scaling constants (the magnitudes are determined by the initial conditions) for the vectors.

$$S_i \bar{e}_{ji} = e_{ji}, \qquad T_i \bar{I}_{ji} = I_{ji}. \tag{3.29}$$

solving the eigenvector equations Eqs. (3.28) yields unscaled eigenvectors

$$\begin{pmatrix} \bar{e}_{11} \\ \bar{e}_{21} \end{pmatrix} = \begin{pmatrix} -0.777991 \\ -0.628275 \end{pmatrix}, \qquad \begin{pmatrix} \bar{e}_{12} \\ \bar{e}_{22} \end{pmatrix} = \begin{pmatrix} 0.332842 \\ -1.01657 \end{pmatrix},$$

$$\begin{pmatrix} \bar{I}_{11} \\ \bar{I}_{21} \end{pmatrix} = \begin{pmatrix} 0.707107 \\ 0.707107 \end{pmatrix}, \qquad \begin{pmatrix} \bar{I}_{12} \\ \bar{I}_{22} \end{pmatrix} = \begin{pmatrix} -0.40797 \\ 1.00624 \end{pmatrix}. \tag{3.30}$$

from Eqs. (3.8)–(3.9) we get the initial values ($t = 0$) on the eccentricity and inclination vectors (inclinations in radians)

$$\begin{aligned} h_1 &= 0.0114692, & h_2 &= 0.0575337, \\ k_1 &= 0.0460556, & k_2 &= 0.00128611 \\ p_1 &= 0.0224566, & p_2 &= 0.0399314, \\ q_1 &= -0.00397510, & q_2 &= -0.0170597 \end{aligned} \tag{3.31}$$

next we use Eqs. (3.20)–(3.21), Eqs. (3.29) and put $t = 0$ to get

$$h_j = S_1\bar{e}_{j1}\sin\beta_1 + S_2\bar{e}_{j2}\sin\beta_2, \qquad k_j = S_1\bar{e}_{j1}\cos\beta_1 + S_2\bar{e}_{j2}\cos\beta_2, \tag{3.32}$$
$$p_j = T_1\bar{I}_{j1}\sin\gamma_1 + T_2\bar{I}_{j2}\sin\gamma_2, \qquad q_j = T_1\bar{I}_{j1}\cos\gamma_1 + T_2\bar{I}_{j2}\cos\gamma_2. \tag{3.33}$$

Then we combine the above four sets of equations to solve for the eight unknowns ($S_1\sin\beta_1$, $S_1\cos\beta_2$, $S_2\sin\beta_2$, ...). For example at $t = 0$:

$$\begin{aligned}
&\left\{\begin{array}{l} h_1 = S_1\bar{e}_{11}\sin\beta_1 + S_2\bar{e}_{12}\sin\beta_2 \\ h_2 = S_1\bar{e}_{21}\sin\beta_1 + S_2\bar{e}_{22}\sin\beta_2 \end{array}\right. \\
\Longrightarrow &\bar{e}_{22}h_1 - \bar{e}_{12}h_1 = \left(\bar{e}_{11}\bar{e}_{22} - \bar{e}_{21}\bar{e}_{12}\right) S_1\sin\beta_1 \\
\Longrightarrow &S_1\sin\beta_1 = \frac{\bar{e}_{22}h_1 - \bar{e}_{12}h_1}{\bar{e}_{11}\bar{e}_{22} - \bar{e}_{21}\bar{e}_{12}} \approx -0.0308089
\end{aligned} \tag{3.34}$$

solving for all unknowns gives the following values

$$\begin{aligned}
&\begin{pmatrix} S_1\sin\beta_1 \\ S_2\sin\beta_2 \end{pmatrix} = \begin{pmatrix} -0.0308089 \\ -0.375549 \end{pmatrix}, \qquad \begin{pmatrix} S_1\cos\beta_1 \\ S_2\cos\beta_2 \end{pmatrix} = \begin{pmatrix} -0.0472469 \\ 0.027935 \end{pmatrix}, \\
&\begin{pmatrix} T_1\sin\gamma_1 \\ T_2\sin\gamma_2 \end{pmatrix} = \begin{pmatrix} 0.0388876 \\ 0.0123566 \end{pmatrix}, \qquad \begin{pmatrix} T_1\cos\gamma_1 \\ T_2\cos\gamma_2 \end{pmatrix} = \begin{pmatrix} -0.0109598 \\ -0.00925221 \end{pmatrix}.
\end{aligned} \tag{3.35}$$

solve the above equations for scaling constants and phases

$$\beta_1 = -146.892^\circ, \qquad \beta_2 = -53.3565^\circ, \qquad \gamma_1 = 105.74^\circ, \qquad \gamma_2 = 126.825^\circ, \tag{3.36}$$
$$S_1 = 0.0564044, \qquad S_2 = 0.0468053, \qquad T_1 = 0.0404025, \qquad T_2 = 0.0154366. \tag{3.37}$$

now we get the scaled eigenvectors, Eqs. (3.29),

$$\begin{aligned}
&\begin{pmatrix} e_{11} \\ e_{21} \end{pmatrix} = \begin{pmatrix} -0.0.0438821 \\ -0.0354375 \end{pmatrix}, \qquad \begin{pmatrix} e_{12} \\ e_{22} \end{pmatrix} = \begin{pmatrix} 0.0155788 \\ -0.047581 \end{pmatrix}, \\
&\begin{pmatrix} I_{11} \\ I_{21} \end{pmatrix} = \begin{pmatrix} 0.0285689 \\ 0.0285689 \end{pmatrix}, \qquad \begin{pmatrix} I_{12} \\ I_{22} \end{pmatrix} = \begin{pmatrix} -0.00629766 \\ 0.015533 \end{pmatrix}.
\end{aligned} \tag{3.38}$$

and finally we have everything in Eqs. (3.20)–(3.21). From the definition of h_j, k_j, p_j and q_j (Eqs. (3.8)–(3.9)) we get the eccentricity as a function of time, $e_j(t) = \sqrt{h_j^2 + k_j^2}$, writing $\sin(g_i t + \beta_i) \equiv s_i$ and $\cos(g_i t + \beta_i) \equiv c_i$ $(i = 1, 2)$,

$$\begin{aligned}
e_j(t) &= \sqrt{e_{j1}^2 s_1^2 + 2e_{j1}e_{j2}s_1 s_2 + e_{j2}^2 s_2^2 + e_{j1}^2 c_1^2 + 2e_{j1}e_{j2}c_1 c_2 + e_{j2}^2 c_2^2} \\
&= \sqrt{e_{j1}^2 + e_{j2}^2 + 2e_{j1}e_{j2}\left(s_1 s_2 + c_1 c_2\right)} \\
&= \sqrt{e_{j1}^2 + e_{j2}^2 + 2e_{j1}e_{j2}\cos\left(\left(\beta_1 - \beta_2\right) + \left(g_1 - g_2\right)t\right)}
\end{aligned} \tag{3.39}$$

we can do the same thing for inclination evolution, $I_j(t) = \sqrt{p_j^2 + q_j^2}$, but here we write
$\sin(f_i t + \gamma_i) \equiv s_i$ and $\cos(f_i t + \gamma_i) \equiv c_i$ $(i = 1, 2)$, to get

$$\begin{aligned} I_j(t) &= \sqrt{I_{j1}^2 s_1^2 + 2I_{j1}I_{j2}s_1 s_2 + I_{j2}^2 s_2^2 + I_{j1}^2 c_1^2 + 2I_{j1}I_{j2}c_1 c_2 + I_{j2}^2 c_2^2} \\ &= \sqrt{I_{j1}^2 + I_{j2}^2 + 2I_{j1}I_{j2}\left(s_1 s_2 + c_1 c_2\right)} \\ &= \sqrt{I_{j1}^2 + I_{j2}^2 + 2I_{j1}I_{j2}\cos\left((\gamma_1 - \gamma_2) + (f_1 - f_2)\,t\right)} \end{aligned} \tag{3.40}$$

finally insert the values of constants to get

$$\begin{aligned} e_1(t) &= \sqrt{0.00217 - 0.00137\cos\left(93.5^\circ - 0.00514t\right)} \\ e_2(t) &= \sqrt{0.00352 - 0.00337\cos\left(93.5^\circ + 0.00514t\right)} \end{aligned} \tag{3.41}$$

for eccentricity evolution and

$$\begin{aligned} I_1(t) &= \sqrt{0.000856 - 0.000360\cos\left(21.1^\circ - 0.00706t\right)} \\ I_2(t) &= \sqrt{0.00106 - 0.000888\cos\left(21.1^\circ + 0.00706t\right)} \end{aligned} \tag{3.42}$$

for the inclination evolution (in radians). The frequencies are in degrees per year. The period of the eccentricity oscillations is $P_e \sim 70100$ years and the period of the inclination oscillations is $P_I \sim 51000$ years. We can see that Saturn's amplitudes are larger, this is because it is less massive. It is also possible to get $\varpi_j(t)$ and $\Omega_j(t)$ with

$$\begin{aligned} \tan\varpi_j(t) &= \frac{h_j}{k_j} \\ \tan\Omega_j(t) &= \frac{p_j}{q_j}. \end{aligned} \tag{3.43}$$

In reality Uranus and Neptune affect as well but not so much. Jupiter and Saturn is also relatively near a 5:2 MMR which could add perturbations on shorter timescales.

3.3 Comparison with N-body simulations

I test the equations derived in the previous section by comparing them to the results from N-body simulations using `MERCURY6` (see Section 4.1 for a description of how to use it). I calculate $e(t)$ and $I(t)$ in the same way as the previous section.

3.3.1 The true Jupiter-Saturn system

I first look at a system with the Sun, Jupiter and Saturn only (a true two-planet system). At epoch J2000 (JD 2451545.0 or 1st January 2000 12:00) Jupiter (m_1) and Saturn (m_2) had the following orbital parameters:

$$\begin{aligned} a_1 &= 5.20336301 \text{ AU} & a_2 &= 9.53707032 \text{ AU} \\ e_1 &= 0.04839266 & e_2 &= 0.05415060 \\ \varpi_1 &= 14.75385^\circ & \varpi_2 &= 92.43194^\circ \\ I_1 &= 1.30530^\circ & I_2 &= 2.48446^\circ \\ \Omega_1 &= 100.55615 & \Omega_2 &= 113.71504^\circ \end{aligned} \tag{3.44}$$

I calculate the equations for the secular oscillations and compare them with the results from a N-body simulation. For the eccentricity evolution I get

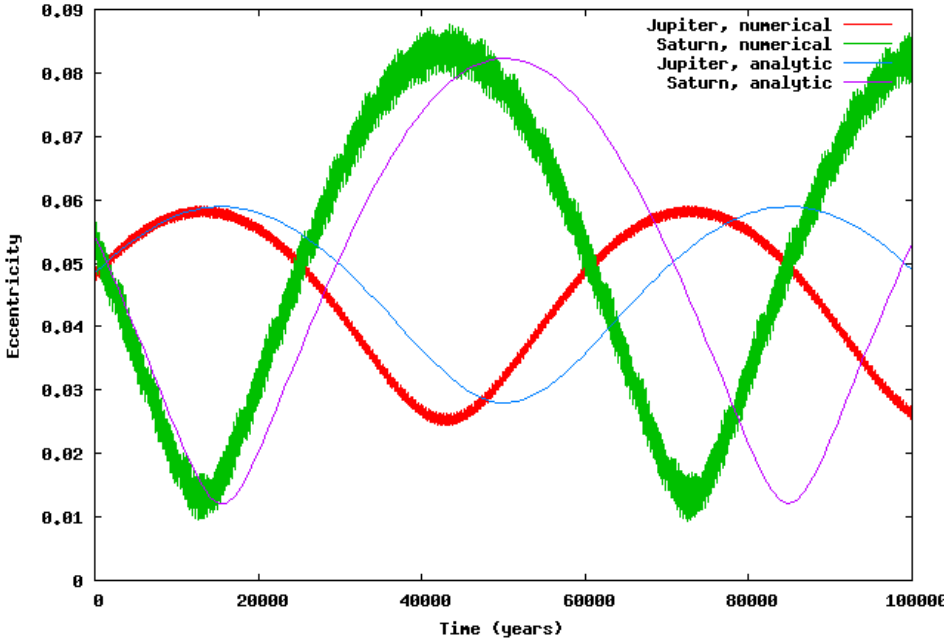

Figure 3.1: Eccentricity oscillations for a planetary system containing the Sun, Jupiter and Saturn. Shows the results from a N-body simulation with Jupiter (red curve) and Saturn (green curve) and the analytically derived equations for Jupiter (blue curve) and Saturn (purple curve).

and for the inclination evolution I get

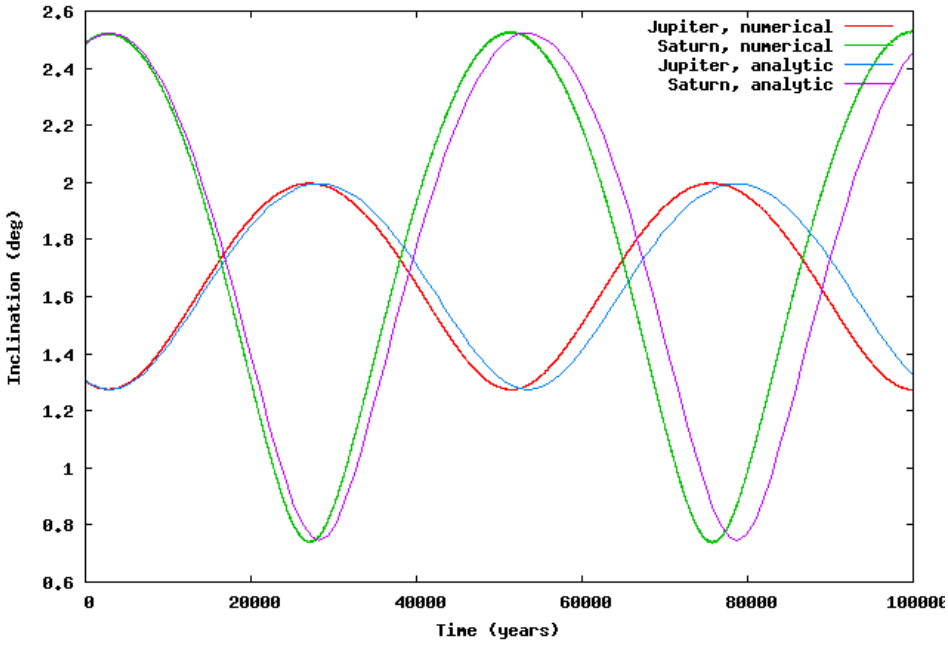

Figure 3.2: Inclination oscillations for a planetary system containing the Sun, Jupiter and Saturn. Shows the results from a N-body simulation with Jupiter (red curve) and Saturn (green curve) and the analytically derived equations for Jupiter (blue curve) and Saturn (purple curve).

You see that you do get oscillations in eccentricity and inclination in the N-body simulation. You also see that the amplitudes match but the frequencies of the oscillations are different between the analytic approximations and the N-body simulations.

3.3.2 Jupiter and Saturn in mean motion resonance

As mentioned before Jupiter and Saturn is relatively close to a 5:2 mean motion resonance $\left(\frac{n_{Jup}}{n_{Sat}} \sim 2.48\right)$. Could this be the reason for the non-perfect fit in Figures 3.1 and 3.2? I change Saturn's semi-major axis to $a_2 = 8.257983581$ AU so they end up in a perfect 2:1 MMR. I now calculate the new secular oscillation equation and compare them with a N-body simulation for the new system.

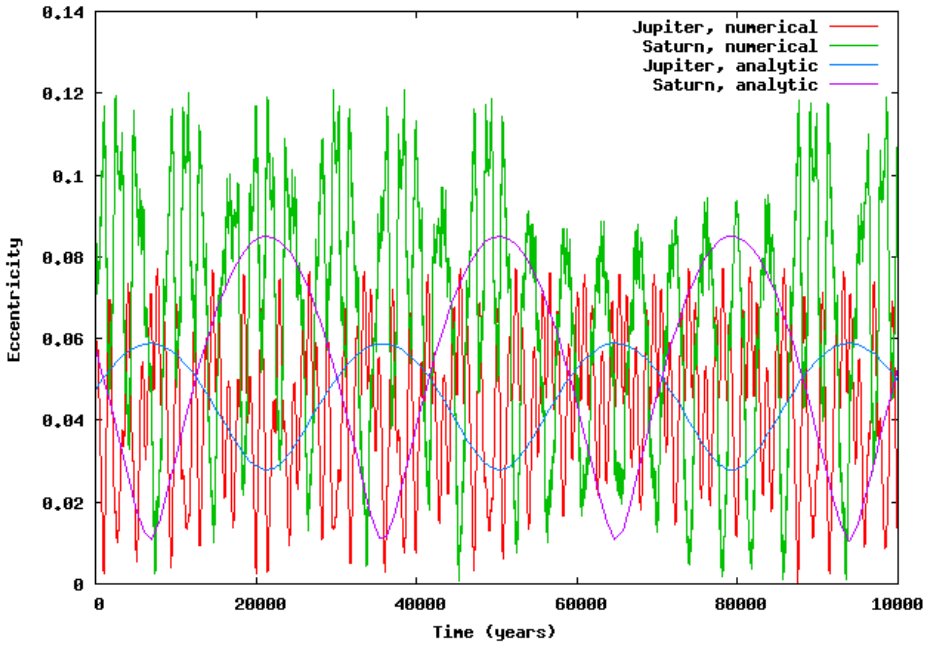

Figure 3.3: Eccentricity oscillations for Jupiter and Saturn in 2:1 MMR. Shows the results from a N-body simulation with Jupiter (red curve) and Saturn (green curve) and the analytically derived equations for Jupiter (blue curve) and Saturn (purple curve).

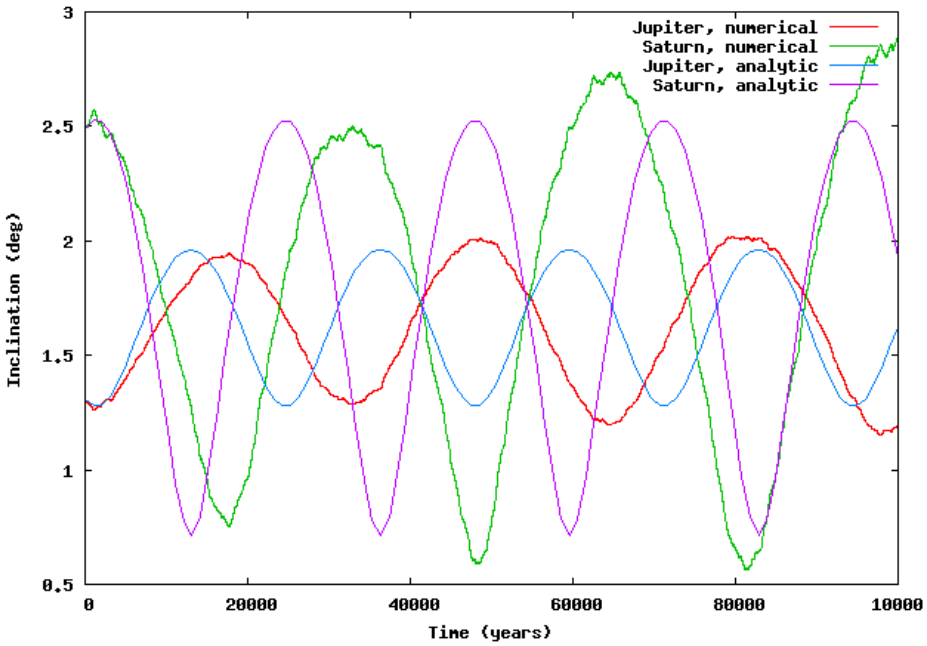

Figure 3.4: Inclination oscillations for Jupiter and Saturn in 2:1 MMR. Shows the results from a N-body simulation with Jupiter (red curve) and Saturn (green curve) and the analytically derived equations for Jupiter (blue curve) and Saturn (purple curve).

In this case the eccentricity evolution don't match at all. The N-body simulation has smaller periods and larger amplitudes. The inclination oscillations have comparable periods but growing amplitudes in the N-body simulation. The differences between simulations and analytic equations are also not the same as for the true Jupiter-Saturn system. The conclusion here is that the equations don't work when the planets are in MMR. The reason for this is that the planets get closer to each other more often leading to larger planet-planet interactions than if they weren't in the resonance.

3.3.3 Jupiter and Saturn far from resonance

What if I have Jupiter and Saturn far from MMR? I use the same initial conditions as before except I set $\frac{n_1}{n_2} = \sqrt{5} \implies a_2 \sim 8.89563148$ AU. I go through the same procedure again and get the following results:

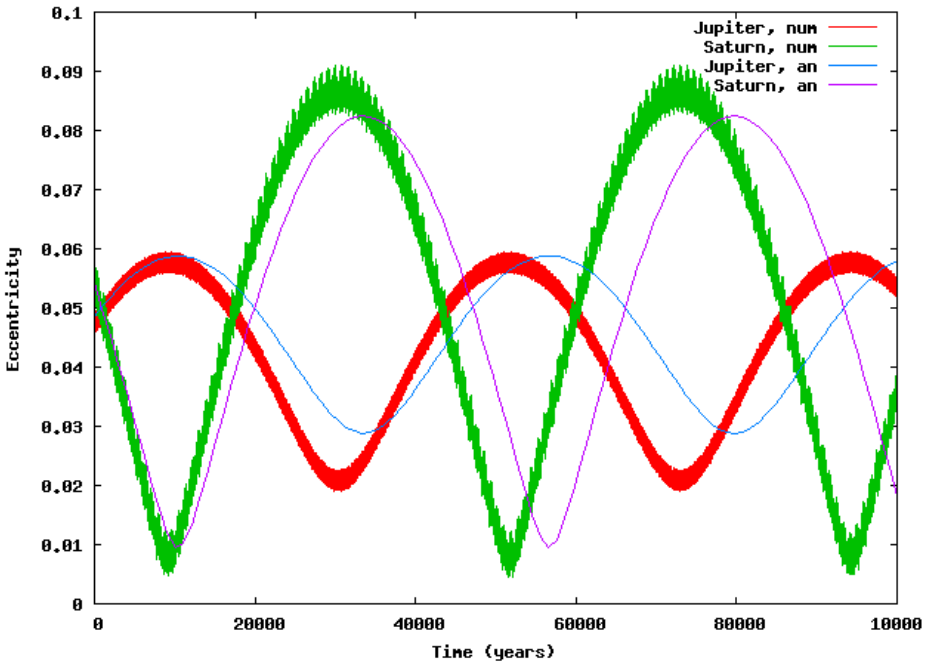

Figure 3.5: Eccentricity oscillations for Jupiter and Saturn far from MMR ($\frac{n_1}{n_2} = \sqrt{5}$). The figure shows the results from a N-body simulation with Jupiter (red curve) and Saturn (green curve) and the analytically derived equations for Jupiter (blue curve) and Saturn (purple curve).

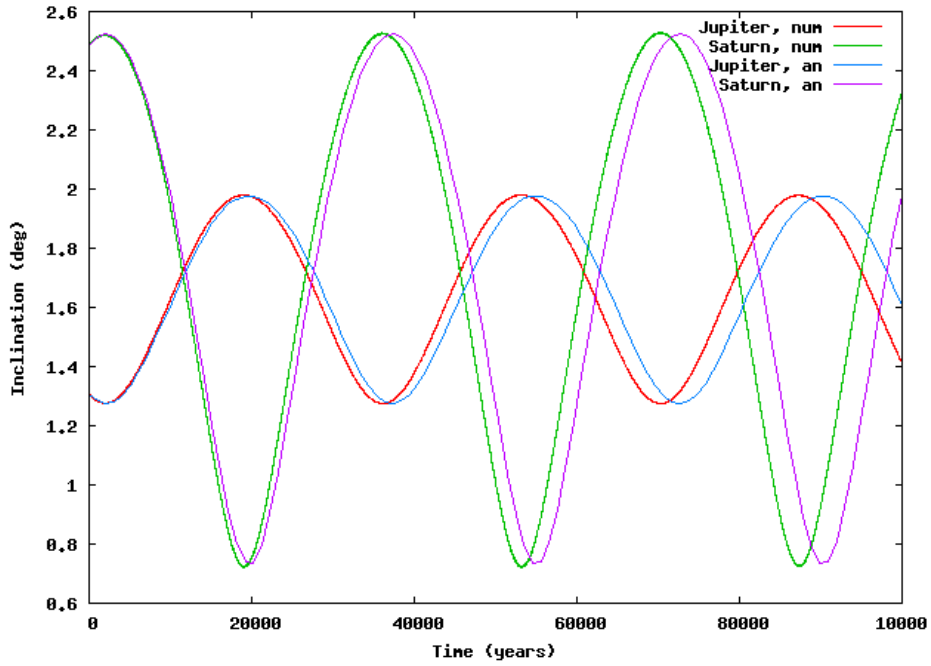

Figure 3.6: Inclination oscillations for Jupiter and Saturn far from MMR ($\frac{n_1}{n_2} = \sqrt{5}$). The figure shows the results from a N-body simulation with Jupiter (red curve) and Saturn (green curve) and the analytically derived equations for Jupiter (blue curve) and Saturn (purple curve).

Here I have the similar errors as for the true Jupiter-Saturn system so it is probably not the almost 5:2 MMR that is the origin of the errors.

3.4 Investigation of the dependence on properties of the two-planet system

In this section I look at how the secular oscillation for a two-planet system depends on different properties of the system. I do this by first selecting a parameter to vary (e.g. the masses of the planets) and a range of values within which I vary the parameter. I then generate 1000 systems within those limits (e.g. masses between one Neptune-mass and one Jupiter-mass). With the same procedure as in Section 3.2 I determine $e(t)$ and $I(t)$ for the two planets with equations from Section 3.1. The periods of the oscillations are typically 10-100 kyr so I evolve systems for 1 Myr. I look at the orbital configurations every 50 yr and find the minimum separation between the orbits. I do this by picking 10 points uniformly distributed in each orbit. Next i find the two points with smallest separation and select 10 points in each orbit around them. I continue until change is small enough (0.1%). I use the following initial conditions if nothing else is mentioned:

$$
\begin{aligned}
m_1 &= 0.5\ \mathrm{M}_{Jup}, & m_2 &= 0.5\ \mathrm{M}_{Jup},\\
a_1 &= 2.0\ \mathrm{AU}, & a_2 &= 5.0\ \mathrm{AU},\\
e_1 &= 0.1, & e_2 &= 0.05,\\
\varpi_1 &= 13.983865^\circ, & \varpi_2 &= 88.71945^\circ,\\
I_1 &= 2.0^\circ, & I_2 &= 4.0^\circ,\\
\Omega_1 &= 100.0381, & \Omega_2 &= 113.1334^\circ.
\end{aligned} \tag{3.45}
$$

The two orbits have the same orientation as the orbits of Jupiter and Saturn but different shapes and masses. These initial conditions lead to: a mutual inclination of $\Delta I \sim 2.10137^\circ$, a mutual Hill radius of $r_{mH} \sim 0.23896$ AU and a separation of $\Delta = \frac{a_2 - a_1}{r_{mH}} \sim 12.3$.

3.4.1 Fixed mass

I first look at systems where I vary the mass of the two planets but keep the total mass constant: $m_1 + m_2 = 1\ \mathrm{M}_{Jup}$. As minimum mass I use $m_{min} = 1\ \mathrm{M}_{Nep}$ and as maximum mass I use $m_{max} = 1\ \mathrm{M}_{Jup} - 1\ \mathrm{M}_{Nep}$. I also define the mass ratio $q = \frac{m_1}{m_2}$. With this setup I get the minimum separation, r_{min}, as a function of mass ratio

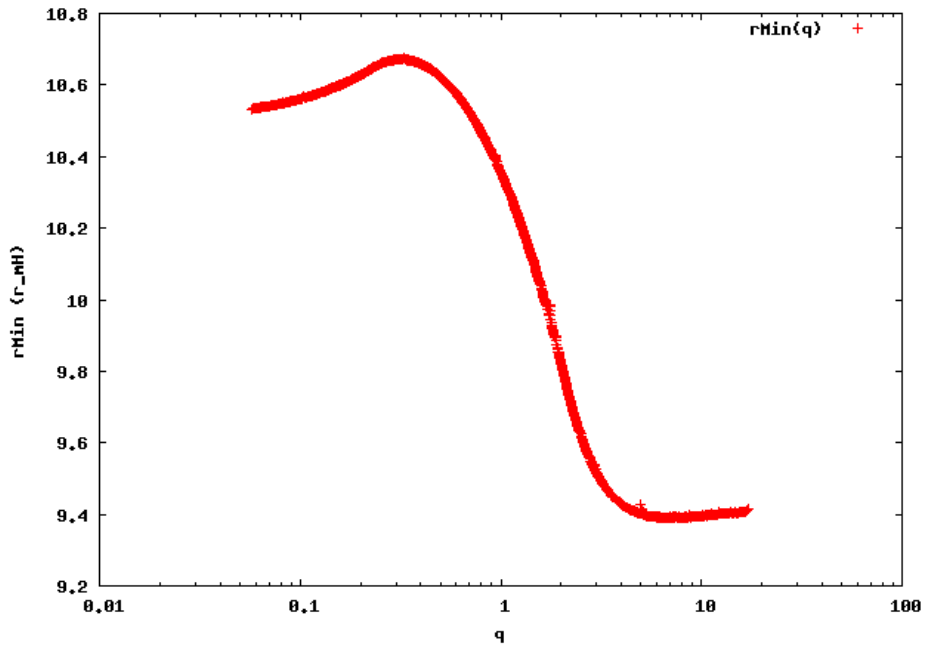

Figure 3.7: Minimum separation between two orbits as a function of mass ratio $q = m_1/m_2$ for a fixed total mass of $m_1 + m_2 = 1\ \mathrm{M}_{Jup}$.

The first thing we see is that r_{min} is smaller for $q > 1$, i.e. when the inner planet is more massive. I select two values on the mass ratio ($q = 0.1$ and $q = 10$) and plot the eccentricity oscillations for those two values:

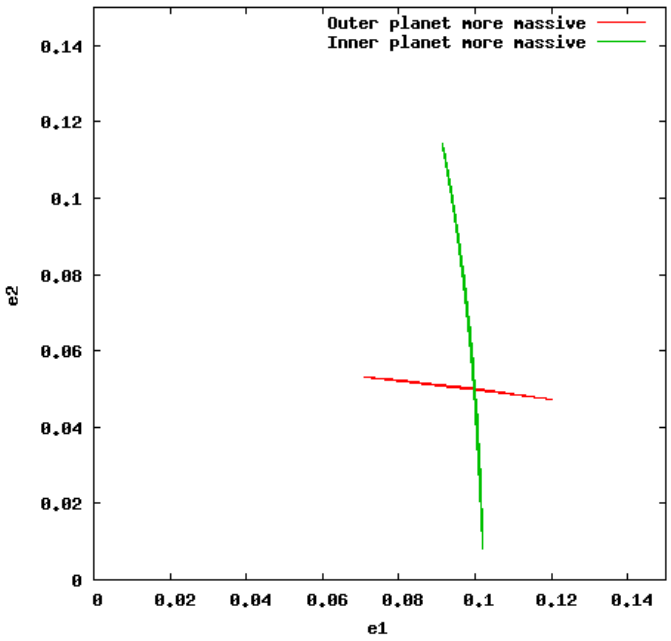

Figure 3.8: Eccentricity oscillations for two values on the mass ratio of the planets. $q = 0.1$ (red line) and $q = 10$ (green line). The total mass of the system is constant, $m_1 + m_2 = 1$ M_{Jup}.

We first see that it is the low-mass planet that has a larger amplitude. In the case of $q = 0.1$ (red line in Figure 3.8) e_1 varies a lot more than e_2. The effect is opposite when the inner planet is more massive (green line in Figure 3.8). We can also see that the eccentricity amplitude of the low-mass planet is larger if it is the outer planet that is low-mass (the green line is longer than the red line). We can then conclude that:

- It is the low mass planet that gets perturbed the most. This is what we should expect since the perturbation on a planet is dependent on the mass of the other planet.
- The effect of the perturbation is larger if the outer planet has low mass. This is also expected since the outer planet is less bound to the star so it is easier to perturb.
- You can do the approximation that the minimum distance between the orbits is the periapsis distance of the outer planet minus the apoapsis distance of the inner planet: $r_{min} \sim r_{per,2} - r_{apo,1} = a_2(1 - e_2) - a_1(1 - e_1) = a_2 - a_1 - a_2e_2 - a_1e_1$. We have $a_2 > a_1$ so r_{min} decreases more with the same change in eccentricity if it is the outer planet that is low mass (i.e. if e_2 inreases rather than e_1).

An inner perturber is more effective if you want a two-planet system to become unstable.

3.4.2 Separation between the planets

Next I look at the dependence on the separation between the planets so I vary $\Delta = \frac{a_1 - a_2}{r_{mH}}$ between 3 and 23 ($\Delta \sim 8$ for Jupiter and Saturn). When $\Delta < 2\sqrt{3}$ a system is always unstable even if it is coplanar (Gladman 1993). I keep the orbit of the inner planet fixed

and vary the semi-major axis of the outer planet's orbit. I first look at the minimum separation as a function of the initial separation

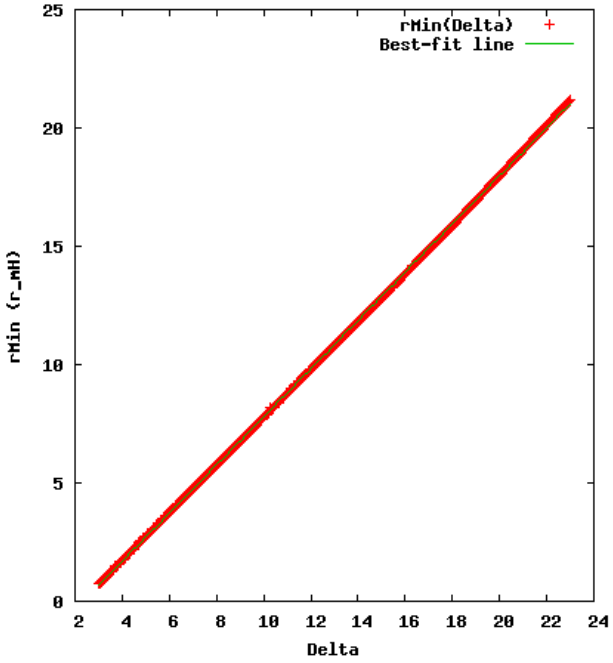

Figure 3.9: Minimum separation of the orbits of the two planets as a function of initial separation, $\Delta = \frac{a_2 - a_1}{r_{mH}}$. In units of mutual Hill radii.

This fits very well with a linear regression: $r_{min} \sim A\Delta + B$ where $A \sim 1.02$ and $B \sim -2.38$ so there is a 1:1 correlation between Δ and r_{min}. We can again use the approximation $r_{min} \sim r_{per,2} - r_{apo,1} = a_2(1 - e_2) - a_1(1 + e_1) = (a_2 - a_1) - (a_2 e_2 + a_1 e_1)$ and conclude that $a_2 e_2 + a_1 e_1$ is constant. This can be explained by the fact that the eccentricity amplitudes decreases as the separation (a_2) increases. I have also looked at the periods of the oscillations as functions of Δ

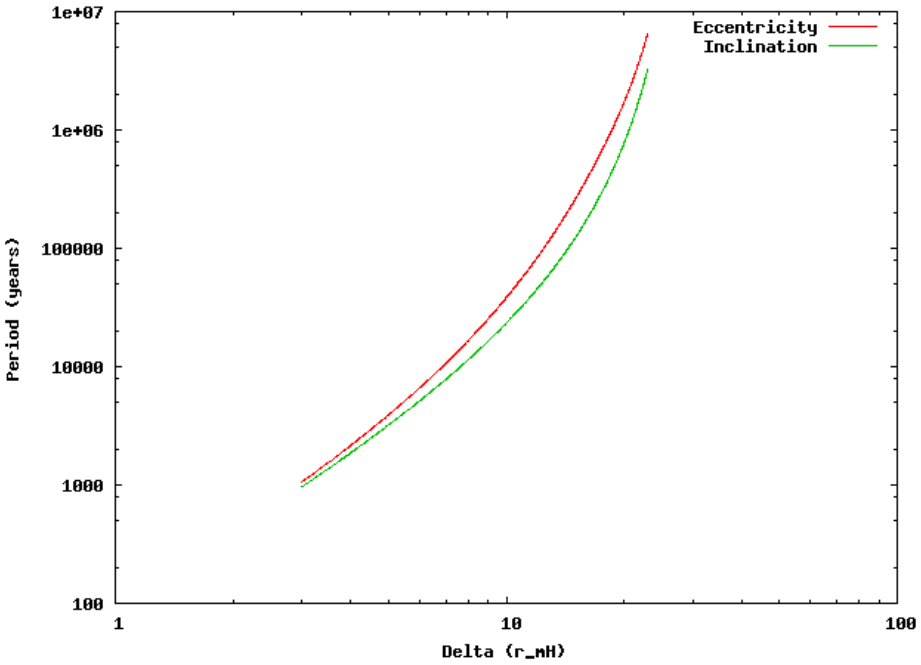

Figure 3.10: Periods of the eccentricity and inclination oscillations of the two planets as a function of initial separation, $\Delta = \frac{a_2 - a_1}{r_{mH}}$.

We see that the periods are very sensitive to the value of Δ. We also see, as for the case of Jupiter and Saturn (Section 3.2), that the period of the eccentricity oscillations is larger than the period for the inclination oscillations.

3.4.3 Stellar mass

How does the secular oscillations depend on the mass of the star? I generate systems where I vary the mass of the star, m_c, between $m_{c,min} = 0.0124$ $M_\odot \sim 13$ M_{Jup} (minimum mass for deuterium fusion) and $m_{c,max} = 16$ $M_\odot$ (a star with a main-sequence lifetime of ~ 10 Myr, similar to the lifetime of a protoplanetary disk). I look at the minimum separation as a function of the mass of the star

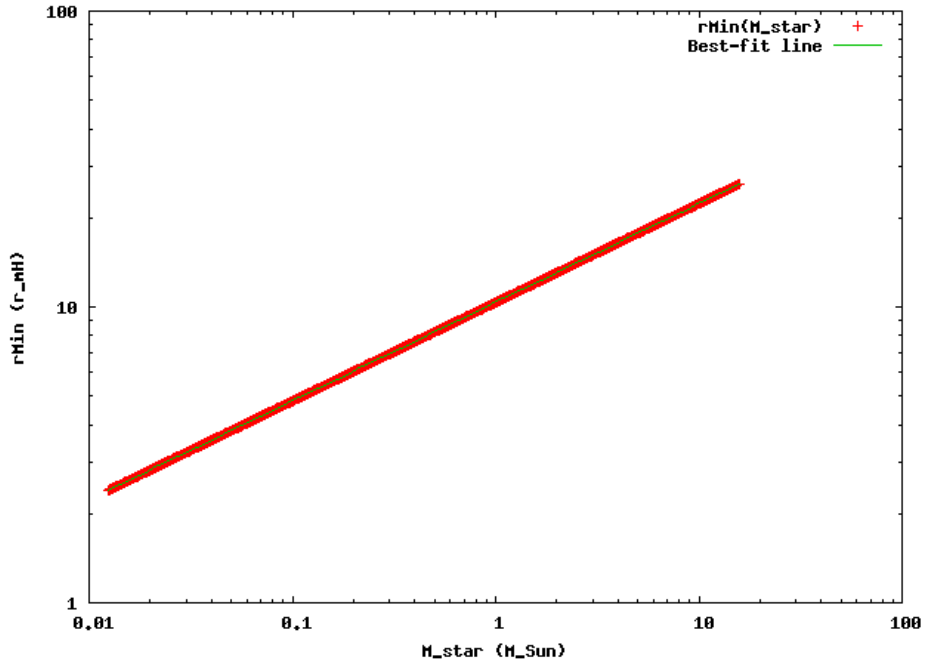

Figure 3.11: Minimum separation of the orbits of the two planets as a function of the mass of the star.

The minimum separation in mutual Hill radii fits very well with a power-law: $\frac{r_{min}}{r_m H} \propto m_c^{1/3}$. But we also know from Eq. (2.10) that $r_{mH} \propto m_c^{-1/3}$ so the amplitudes of eccentricity oscillations are not dependent on the mass of the star. On the other hand the periods are dependent on the mass of the star

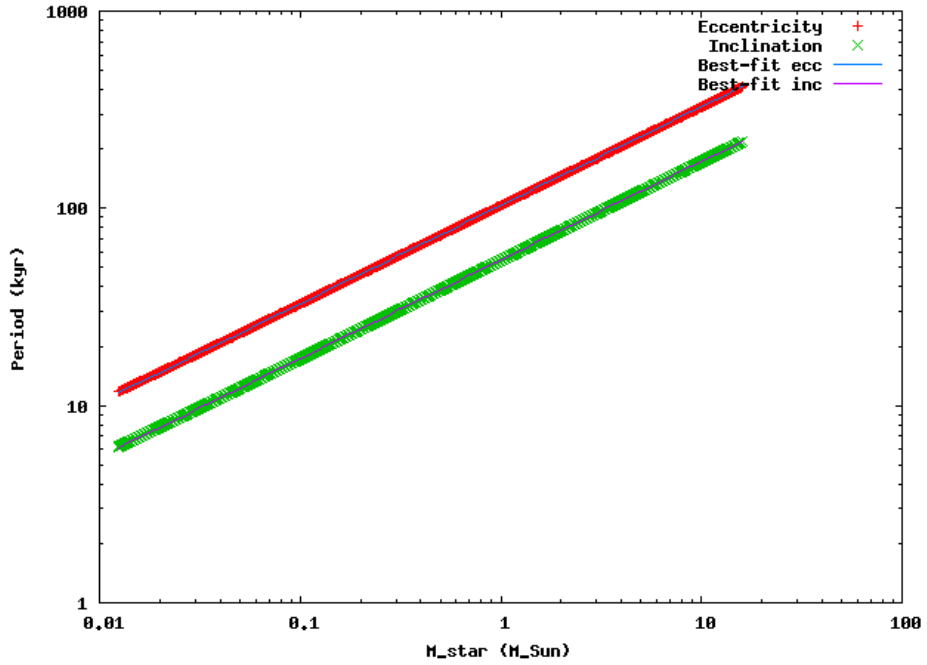

Figure 3.12: Periods of the eccentricity and inclination oscillations of the two planets as a function of the mass of the star.

The periods of the oscillations both fits with a power-law $\propto m_c^{1/2}$. This can be explained by looking at Eqs. (3.4)–(3.5). We see that the matrix elements are $\propto \frac{n}{m_c} \propto m_c^{-1/2}$. The frequencies are then the eigenvalues of the matrices which are proportional to the matrix elements and finally the periods are proportional the the inverse of the frequencies i.e. $\propto m_c^{1/2}$. This explains the slope of the curves in Figure 3.12.

3.4.4 Equal-mass planets

The final investigation I do with this method is looking at the dependence on the mass of equal-mass planets, $m_1 = m_2 = m$. I vary the masses between $m_{min} = 1$ M_{Nep} and $m_{max} = 2$ M_{Jup}. I first look at the minimum separation as a function of planet mass

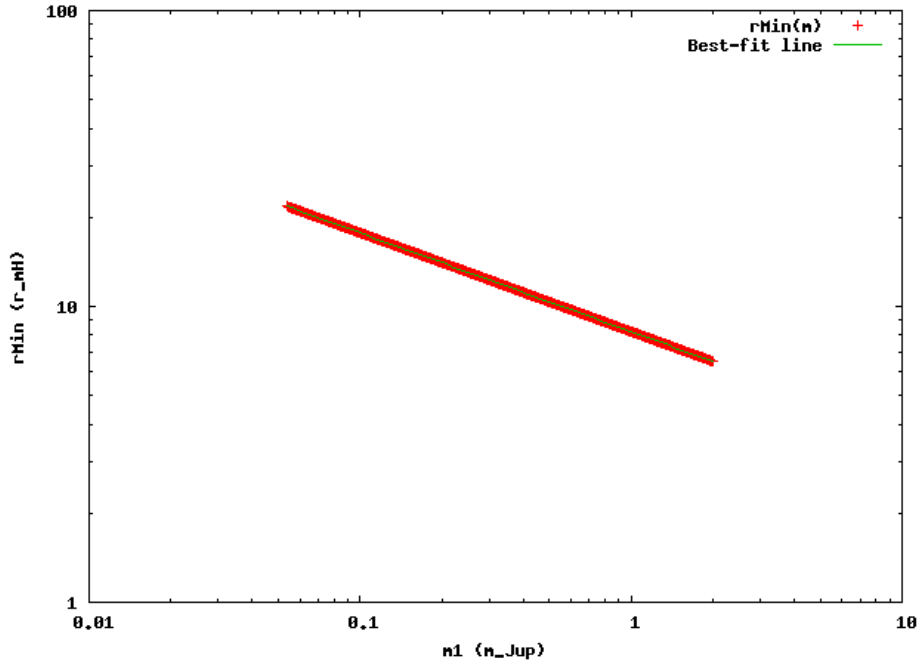

Figure 3.13: Minimum separation of the orbits of the two planets as a function of the mass of the equal-mass planets.

The minimum separation in mutual Hill radii fits very well with a power-law: $\frac{r_{Min}}{r_m H} \propto m^{-1/3}$. But we also know from Eq. (2.10) that $r_{mH} \propto (m_1 + m_2)^{1/3}$ so the amplitudes of eccentricity oscillations are not dependent on the mass of the planets. On the other hand the periods are dependent on the planet mass

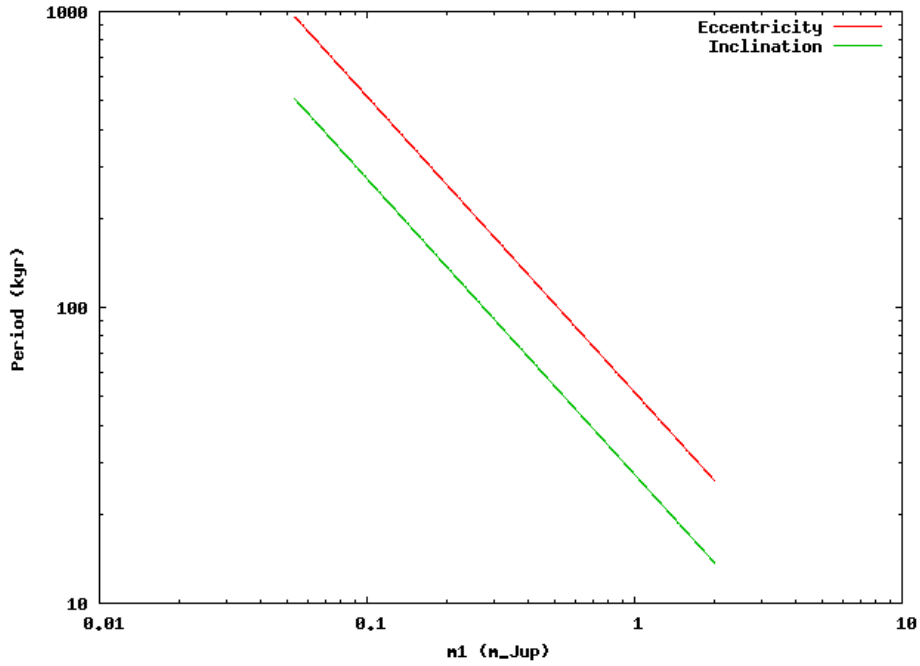

Figure 3.14: Periods of the eccentricity and inclination oscillations of the two planets as a function of the mass of the equal-mass planets.

The periods of the oscillations both fits with a power-law $\propto m^{-1}$. This can be explained by looking at Eqs. (3.4)–(3.5). We see that the matrix elements are $\propto m$. The frequencies are then the eigenvalues of the matrices which are proportional to the matrix elements and finally the periods are proportional the the inverse of the frequencies i.e. $\propto m^{-1}$.

4 Simulation setup

4.1 MERCURY6

In my project I have made many N-body simulations of multiple-planet systems (e.g. $\sim$ 1500 in Section 8 alone). To do the simulations I use MERCURY6 (Chambers 1999) which is a package designed for making N-body simulations where you have small bodies orbiting around a single massive object (e.g. planetary systems, moons around a planet, ...). The code is written in Fortran 77 and contains several integrators to solve the equations of motion:

- Mixed-variable symplectic: A fast, moderately accurate integrator which cannot handle close encounters between objects. It is designed to solve Hamilton's equations and almost perfectly conserve the energy of a system.
- Bulirsch-Stoer: A slow but very accurate integrator that can handle close encounters between two objects. It increases the accuracy by splitting one time step into smaller steps.
- Conservative Bulirsch-Stoer: Similar to the Bulirsch-Stoer but two times faster. It only works for conservative forces, i.e. when the force is a function of position only (e.g. gravity).
- Everhart's RA15: An integrator that is faster than the Bulirsch-Stoer. It is accurate but has problems with close encounters.
- Hybrid symplectic-BS: This is the integrator that I have used the most. When planets are far away from each other it uses the mixed-variable symplectic integrator but changes to Bulirsch-Stoer if two planets gets close to each other. This makes it fast, relatively accurate and able to handle close encounters.

So how do I do an integration?

i) First I compile three files included in the MERCURY6-package: mercury6_1.for (program containing the integrators), element6.for (program for producing output in readable format), close6.for (program for producing output on close encounters)

ii) Next I set the initial conditions:

- Set the masses, densities and orbital parameters for the bodies in the system. Set the epoch at which they had those parameters. Define the close encounter limit (in units of r_{mH}). The orbital parameters can be expressed in different formats: Keplerian or Cartesian coordinates.
- Decide which integrator I want to use, at which times I want to start and stop the integration, how often I want output, which time step I want to have, if I want to stop the integration if there is a close encounter, the mass of the central body, at what separation between two objects I want to change integrator if I use the Hybrid symplectic-BS integrator.

iii) After the initial conditions are set I run the program (mercury6_1).

iv) When it is finished I decide which orbital elements I want output for and to what precision.

v) Then I run element6 to get the output in a readable file.

vi) Finally I run close6 to get information on close encounters in a readable file

Throughout the N-body integration the program produces dump files so I can continue an integration from them if the computer crashes during a run and I can also extend a finished run.

4.2 How to decide initial conditions

How do I decide what initial conditions to use for my simulations?

- **Eccentricity and mutual inclination:** From Section 3 we know that if two orbits are mutually inclined you get secular oscillations in e, I, ϖ and Ω. So I pick small, non-zero, e and ΔI (except when I am investigating the Kozai mechanism, see Section 6.4).

- **Masses:** When I chose masses of the planets in planetary systems I generate myself I pick either Jupiter-Saturn masses, equal masses or masses that are well explained in the relevant sections. For self-generated systems I use 1 $M_\odot$ as the mass of the star.

- **Semi-major axes:** I want planets that are relatively close to each other so I get large planet-planet interactions on reasonably small timescales. I try to have planets on orbits around 1 AU.

- **Alignment of the orbits:** For self-generated systems I pick longitude of periapsis (ϖ) and Longitude of ascending node (Ω) such that they are equal to the values for Jupiter and Saturn (Section 3) or such that the orbits are perfectly aligned ($\varpi_i = \varpi_j$ and $\Omega_i = \Omega_j$, Sections 5, 8 and 9).

- **Initial positions of the planets:** In Section 3 I neglect the initial positions of the planets in their orbits to be able to analytically approximate the secular oscillations. However, for N-body simulations that I have made I have seen that the initial positions of the planets are important for the outcome, see Section 7.3.4. Planetary systems are typical examples of chaotic systems, where small changes in initial conditions result in large differences in outcome. The reason it is like this is because the disruption of a system (collision between planets or ejection of a planet) is caused by discrete events, close encounters, eventually leading to ejections and collisions. In Sections 5, 8 and 9 I make many simulations for the same orbital configurations by changing the initial positions of the planets in their orbits.

4.3 Fitting method

At several points in my project I need to fit analytic functions to simulation results (e.g. periods and minimum separation as functions of masses and initial separation in 3.4, timescales as functions of separations in Sections 5, 8 and 9 and timescales as functions of mass in Section 9). To do this I use the plotting software gnuplot's built-in non-linear

least square method. It uses a Marquardt-Levenberg algorithm which is slower but safer than other algorithms to minimize:

$$S(\boldsymbol{\beta}) = \sum_{i=0}^{n} \left(y_i - f(x_i, \boldsymbol{\beta})\right)^2 \tag{4.1}$$

where y_i and x_i are the data, n is the number of data points, $\boldsymbol{\beta}$ are the free parameters and $f(x_i, \boldsymbol{\beta})$ is the function to be fitted.

5 Three-planet systems with equal separations, $\Delta_{12} = \Delta_{23}$

5.1 Simulation setup

In this section I investigate the stability of three-planet systems as a function of the separations between the planets. If you have a system with three planets the parameter space is very large. The simplifications I make are:

- Equal-mass planets (1 M_{Jup}).
- Aligned orbits ($\varpi_1 = \varpi_2 = \varpi_3$ and $\Omega_1 = \Omega_2 = \Omega_3$).
- Small, non-zero, eccentricities ($e_1 = 0.01$, $e_2 = 0.02$ and $e_3 = 0.015$) and inclinations ($I_1 = 0°$, $I_2 = 1.5°$ and $I_3 = 3.0°$).
- Equal separations between the planets (Δ_{12} and Δ_{23}) in units of mutual Hill radii:

$$\Delta_{12} = \frac{a_2 - a_1}{r_{mH,12}} = \Delta_{23} = \frac{a_3 - a_2}{r_{mH,23}} \equiv \Delta \tag{5.1}$$

The parameter I vary for my simulations is Δ and I chose 13 values between 3.0 and 5.25 (3.0, 3.25, 3.5, 3.75, 3.9, 4.0, 4.1, 4.25, 4.5, 4.75, 5.0, 5.1 and 5.25). I put the inner planet at an orbit with $a_1 = 1$ AU and from that I can get the values on a_2 and a_3 given Δ. I make several (~ 30) simulations for each value on Δ (I chose initial position of the outer two planets in their orbits randomly). I run each simulation until a planet is ejected or for a maximum of 500 Myr. I am interested in what happens and when it happens. Secular oscillations in e and I will change the orbits of the planets and may lead to close encounters (when two planets are within one r_{mH} of each other) and ejections of planets. In total I have made 530 N-body simulations for these studies.

5.2 Timescales

The events I am interested in are close encounters, especially the first close encounter, and ejection of planets. The first thing I look at is the time it takes to get a close encounter (τ_{CE}) for the simulations and plot it versus Δ:

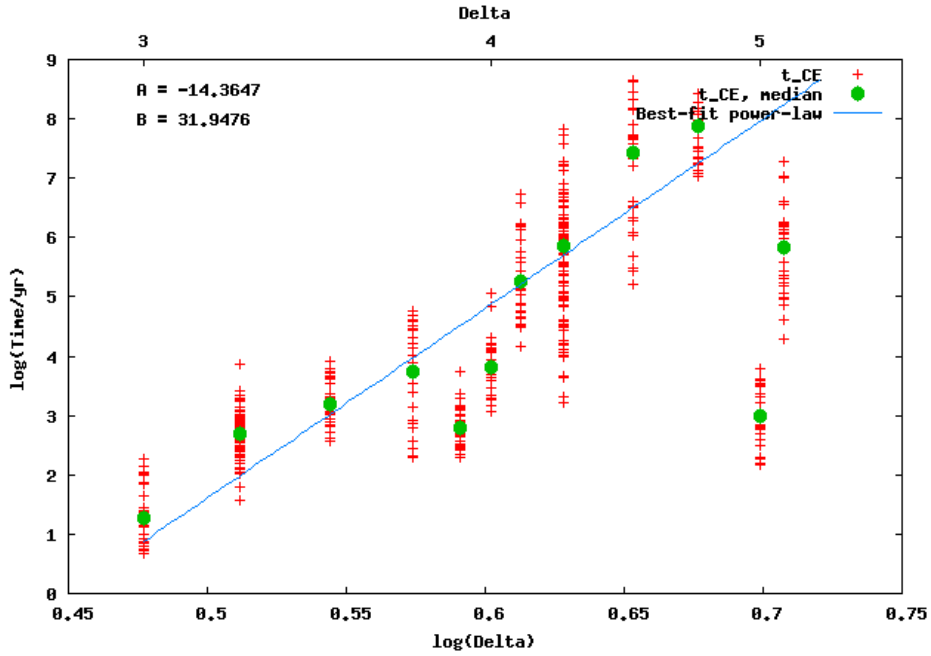

Figure 5.1: Time until first close encounter between two planets as a function of $\Delta_{12} = \Delta_{23}$. Red crosses are the data for each simulation and green dots are the median values of the time until first close encounter. Best-fit power-law, $\log \tau_{CE} = A + B \log \Delta$ also added (blue line).

The medians of the data points in Figure 5.1 fits relatively well with a power-law (I do the fitting with the method described in Section 4.3):

$$\log \tau_{CE} = A + B \log \Delta \tag{5.2}$$

where $A = -14.3674$ and $B = 31.9476$. As we can see the time to get to first close encounter is extremely dependent on the initial separation. We also see dips in close encounter timescale here and there e.g. at $\Delta = 5.0$. With the orbital configurations of the $\Delta = 5.0$ simulations the planets in the system are relatively close to MMRs (Eq. (2.11)):

$$\frac{n_1}{n_2} \sim 1.9260 \qquad \frac{n_2}{n_3} \sim 1.9260 \qquad \frac{n_1}{n_3} \sim 3.7096 \tag{5.3}$$

MMRs can lead to planets being closer to each other more often and hence increasing the planet-planet interactions, remember that we assumed no MMR in our derivation of the secular oscillation equations (Section 3). One thing I also have found is that not all simulations have a close encounter which means that this is a good regime of separations to investigate (discussed further in Section 5.3).

The next thing I am interested in is ejections of planets. Therefore I plot the time it takes to eject one planet from the system:

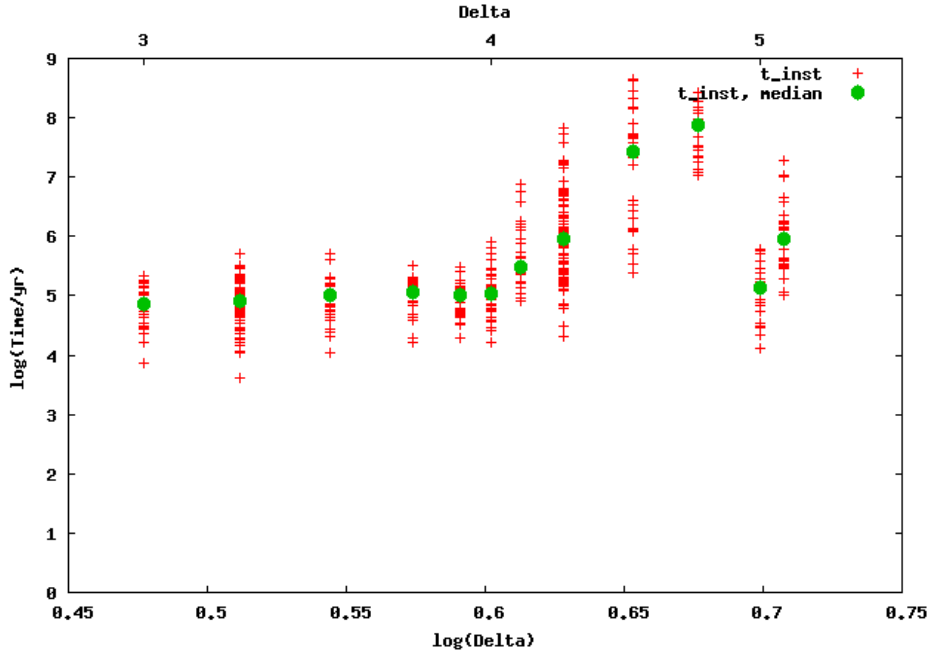

Figure 5.2: Time until first ejection of a planet as a function of $\Delta_{12} = \Delta_{23}$. Red crosses are the data for each simulation and green dots are the median values of the time until ejection of a planet.

Compared to Figure 5.1 there is no simple relation between the ejection time and Δ. For small Δ it seems to be constant while it is increasing for larger Δ. One thing I find, though, is that all systems with at least one close encounter continue to have more and more close encounters until they eventually eject a planet (see Section 5.3). I find that the systems have a total of ~ 500 close encounters (se Table 5.4).

If I instead look at the time between the first close encounter and ejection of a planet I find something very interesting:

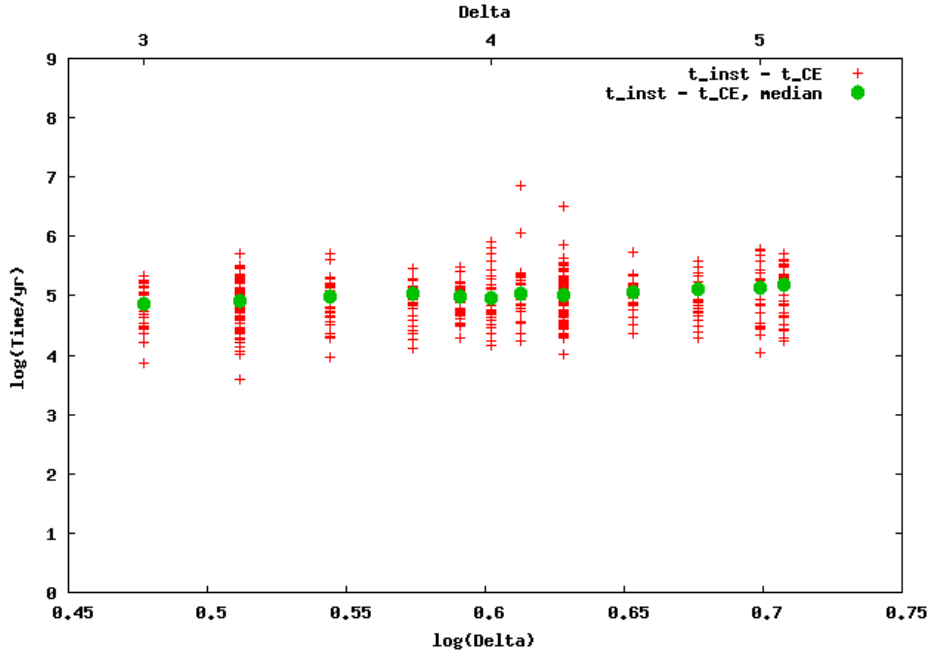

Figure 5.3: Time between first close encounter and ejection of a planet as a function of $\Delta_{12} = \Delta_{23}$. Red crosses are the data for each simulation and green dots are the median values of the time until ejection of a planet.

We see that it is constant ~ 100 kyr or at least independent of the initial separations. Even the systems which had a smaller τ_{CE} than expected from Eq. (5.2) (the MMR systems) are now the same as all other systems. My explanation for this is that the first close encounter stir up the system so that it loses its identity and you can't separate it from the other systems. This might sound like it shouldn't work since the systems have different Δ but the differences in absolute separations are not very large:

Δ	a_1 (AU)	a_2 (AU)	a_3 (AU)
3.00	1.00	1.30	1.68
4.00	1.00	1.42	2.00
5.00	1.00	1.55	3.40

Table 5.1: Semi-major axes for the three planets for three different values of Δ.

We can also do an approximation of the time between first close encounter and ejection of a planet.

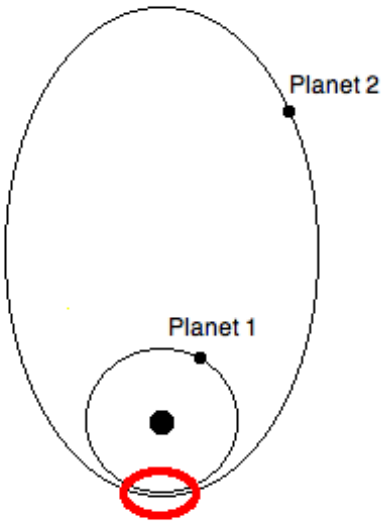

Figure 5.4: The orbits of two planets that can have close encounters. These close encounters can occur in the red region where the two orbits are as close as possible to each other.

Figure 5.4 shows the orbits of two planets that can have close encounters. These close encounters will in that case happen inside the red region. The outer planet is in that region once every orbit. To find how often the inner planet is in that region we need to know the fraction of its orbit that is inside the red region. Say the planets have semi-major axes of 1 and 10 AU. I pick 1 AU because it is roughly equal to the initial semi-major axes of the planets in the simulations and 10 AU since as time goes by the semi-major axis of the ejected planet increases so it is somewhere in between initial and ejected. With these values the mutual Hill radius becomes $r_{mH} \sim 0.5$ AU. Then the fraction, η, of the orbit of the inner planet that is inside the red region becomes

$$\eta = \frac{2 \cdot 0.5}{2\pi} \sim \frac{1}{6} \tag{5.4}$$

That means that every sixth time the outer planet is in the red region the inner planet will also be there and we have a close encounter. The period of the outer planet is $T_2 \sim 30$ years so the time between each close encounter, Δt, becomes

$$\Delta t = 6T_2 \sim 300 \text{ yr} \tag{5.5}$$

We can now finally get the time between first close encounter and ejection, $\tau_{ej} - \tau_{CE}$ as the number of close encounters, N_{CE}, multiplied with the time between each close encounter

$$\tau_{ej} - \tau_{CE} = N_{CE}\Delta t \sim 500 \cdot 300 \text{ yr} = 10^5 \text{ yr} \tag{5.6}$$

Which is surprisingly similar to the results in Figure 5.3.

5.3 Planets involved in close encounters and ejections

I next investigated in more detail the first close encounter. Which planets are involved in the first close encounter? Is it always the same two planets?

Δ	η_{CE}	1:2	1:3	2:3
3.00	30/30	16.67%	3.33%	80.0%
3.25	100/100	64.0%	1.0%	35.0%
3.50	30/30	60.0%	0.0%	40.0%
3.75	30/30	53.33%	0.0%	46.67%
3.90	30/30	56.67%	0.0%	43.33%
4.00	30/30	43.33%	3.33%	53.33%
4.10	30/30	43.33%	0.0%	56.67%
4.25	100/100	46.0%	2.0%	52.0%
4.50	28/30	46.43%	0.0%	53.57%
4.75	26/30	46.15%	0.0%	53.85%
5.00	30/30	73.33%	0.0%	26.67%
5.10	30/30	66.67%	0.0%	33.33%
5.25	0/30	0.0%	0.0%	0.0%

Table 5.2: Fraction of systems that have at least one close encounter, η_{CE}, and which planets are involved in the first close encounter (column three, four and five).

Intuitively I thought that it should be either the two inner or the two outer planets that had the first close encounter. The reason I didn't expect that the innermost and the outermost planets were going to have the first close encounter was that you have one planet in between them. In most cases I am right but in five of my simulations it is planet 1 and 3 that has the first close encounter. One reason why this is possible is because I have a strict definition of what a close encounter is: two planets within one mutual Hill radius. A system where planet 1 and planet 3 have the first close encounter could have had several 'almost' close encounters which changed the orbits. If we look at the other simulations the first close encounter is between the inner two planets roughly equally often as it is between the outer two planets.

Next I investigated if there is any trends when it comes to which planet is ejected from a system. I get the following results:

Δ	η_{ej}	Planet 1	Planet 2	Planet 3
3.00	30/30	36.67%	23.33%	40.0%
3.25	100/100	25.0%	42.0%	33.0%
3.50	30/30	50.0%	23.33%	26.67%
3.75	30/30	33.33%	26.67%	40.0%
3.90	30/30	43.33%	26.67%	30.0%
4.00	30/30	36.67%	33.33%	30.0%
4.10	30/30	33.33%	30.0%	36.67%
4.25	100/100	33.0%	37.0%	30.0%
4.50	28/30	32.14%	32.14%	35.71%
4.75	26/30	38.46%	38.46%	23.08%
5.00	30/30	40.0%	33.33%	26.67%
5.10	30/30	26.67%	40.0%	33.33%
5.25	0/30	0.0%	0.0%	0.0%

Table 5.3: Fraction of systems that are unstable and ejects a planet η_{ej} and how often the each planet is ejected (column three, four and five).

The first thing we see is that there is no real preference which planet is ejected, all planets are ejected roughly one third of the simulations with ejections. By comparing Tables 5.2 and 5.3 I find that all systems with a close encounter eventually ejects one planet. One interesting thing we see in Table 5.3 is that planet 2 is not ejected in 50% of the simulations. This suggests that the planets lose their identity after one or a few close encounters. One could have thought that, in the simulations, one of the planets is a 'spectator', i.e. it stays where it is while the other two planets keep having close encounters until one of them gets ejected. If that had been the case planet 2 would have been ejected $\sim 50\%$ of the time since (from Table 5.2) it is involved in $\sim 100\%$ of the first close encounters.

I have also looked at the distribution of close encounters after the first one:

Δ	$\overline{N}_{CE}$	1:2	1:3	2:3
3.00	463	39.05%	33.52%	27.42%
3.25	484	31.99%	34.59%	33.41%
3.50	524	31.67%	26.03%	42.3%
3.75	536	32.19%	35.43%	32.38%
3.90	592	38.85%	38.51%	22.63%
4.00	584	25.52%	38.8%	35.68%
4.10	663	42.89%	33.31%	23.79%
4.25	543	39.18%	34.7%	26.12%
4.50	469	33.68%	42.22%	24.1%
4.75	533	45.03%	27.96%	27.01%
5.00	558	27.5%	46.14%	26.37%
5.10	588	33.11%	33.35%	33.54%
5.25	0	0.0%	0.0%	0.0%

Table 5.4: Mean number of close encounters $\overline{N}_{CE}$ for the simulations and which planets are involved in the close encounters (column three, four and five).

From this we see that there is no preferred pair to have a close encounter after the first which Table 5.3 also indicated. Another thing we can see is that a system has many close encounters ($\sim 500 - 600$) before the ejection of a planet. The system, so to say, 'builds up' the eccentricity to eject a planet rather than having one extreme close encounter.

5.4 Evolution of the structure of the systems

As we have seen in previous sections it is relatively random which planets have close encounters and which planets are ejected. What could be interesting is to see how the structure of the systems change as the have close encounters. To visualize this I select a value of Δ and plot all the systems with that separation in a-e-space right after the first close encounter and just before the ejection of a planet. I have chosen $\Delta = 4.1$ and the reason for that is that I find it to be a representative set of simulations. If we look in Figure 5.1 its median is right on the best-fit line, we see in Table 5.2 that it has roughly the same number of first close encounters between planet 1 and planet 2 as between planet 2 and planet 3 and finally in Table 5.3 we see that all planets are ejected in roughly the same number of simulations. I first plot the systems in a-e-space right after the first close encounter:

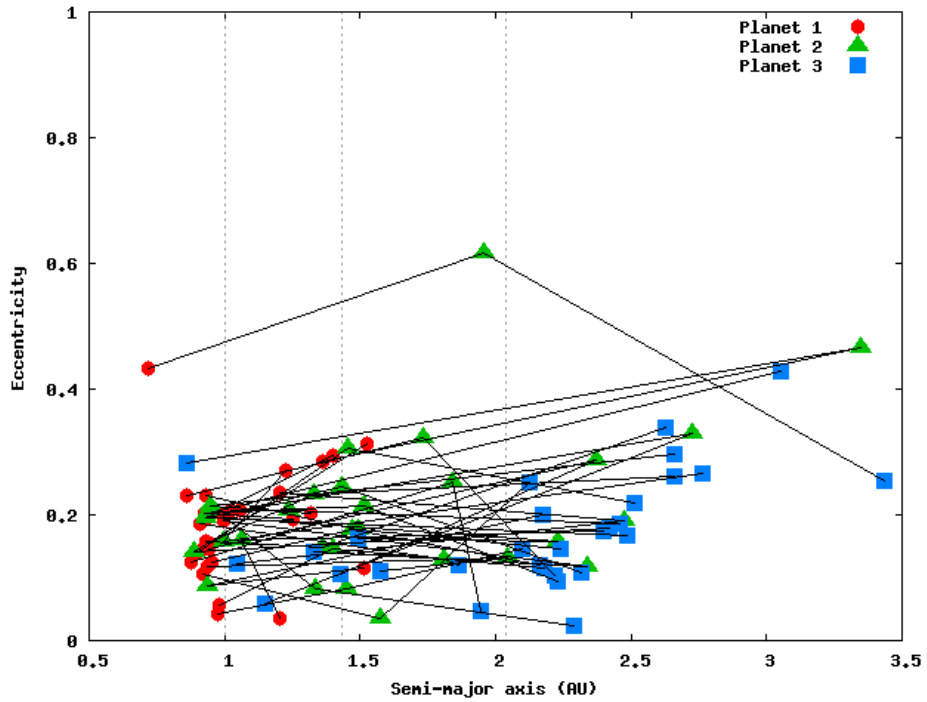

Figure 5.5: Structure of the $\Delta = 4.1$ systems right after the first close encounter (two planets within 1 r_{mH}). The initially innermost planet is plotted as a red circle, the middle planet as a green triangle and the outer planet as a blue square. Planets belonging to the same system are connected with a black line. The initial semi-major axes are also included as vertical dotted lines ($a_{1,0} = 1$ AU, $a_{2,0} = 1.43$ AU and $a_{3,0} = 2.04$ AU).

One thing we can see in Figure 5.5 is that most of the red circles (initially innermost planet) are to the left (close to the star) and most of the blue squares (initially outermost planet) are to the right (far away from the star) which makes sense since they started out with that configuration and there has been only one or at least very few close encounters so they haven't had much time to rearrange. Even if the planets still are relatively ordered most of them have a new value on their semi-major axis. This means that they have at some point exchanged energy with another planet and the evolution is then not purely secular (remember we assumed a constant semi-major axis in Section 3). It is however quite easy to explain: this is the configurations after the first close encounter but since I have a strict definition of what a close encounter is (two planets within one mutual Hill radius) the system could have had several 'almost' close encounters which could involve some energy transfer. We can also see that the heating of the system (i.e. the growth of eccentricity) is democratic meaning that all planets increase their eccentricity. It isn't only one planet in each system that has a larger eccentricity as it would have been if the growth was hierarchical.

Next I investigate what the same systems look like right before one planet is ejected:

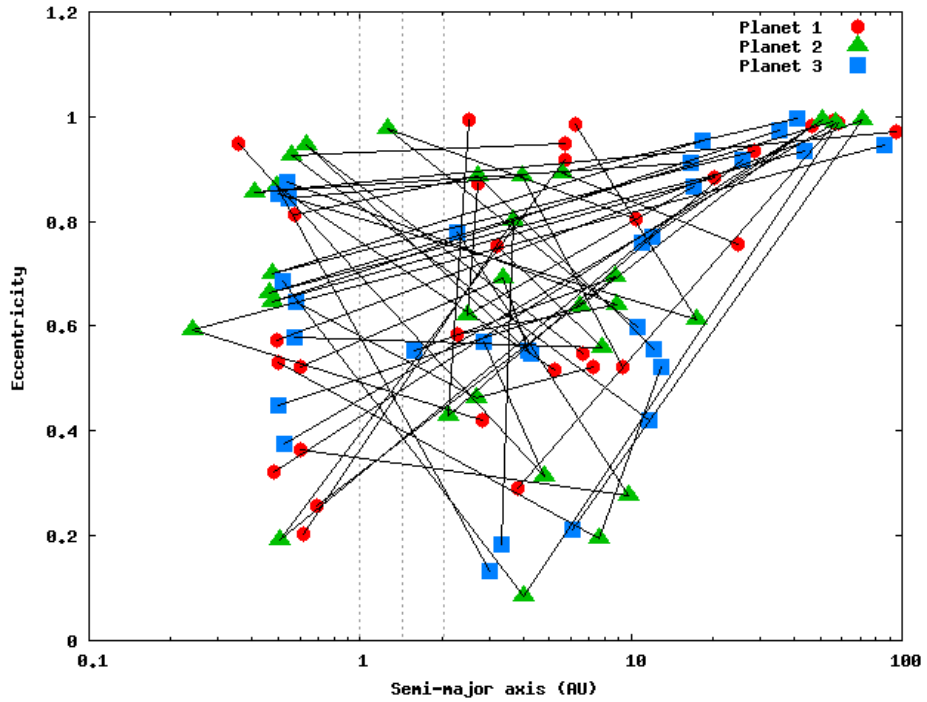

Figure 5.6: Structure of the $\Delta = 4.1$ systems right before one planet is ejected. The initially innermost planet is plotted as a red circle, the middle planet as a green triangle and the outer planet as a blue square. Planets belonging to the same system are connected with a black line. The initial semi-major axes are also included as vertical dotted lines ($a_{1,0} = 1$ AU, $a_{2,0} = 1.43$ AU and $a_{3,0} = 2.04$ AU).

The first thing we see in Figure 5.6 is that we have planets with large eccentricity for all possible semi-major axes but only planets close to the star can have low eccentricity. This is quite natural since the close encounters take place close to the star and planets on wide orbits can only get there if they have a high eccentricity. The close encounters have to take place close to the star since that is where the planets start and the total energy is conserved. We can also see that the planets have been mixed, there is no preferred semi-major axis or eccentricity for the different planets. Again this is a sign of democratic heating of the system. These results could affect the observability of the systems. If you have a system with a planet on a very wide orbit ($a \sim 100$ AU) it could be observed via direct imaging (see Section 7.1). The fact that the planets are very mixed is a consequence of the fact that they are equal mass. If they had had different mass it would have been the low-mass planet that was on a wide orbit and eventually ejected (see results in Section 7.2). By comparing Figure 5.5 to Figure 5.6 we find the same result as in Table 5.4, namely that it is not enough to have one close encounter to eject a planet. We can do an approximation of how many close encounters is needed to eject a planet with the help of Figure 5.7.

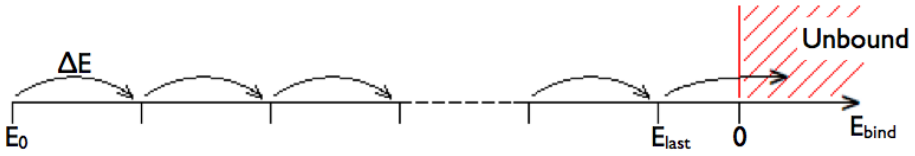

Figure 5.7: The evolution of the binding energy of a planet that eventually gets ejected. E_0 is the initial binding energy, E_{last} is the binding energy before the last close encounter and ΔE is the energy change per close encounter.

Figure 5.7 shows how the binding energy of the ejected planet evolves with time. The planet that eventually gets ejected has an initial binding energy E_0 and right before the last close encounter it has the binding energy E_last. We, again, assume that the binding energy increases in steps (close encounters) and at each close encounter the planet gains an energy ΔE. To get unbound to the star the planet neads a binding energy that is > 0 and before ejection the binding energy is E_{last} and we need only one more close encounter so we get that

$$E_{last} \sim \Delta E \tag{5.7}$$

In Figure 5.6 we see that the semi-major axis of the ejected planet has increased with a factor $\sim$ 100 from the initial value. We also know from Eq. (2.6) that the binding energy is inversely proportional to the semi-major axis. This means that the binding energy right before ejection becomes

$$E_{last} \sim \frac{1}{100} E_0 \tag{5.8}$$

Finally we also know that the planet that eventually gets ejected needs to increase its energy with E_0 to get a positive binding energy. This process has N_{CE} close encounters where in each close encounter it increases its energy with ΔE. Combining this with Eqs. (5.7)–(5.8) and we get

$$E_0 = N_{CE}\Delta E \Longrightarrow N_{CE} = \frac{E_0}{\Delta E} \sim \frac{100\Delta E}{\Delta E} = 100 \tag{5.9}$$

which is of the same order as the values I found in Table 5.4. The reason it is a bit smaller is because I have assumed that the planet that eventually gets ejected is involved in all close encounters (which is not true from Table 5.4). I also assume that it always gains energy in a close encounter which is not necessarily true. In some close encounters it could very well lose energy and get more tightly bound to the star but in the end it gains enough energy to get ejected. The important result here is that it requires more than one close encounters to eject a planet.

5.5 Conclusions

My conclusions for the simulations in this section are that the time it takes to get to the first close encounter is very dependent on Δ and can be described with a power-law (see

Eq. (5.2) and Figure 5.1). However, I have also found that MMRs can lower it (certain values of Δ in Figure 5.1). One very interesting thing I have found is that the time between the first close encounter and the ejection of a planet, $\tau_{ej} - \tau_{CE}$, is independent of the initial separation Δ (Figure 5.3). I find that already the first close encounter stirs up the system a bit (Figure 5.5) and with further close encounters the planets completely lose their identity (Figure 5.6). This means that there is no preferred pair of planets for the close encounters (Tables 5.2 and 5.3) except the first close encounter where there are very few (but still some) first close encounters between planet 1 and planet 3. I find that all systems that have a close encounter eventually eject a planet and they do it in the sense that they 'build up' the eccentricities of the planets with many ($\sim 500 - 600$) close encounters rather than a really strong one (Table 5.4).

From my power-law fit of the close encounter timescale (Eq. (5.2)) I find that the maximum separation for a three-planet system is $\Delta_{max} \approx 5.8$ to get a close encounter within age of the universe ~ 10 Gyr and after that it will eventually eject a planet on a much shorter timescale (see Figure 5.3). If we look at the observed systems (Figure 7.1) many systems have planets within those limits, however, I have made many simplifications (especially $a_1 = 1$ AU, equal-mass planets and the alignment of the orbits) in this model. The close encounter timescales should also be dependent on the periods of the secular oscillations which are dependent on many of the properties of the planetary system (Section 3.4).

6 Instability mechanisms

6.1 Stages in the evolution of a multiple-planet system

The evolution of a multiple-planet system can be split up into three stages (see Figure 6.1):

A) Systems with nice, non-crossing orbits. Stable systems stay here, e.g. the Solar System. For some of these systems (systems with planets on widely separated orbits with small eccentricities and low mutual inclinations) you can use the analytic approximations made in Section 3 to investigate the evolution of the system. If the orbits are close to each other or have large eccentricities the planet-planet interactions become too large and you need N-body simulations to do investigations.

B) Systems where two of the planets have crossing orbits or have a close encounter. The system has become unstable and you get scattering events between planets. Systems which come to this stage eventually also end up in stage C (see Section 5). At this stage the analytic approximation from Section 3 no longer works. Many of the observed multiple-planet systems seem to reach this stage (see Section 7.2).

C) Disrupted systems. A planet is ejected, two planets collide or a planet collides with the star. After the ejection of a planet the remaining planets are usually left on orbits with high eccentricity. The system is left with certain values on the binding energy, E, and angular momentum, h. From Eq. (A.28)

$$e = \sqrt{1 - \frac{2Eh^2}{\mu^2}} \tag{6.1}$$

we can see that it is very unlikely that the orbits are circular, $e = 0$. You need a specific combination of energy and angular momentum. This is interesting since many of the observed exoplanets have eccentric orbits close to the star. By ejecting a planet from a system the remaining planets lose energy (the orbit shrinks) and they are likely to end up on eccentric orbits. Kill two birds with one stone so to say. Whether a system gets disrupted by ejection of a planet or collision between two planets can be quantified with the Safronov number (Ford & Rasio 2008)

$$\theta^2 = \frac{1}{2}\frac{v_{esc}^2}{v_{orb}^2} = \left(\frac{Gm}{R_p}\right)\left(\frac{r}{Gm_c}\right) \tag{6.2}$$

where R_p is the radius of the planet, m is the mass of the planet, m_c is the mass of the star and r is the distance to the star at the final close encounter. If $\theta \gg 1$ the planets are massive enough to eject each other while if $\theta < 1$ collisions will be more frequent (for further discussion see Section 9).

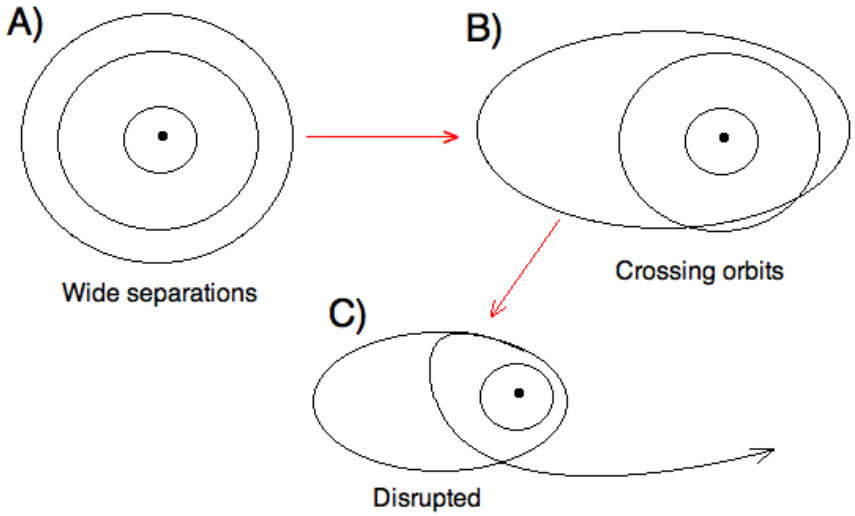

Figure 6.1: Evolutionary stages of a multiple-planets system. A) System with non-crossing orbits. B) System with crossing orbits and/or close encounters. C) Disrupted system. A planet is ejected, two planets collide or a planet collides with the star.

There are several ways multiple-planet systems can move between the stages in Figure 6.1. In the following three sections I describe three different mechanisms: planet-planet interactions, fly-by stars and the Kozai mechanism.

6.2 Planet-planet interactions

This is the mechanism that made the systems in Section 5 unstable. The systems initially have orbits with small eccentricities and low mutual inclinations, i.e. they start out in stage A. However, as time goes by the secular oscillations due to planet-planet interactions described in Section 3 change the orbits. This can then lead to even larger planet-planet interactions and if the interactions are large enough they can lead to crossing orbits and close encounters, the system has moved from stage A to stage B. This happens on a timescale $\tau \propto \Delta^B$ where $B \sim 32$ for three, equally separated, Jupiter-mass planets (Section 5). I find lower values of B for planets of lower mass in Section 9 which is described in that section. After the first close encounter the system continues to have close encounters ($\sim 500 - 600$) and the system eventually moves from stage B to stage C (this happens to all systems that reach stage B). The timescale for this is independent of the initial separation, $\tau = const \sim 10^{5\pm1}$ yr. I get a different value for this time for low-mass planets in Section 9 which I describe in that section. What has happened in the time between the first close encounter and the ejection of a planet is that through multiple close encounter the system has been heated and the semi-major axis of one planet has increased in small steps. For this mechanism to work on reasonable timescales you need planets on relatively tight orbits and close to each other (Eq. (5.2)). The first phase (stage A to stage B) has previously been investigated analytically by Quillen (2011) and numerically by e.g. Chambers et al. (1996). Chambers et al. (1996) find an exponential relationship between the close encounter time and initial separation in mutual Hill radii. Quillen (2011) investigate the time it takes for a system to get in a three-body resonance

$$pn_1 - (p+q)n_2 + qn_3 \sim 0 \tag{6.3}$$

where p and q are integers and n_i ($i = 1, 2, 3$) are the mean motions of the planets. Compare to Eq. (2.11) for the difference between two- and three-body resonances. If you have systems in resonance the Analytic approximations made in Section 3 are no longer valid and the time to get a first close encounter can be reduced drastically (e.g. for $\Delta = 5.0$ in Figure 5.1).

6.3 Fly-by stars

Many stars resides in stellar clusters and in those clusters there is a non-negligible probability that stars get close to each other. If a star hosts a planetary system, such a close encounter would of course affect the planets as well. A star passing by a planetary system (fly-by star within $r_{min} < 1000$ AU) could change the orbital configurations of the planets and make a system go from stage A to stage B without the need of any planet-planet interactions. The timescale for this would be of the same order as the time it takes the fly-by star to pass the system, $\tau \sim 10000$ (Malmberg et al. 2011), or rather the time it takes for the fly-by star to pass the system. After the fly-by has passed, given you get crossing orbits, the system will continue to have close encounters between planets and eventually go from stage B to stage C again on a constant timescale, $\tau = const.$ This mechanism can destabilize systems with planets on wider orbits where the planet-planet interactions aren't enough. Fly-by stars are relatively common in stellar clusters and has been investigated in more detail by Malmberg et al. (2011). The effect of a fly-by star depends on how close to the planetary system it gets:

i) Close fly-by ($r_{min} \lesssim 100$ AU): Very close interactions can lead to immediate ejection/ejections of planets. You could say that the fly-by star 'steals' one or more planets.

ii) Wider fly-by ($100 < r_{min} < 1000$ AU): If the fly-by star is further away from the planetary system it cannot immediately disrupt the system, it can, however, change the orbits of the planets. One thing that can happen is that the system jumps from stage A to stage B on the fly-by timescale. If the fly-by star is even further away it may perturb the system slightly (e.g. increase eccentricities or change semi-major axes). This can increase the planet-planet interactions and shorten the close encounter timescale (the time it takes to go from stage A to stage B). In this case the fly-by star 'heats' the system. One final thing that can happen which also can lead to instability is if it changes the mutual inclinations of the planets. If the change is large enough the system could enter the Kozai threshold (see Section 6.4) leading to large oscillations in eccentricities and possibly to close encounters between planets.

6.4 Kozai mechanism

Another type of secular interaction (the timescale of the interactions is much longer than the orbital timescale) leading to oscillations in eccentricity and inclination is the Kozai mechanism. These oscillations start when the mutual inclination between two objects is $\Delta I \gtrsim 39.2°$ (Kozai 1962) and occurs because of angular momentum transfer. The two object don't necessarily have to be two planets but could be a planet and a binary companion to the host star. These oscillations are separate from the secular oscillations described in Section 3 and the two oscillations can work together (see Figure

7.4). An object in so called Kozai resonance, undergoing the oscillations, has the following conserved quantity:

$$\sqrt{1-e^2}\cos\Delta I \tag{6.4}$$

where e is the eccentricity of the orbit and ΔI is the mutual inclination. Basically you trade inclination for eccentricity. Changing the eccentricity of a planet's orbit can lead to close encounters and you go from stage A to stage B on a timescale that is different from the timescale for secular instability. Ford et al. (2000) made an approximation of the period of the oscillations:

$$P_{Kozai} \approx 2\pi\sqrt{\frac{a_1^3}{G\left(m_c+m_1\right)}}\left(\frac{m_c+m_1}{m_2}\right)\left(\frac{a_2}{a_1}\right)^3\left(1-e_2^2\right)^{3/2} \tag{6.5}$$

where subscript 2 is used for the outer body's properties. The maximum eccentricity of the inner body can also be estimated (Takeda & Rasio 2005):

$$e_{1,max} \approx \sqrt{1-\frac{5}{3}\cos^2\Delta I_0} \tag{6.6}$$

where ΔI_0 is the initial mutual inclination. The Kozai oscillations typically have larger amplitudes than the secular oscillations (at the limit $\Delta I_0 \sim 40^\circ \implies e_{1,max} \sim 0.64$, while the secular have amplitudes of order 0.1 Figure 3.8). There are two types of Kozai oscillations:

- Self-Kozai: Occurs in multiple-planet systems with planets on highly mutually inclined orbits.
- External Kozai: Occurs in planetary systems where the host star has a binary companion on a highly mutually inclined orbit.

The external Kozai oscillations usually have longer period since $P_{Kozai} \propto \frac{a_2^3}{m_2}$. The mass of a star is $m_\star \sim 1000 m_{planet}$ but typically $a_{binary} > 10 a_{planet}$. To do an estimation of the period of self-Kozai we can use the initial conditions in Section 3.4.4: $m_1 = m_2 = 1$ M_{Jup}, $a_1 = 2$ AU, $a_2 = 5$ AU. This results in a period: $P_{Kozai,self} \sim 22$ kyr. If we, on the other hand, estimate the period for external Kozai oscillations we can set the initial conditions to: $m_2 = 1$ $M_\odot$, $a_2 = 100$ AU and end up with $P_{Kozai,ext} \sim 175$ kyr. As we can see the values are a bit different which affects how fast you go from stage A to stage B. We can also compare it to the periods of the secular oscillations: $P_{e,sec} \sim 30$ kyr and $P_{I,sec} \sim 55$ kyr (Figure 3.14). I have found that even if you start out with a multiple-planet system that are not in the Kozai regime (i.e. $\Delta I_0 < 39.2^\circ$) secular oscillations can increase the mutual inclination of two planets so that it gets large enough for Kozai oscillations to start.

My conclusion is that if the mutual inclination of two objects (two planets or a planet and a binary companion) is large enough Kozai oscillation can take a multiple-planet system from stage A to stage B on a different timescale than the secular timescale. After the first close encounter between planets you go from stage B to to stage C on a constant timescale ($\tau = const$) if it is self-Kozai while if it is external Kozai the binary companion still can affect the evolution of the planetary system.

7 The observed multiple-planet systems

7.1 Observation methods

Exoplanets can be detected in several ways. You can either measure the effect the planets have on their host stars (indirect methods) or measure the light coming directly from the planet itself (direct methods). The main methods are

- **Radial velocity measurements:** Even if a planet is much smaller than its host star the star will still be affected by the planet and they will both orbit around their common center of mass. The motion of the star will doppler shift the light and this can be measured from the Earth if the orbital plane is not perpendicular to the line-of-sight. The velocity of the star will vary periodically and from the period you can get the semi-major axis of the planet's orbit through Kepler's third equation (Eq. (A.19)). The shape of the velocity curve can also give you the eccentricity of the orbit. The more inclined the orbit is to the line-of-sight the smaller the effect of the planet on the star and you can only measure the minimum mass of the planet, $m \sin i$ (**N.B.** i is the angle between the normal of the orbit and the line-of-sight, i.e. not the same as previously used inclination I which is the angle between the normal of the orbit and an arbitrary reference plane). This method gives a large bias to massive planets close to the star because they affect the star more than small planets far away. The periods of planets close to the star is also smaller so it takes shorter time to complete an orbit.

- **Planet transits:** If the line-of-sight lies in the orbital plane of the planet at some point the planet will pass in front of the star and hence block some of the star's light. This can be observed and gives the radius of the planet if you know the radius of the star. From models you can then get the mass of the planet. From the period of these transits you get the semi-major axis of the orbit. With this method it is easier to detect smaller planets compared to radial velocity measurements.

- **Direct imaging:** Planets are much fainter than their host stars but if an exoplanet is massive enough and far away from the star you can sometimes measure light coming directly from it. This method has a large bias to large, massive planets far away from their star. One example of a multiple-system that has been observed with this method is HR 8799 (see Figure 7.1).

- **μ-lensing:** If a star passes in front of a background light source it will gravitationally lens the background light source making it look brighter. If the star has a planet you can get an extra 'bump' in the light curve caused by the planet. Using this method you are capable of detecting Earth-like planets, however, the measurements are not repeatable since the star only passes in front of the light source once.

- **Astrometry:** As mentioned in the radial velocity method the star moves because of the planet. With precise astrometric measurements of the position of the host star this motion can be detected.

When it comes to naming the planets the convention is that the name of a planet is the name of the host star plus one lowercase letter. The first planet detected around a star gets the letter 'b', the second detected planet gets 'c', the third 'd', and so on.

For example the star HD 125612 has three planets: HD 125612b, HD 125612c and HD 125612d.

7.2 The observed systems

As mentioned before, some multiple exoplanet-systems have been observed (data from exoplanet database `exoplanet.eu`, Schneider et al. (2011))

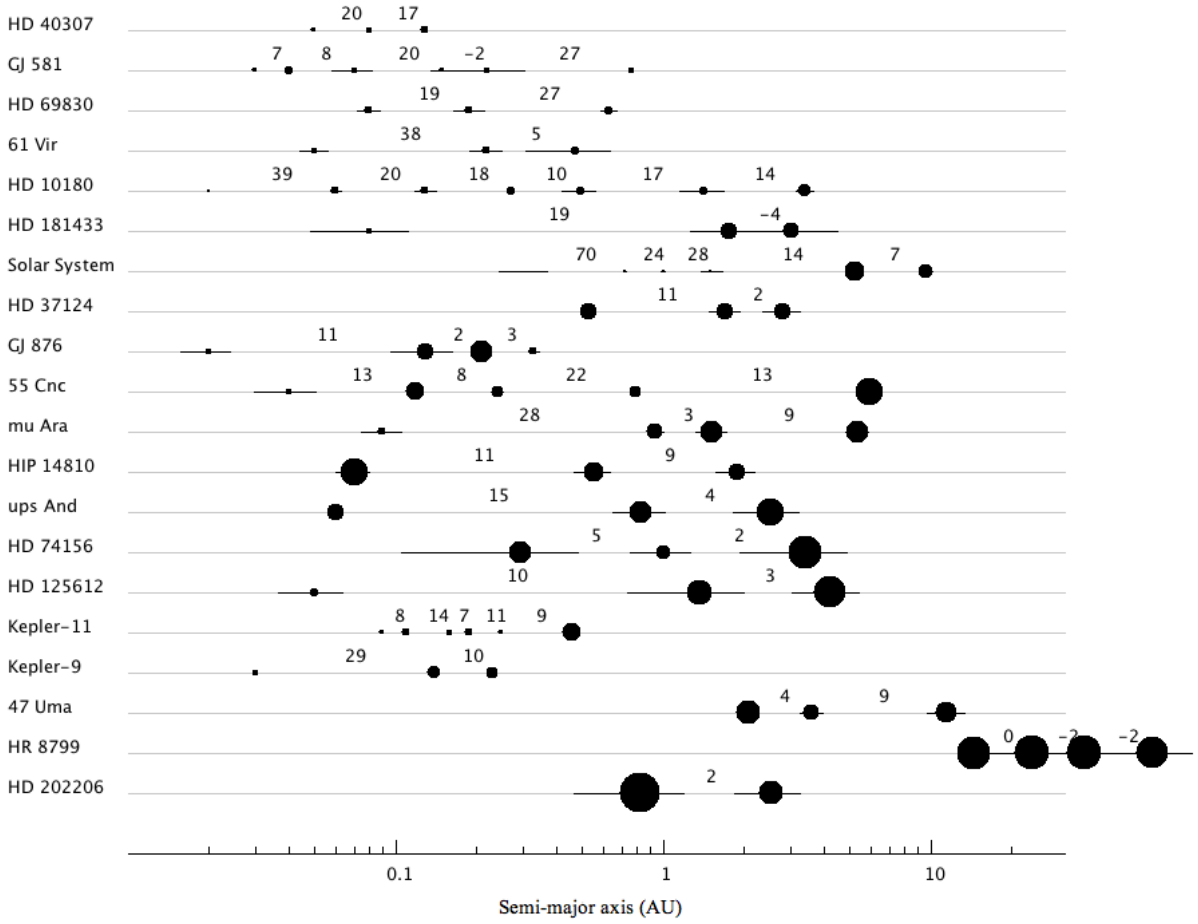

Figure 7.1: Plot of all observed multiple-planet systems. The name of the star is in the column to the left. The dots are the planets, the size of a dot is proportional to $m^{1/4}$, the position on the thin line is the semi-major axis, the thicker line going through each dot shows the extent of the orbit (periapsis and apoapsis distances) and the value above the line between two planets is the separation between the planets in units of mutual Hill radii Eq. (2.10). I have made this figure myself but used the same format as in Figure 13 in Lovis et al. (2011). These kind of plots will henceforth be called Lovis plots.

In Figure 7.1 we have the name of the star in the column to the left. The dots are the planets, the sizes of the dots represent the mass (**N.B.** minimum mass since most systems are observed with radial velocity measurements) of the planets ($\propto m^{1/4}$), the positions of the planets on the thin lines shows the semi-major axes, the slightly thickened lines shows the extent of the orbits (periapsis and apoapsis) and the value above the line between two planets is the separation between the planets ($r_{per,2} - r_{apo,1}$) in units of mutual Hill radii Eq. (2.10).

We know that these planetary systems, with their configurations, have to be stable since they are observed. If they had been born to become unstable they would already have been destroyed since the age of the stars are larger than instability timescales (see Section 6). The age of of e.g. HD 37124 is $\sim$ 3.33 Gyr (Saffe et al. 2005) and the age of HD 74156 is $\sim$ 3.7 Gyr (Meschiari et al. 2011). I have selected a few of these systems which I find dynamically interesting systems:

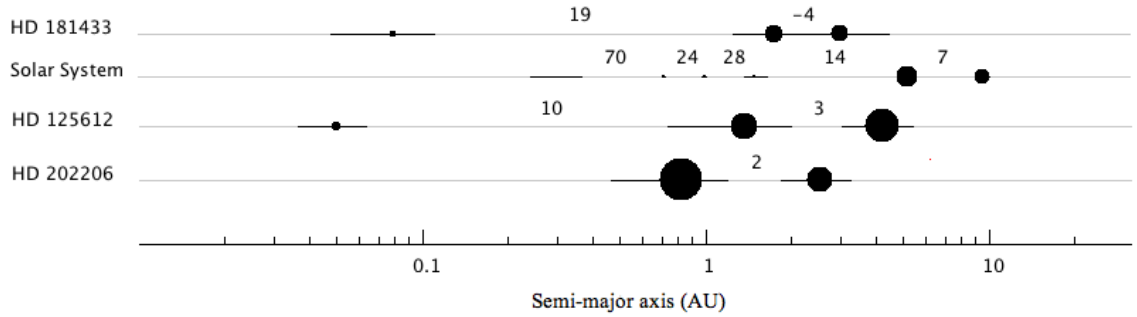

Figure 7.2: Lovis plot (see Figure 7.1) of dynamically interesting multiple-planet systems.

The common denominator of these systems (except the Solar System) is that they have massive planets close to each other. In the case of HD 181433 two of the planets even have crossing orbits (see Section 7.3.2 for further discussion). I include the Solar System as well since it is a multiple-planet system, it has known secular oscillations and the data for it is much more accurate than for any other multiple-planet system.

7.3 Simulations

To investigate the stability of the dynamically interesting multiple-planet systems in Figure 7.2 I make N-body simulations using `MERCURY6` (see Section 4.1). For the simulations and results I present in this section I have taken the initial conditions from the exoplanet database `exoplanet.eu` (Schneider et al. 2011) except when it comes to the Solar System where I take the data from the `MERCURY6`-package (Chambers 1999). Note that the masses given are the minimum masses since most planetary systems are observed with radial velocity measurements. However, when I run simulations and put the planets on inclined orbits I adjust the mass with a factor $\frac{1}{\sin i}$ where i is the angle between the normal of the orbit and the line-of-sight to the star.

7.3.1 The Solar System

The Solar System has known secular oscillations for Jupiter and Saturn (see Sections 3.2 and 3.3). I have already shown that `MERCURY6` really gives you those secular oscillations. Here I test the Kozai-mechanism discussed in Section 6.4, i.e. oscillations in eccentricity and inclination when the mutual inclination of two orbits is large enough ($> 39.2°$). I first test external Kozai by adding a binary companion to the Sun (it is then not really an observed system but I investigate it in this section in any case). I set the mass of that companion to $m_{c,2} = 0.5$ M$_\odot$ put it in an orbit with semi-major axis $a_{c,2} = 300$ AU, eccentricity $e_{c,2} = 0$ and inclination to the ecliptic $I_{c,2} = 45°$. To make the simulations

run faster I only include the giant planets. From the results shown in Figures 7.3 and 7.4 the eccentricities are sometimes larger than 0.7 and the inclinations are sometimes over 90°.

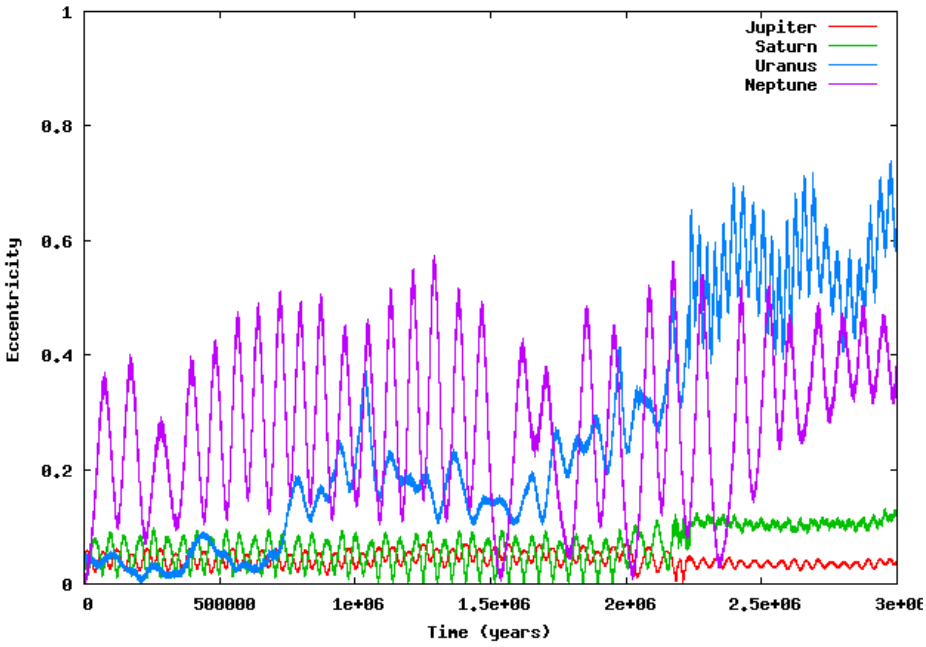

Figure 7.3: Eccentricity oscillations for the giant planets in the Solar System with a 0.5 $M_{\odot}$ binary companion to the Sun on an inclined orbit to test the Kozai mechanism.

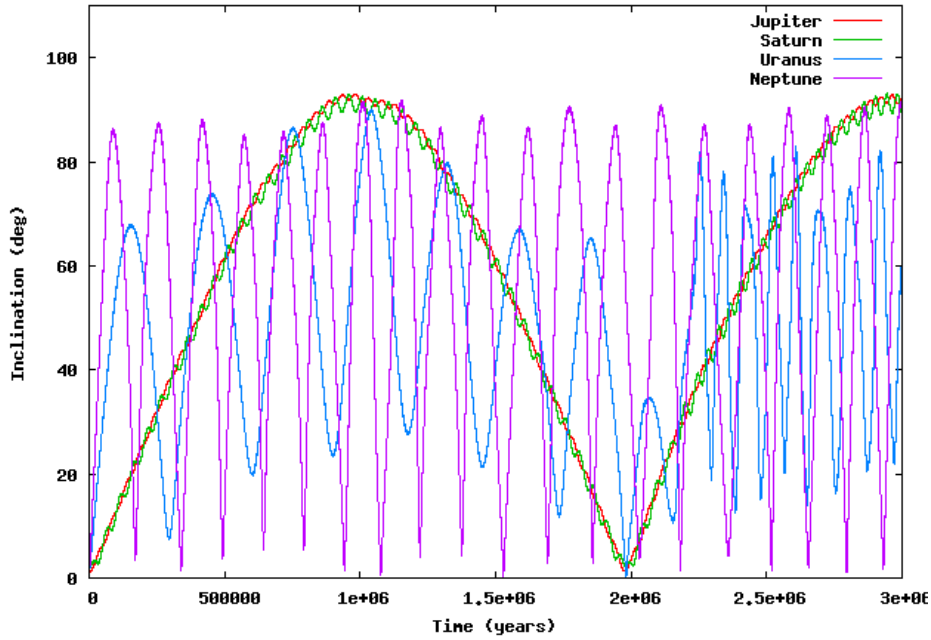

Figure 7.4: Inclination oscillations for the giant planets in the Solar System with a 0.5 $M_\odot$ binary companion to the Sun on an inclined orbit to test the Kozai mechanism.

What we see in Figure 7.4 is that Jupiter, Uranus and Neptune has regular, large amplitude, Kozai oscillations. However, the period of the inclination oscillations of Saturn has the same period as Jupiter's oscillations which is odd since it has a different semi-major axis. The explanation for this is that Saturn is less massive than Jupiter and ends up following Jupiter on its oscillations. We can also see that Jupiter and Saturn also has short period, small amplitude, oscillations which are the secular oscillations described in Section 3. My conclusion is that the external Kozai mechanism works and you get it from `MERCURY6` simulations. If I increase the mass of the binary companion to $m_{c,2} = 0.6$ $M_\odot$ the Solar System becomes disrupted within 2.5 Myr and both Uranus and Neptune are ejected in 4 Myr.

The Solar System has many planets and there are a lot of planet-planet interactions. However, it is also very stable:

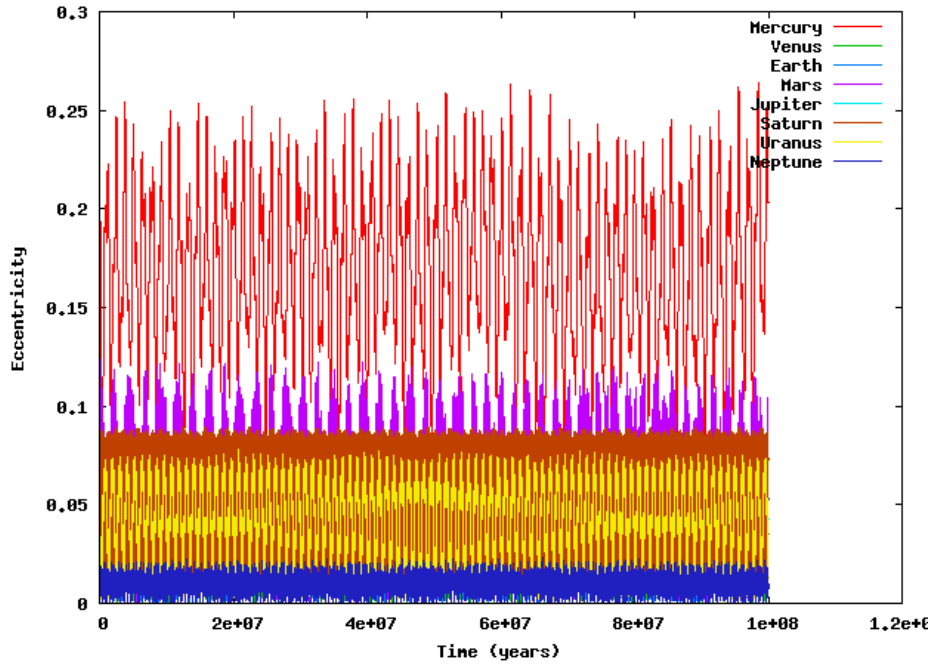

Figure 7.5: Eccentricity oscillations for all planets in the Solar System for 100 Myr.

Figure 7.5 shows the eccentricity evolution for all planets in the Solar System for 100 Myr. It is a messy plot since it shows the eccentricity for all planets but we can see it is stable and the eccentricities are less then 0.3 for all planets at all times.

7.3.2 HD 181433

The star HD 181433 is a Sun-like star ($m_c \sim 0.8$ $M_\odot$ (Bouchy et al. 2009)) and has three planets. Two of the planets are Jupiter-sized ($m_c \sin i_c = 0.64$ M_{Jup} and $m_d \sin i_d = 0.54$ M_{Jup}) at Mars-like distances ($a_c \sim 1.8$ AU, $a_d \sim 3$ AU) and the last planet is smaller ($m_b \sin i_b \sim 8$ $M_\oplus$) and closer to the star ($a_b \sim 0.08$ AU). If we look in Figure 7.2 planet c and d have crossing orbits. This means that it already is at stage B in Figure 6.1 and should end up unstable with the arguments made in section Section 6.1. Simulations that I have made show that it is a very unstable system (planets are ejected within a few 100 kyr). I have also seen that even coplanar versions of the system are unstable. It is always the lower mass planet (planet d) that is ejected. I find three possible explanations for the fact that this system is observed:

- It is a very lucky find. Planetary systems that reach stage B in Figure 6.1 stay in that stage before a planet is ejected for a few 100 kyr (Figure 5.3).
- The system could be stable because of a MMR (like the Galilean satellites of Jupiter). The mean motion ratio of planets c and d is $\frac{n_c}{n_d} \sim 2.23 \sim \frac{9}{4}$.
- There could be more, undiscovered, planets in the system. Those planet could make it look like there are two planets with eccentric, crossing orbits when there in fact are more planets on more circular orbits.

7.3.3 HD 125612

HD 125612 is a Sun-like star ($m_c \sim 1.1$ $M_\odot$ (Fischer et al. 2007)) with three planets. Two of the planets are more massive than Jupiter ($m_b \sin i_b \sim 3$ M_{Jup} and $m_d \sin i_d \sim 7$ M_{Jup}) with semi-major axes between Earth and Jupiter ($a_b \sim 1.4$ AU and $a_d \sim 4.2$ AU). The third planet is less massive ($m_c \sin i_c \sim 20$ $M_\oplus$) and has a period of only four days (corresponds to a semi-major axis of $a_c \sim 0.05$ AU). The reason I chose this system is because I have found no stability analysis of it and it has massive planets close to each other. The first thing we can say is that it is very sensitive to the choice of time step since the period of the inner planet is only ~ 4 days.

I have used this system to test the self-Kozai mechanism described in Section 6.4. I have investigated at which mutual inclination the Kozai oscillations. What I found is that I get new kinds of oscillations (i.e. not just the secular oscillations) already at initial mutual inclinations that are smaller than the Kozai limit (at $\Delta I_0 \sim 20°$ rather than at $\Delta I_0 \sim 40°$) The reason for this is that the secular oscillations changes the mutual inclination over time and can make it cross the limit. Here I show such a situation. The first plot is the results from a simulation where I put planets b and d on orbits with an initial mutual inclination of a few degrees ($\Delta I = 5°$, non-Kozai regime) and I get the following evolution in eccentricity

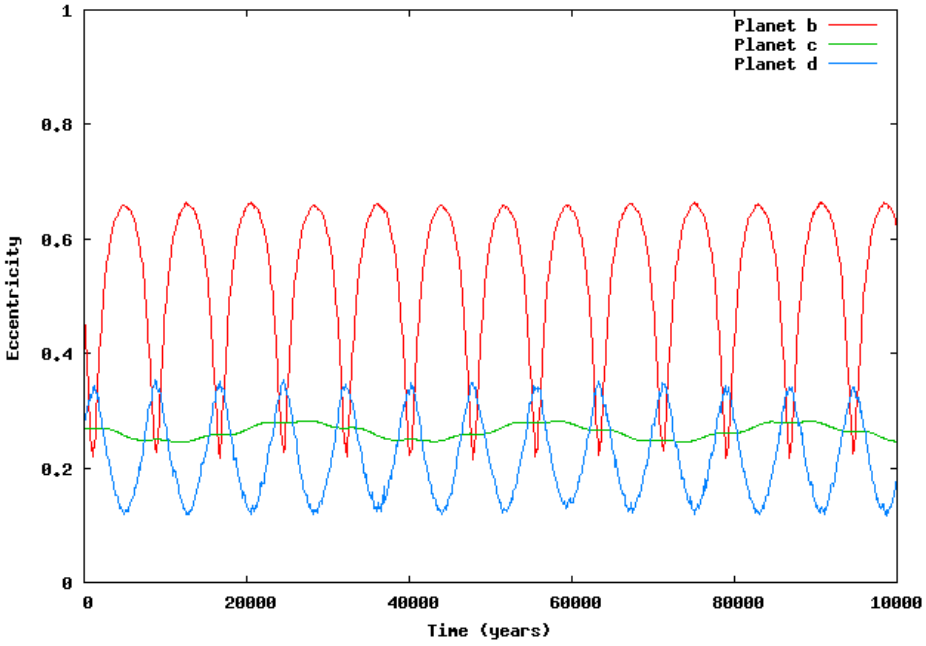

Figure 7.6: Eccentricity oscillations for HD 125612 b, c and d. Planets b and d have an initial mutual inclination of 5°.

As we can see we get nice, stable, secular oscillations like in the Solar System. The mutual inclination of the orbits of planets b and c is never larger than 10°. Next I run a simulation where I set the initial mutual inclination to $\Delta I = 20°$, i.e. still smaller than the Kozai limit ($\Delta I_{min} \sim 39.2°$) but as the system evolves it crosses the limit at some point. I plot the eccentricity evolution in Figure 7.7:

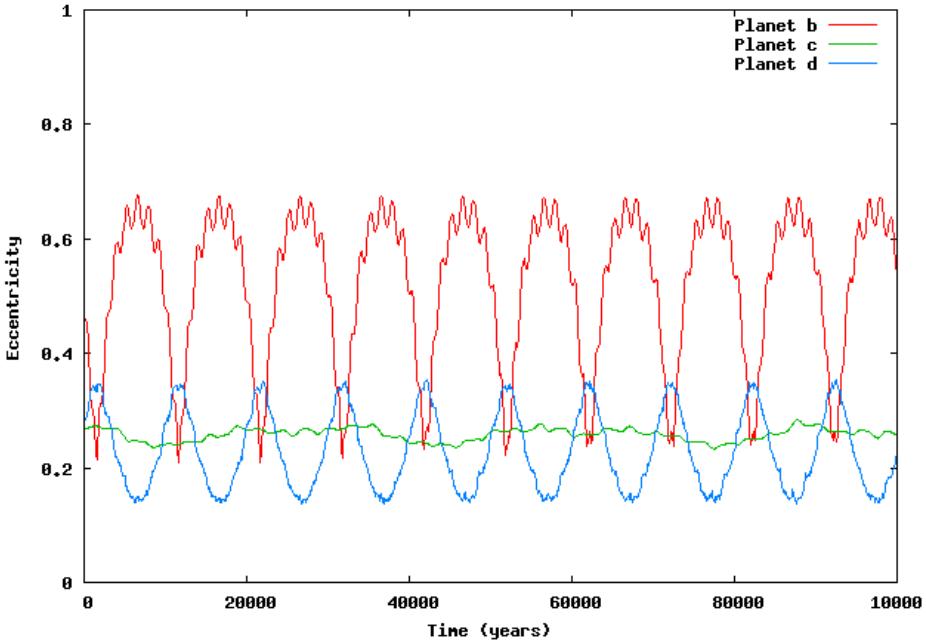

Figure 7.7: Eccentricity oscillations for HD 125612 b, c and d. Planets b and d have an initial mutual inclination of 50°.

If we compare Figure 7.7 to Figure 7.6 the system is still stable but we get two kinds of oscillations in the simulation with 20° mutual inclination: short period self-Kozai oscillations (best seen when planet b has large eccentricity) and long period secular oscillations. We see that the self-Kozai oscillations has shorter period than the secular oscillations while the external Kozai has longer period (Figure 7.4). The reason for this we can find in Kozai period's dependence on semi-major axis and mass of the outer body, Eq. (6.5).

One idea I had was that maybe you can treat HD 125612 as a two-planet system. After all $m_c \ll m_b, m_d$. The advantage of this would be that the period of the innermost planet would be 336.6 days instead of 4.15 days and also you only have to integrate two planets instead of three. However, from the 20 simulations I made to investigate this I found that the evolution of the orbits of the two massive planets changes if planet c is removed. For the simulations I have made I have found that the integrator has problem with energy conservation. This could be because, even though it is less massive, planet c carries a significant part of the total binding energy of the system.

The stability analysis I have done for this system I have mainly looked at the effect of Kozai oscillations and the effect of the inner planet. I look at systems both where I use the minimum mass for the planets and systems where I adjust the mass because of the inclination.

I have run 40 simulations where I vary the inclination of the outer planet (planet d) between 5° and 100°. I find that if the mutual inclination of planet b and d is $\geq 50°$ the system is unstable and planet b is ejected and/or planet c collides with the star. This is true for both systems where I use the minimum mass of the planets and systems where the mass has been adjusted.

For the above simulations I only ran one simulation per inclination. After that I

chose one value of the inclination ($I_d = 45°$) and ran 20 more simulations. The difference between the simulations is the initial positions of the planets in their orbits (explained in Section 4.2). From my results I find that 8 out of 20 simulations are unstable within 10 Myr and planet b is ejected and/or planet c collides with the star. My conclusion is then that even if this system has quite large planet-planet interactions there are definitely orbital configurations that makes i stable for a long time.

The final thing I did with this planetary system was to compare two of the integrators described in Section 4.1, namely the Hybrid symplectic and the Bulirsch-Stoer. I make 20 sets of initial conditions (again different initial positions of the planets in their orbits) and run the systems with both integrators. I find that the outcome of a system can vary depending on which integrator I use. Most importantly some systems are stable for one integrator and unstable with the other. I trust the Bulirsch-Stoer most since it has a variable size of the time step. The Hybrid symplectic integrator also has problem with conserving energy mainly because of the fact that planet c is so close to the star.

7.3.4 HD 202206

HD 202206 is also a Sun-like star ($m_c \sim 1.13$ $M_\odot$). It has two planets that are more massive than Jupiter ($m_b \sin i_b = 17.4$ M_{Jup} and $m_c \sin i_c = 2.44$ M_{Jup}). The planets have semi-major axes of $a_b = 0.83$ AU and $a_c = 2.55$ AU.

I started off by comparing the two integrators with the same approach as for the HD 125612 system. I have run 20 simulations (10 for each integrator) with a mutual inclination of 45°. I find that all these simulations are unstable and planet c is ejected within 2 Myr. Clearly the mutual inclination is too high so I run more simulations with lower inclination. When I run 20 simulations with a mutual inclination of 2° I find that 16 of them are unstable and eject planet c within 250 kyr. For two of the sets of initial positions the system is stable for at least 100 Myr (same initial conditions for both integrators). My conclusion is that the initial positions of the planets in their orbit are important (already discussed in Section 4.2). These are the results for two simulations with a mutual inclination of $\Delta I = 2°$ where the only difference in initial conditions between the two simulations is the initial position of planet c (it has been moved one tenth of an orbit in its orbit)

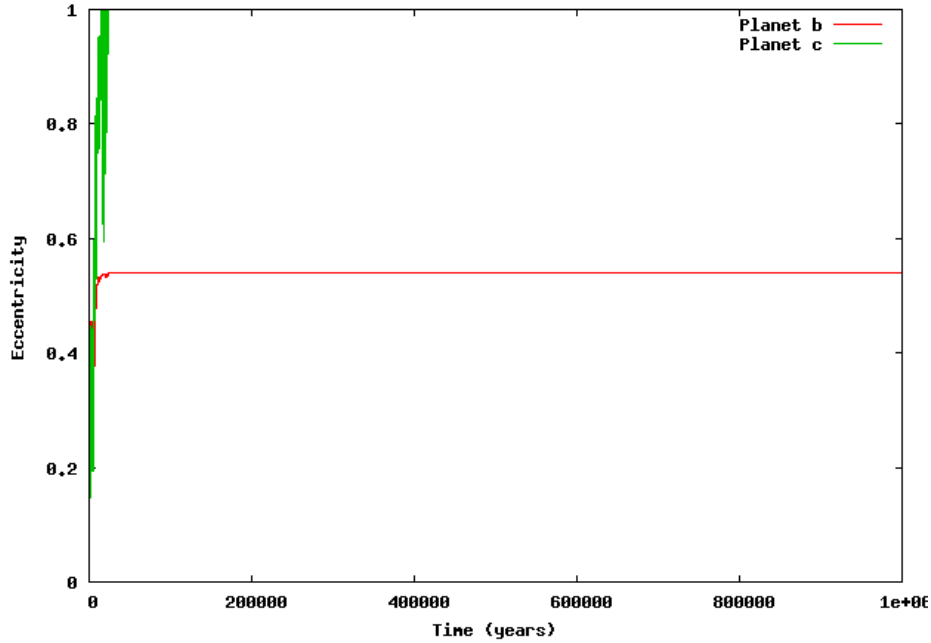

Figure 7.8: Eccentricity oscillations for planetary system HD 202206. Mutual inclination of 2°. The planetary system is unstable and planet c is ejected from the system within 100 kyr.

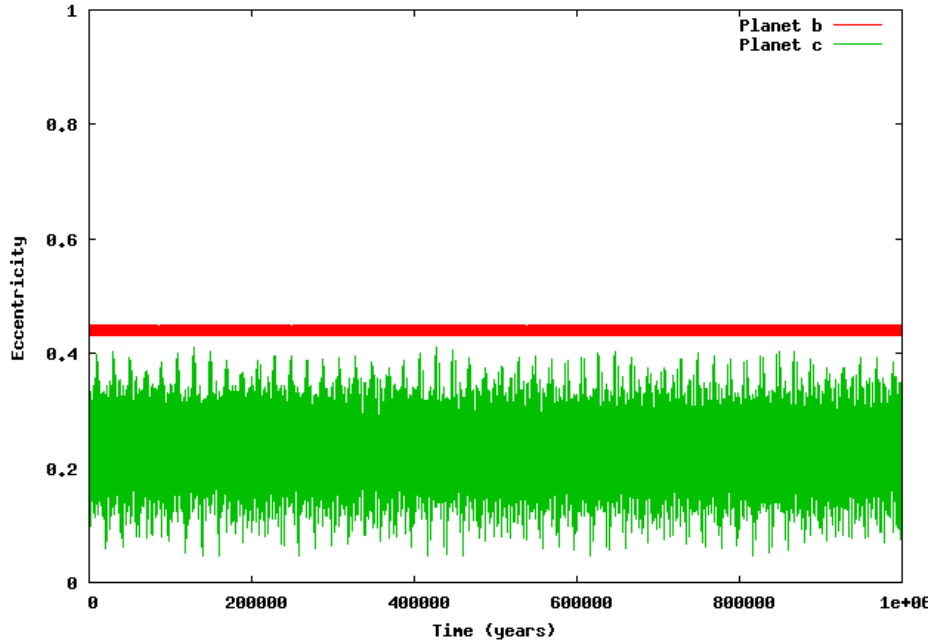

Figure 7.9: Eccentricity oscillations for planetary system HD 202206. Mutual inclination of 2°. In this simulation the planetary system is stable for more than 100 Myr.

As we can see if we compare Figures 7.8 and 7.9 the outcome is very different. In the first simulation planet c is ejected within 100 kyr while the other simulation is stable

for at least 100 Myr (only first 1 Myr is shown in the figure). This is a typical example of a chaotic system where small changes in initial conditions lead to large differences in outcome. The reason that the difference can be so large is because it is discrete events (close encounters) that eject one of the planets. The planets are further away from the star than for the HD 125612-system so the integrator doesn't have the same problems with size of time step and energy conservation.

7.4 Conclusions

My conclusions made from my simulations of the observed multiple-planet systems are:

- The Solar System
  - By running N-body simulations of the Solar System I confirm that it undergoes secular oscillations described in Section 3.
  - If I put the Solar System in a binary where the orbital plane of the binary is very inclined to the orbits of the planets ($\Delta I_0 > 39.2°$, Kozai (1962)) I get external Kozai oscillations (Section 6.4).
  - Even if the Solar System has many planets it is very stable.
- HD 181433:
  - HD 181433 has planets on crossing orbits so it should eventually become unstable within a few 100 kyr (see Section 5). This means that it is either a lucky find, that it is stable because of some resonance or that it has some undiscovered planets that stabilizes the system. The two planets with crossing orbits are relatively close to a 9:4 MMR.
- HD 125612:
  - The HD 125612 system is very sensitive to the choice of time step. This, I think, is because the inner planet is very close to the star with a period of only 4 days. I need to have a time step of less than $\sim \frac{1}{40}$ before the system becomes insensitive to changes of the initial position of the inner planet.
  - If I have some mutual inclination between planet b and d I get Jupiter-Saturn like secular oscillation in inclination and eccentricity.
  - When the initial mutual inclination of planet b and d reaches $\sim 40° - 45°$ I get new kinds of oscillations beside the secular oscillations. These are self-Kozai oscillations (Section 6.4), which theoretically should start when $\Delta I_0 > 39.2°$ (Kozai 1962).
  - For even larger mutual inclinations the system becomes unstable within 1 Myr and sometimes the planets become retrograde.
  - If a system is unstable planet c more often collides with the star than is ejected while planet b is more often ejected. This is probably due to the fact that planet c is really close to the star while planet b is further away.
  - With a planet with such small period I'm starting to get worried that you need to take relativistic effects into account which I haven't done since it's not included in the `MERCURY6`-code.

  - If you treat the system as a two-planet system by removing the inner, low-mass planet (planet c) you get a different evolution of the system compared to when you keep it.

- HD 202206:

  - The initial positions of the planets in their orbits are important for the stability of the system. It is a typical example of a chaotic system: small changes in initial conditions leads to large differences in the outcome.

    The planets in this system are further away from the star than the planets around HD 125612 so the integrators have less problem with the conservation of energy.

- General planetary system conclusions:

  - With radial velocity measurements of stars we can only find the minimum mass of the planet we need to adjust the mass of a planet if it's orbit happens to be inclined. This adjustment is done by multiplying the minimum mass with a factor of $\frac{1}{\sin i}$ where i is the angle between the line-of-sight and the normal of the planet's orbit.
  - Fusion of deuterium starts at $\sim 13 M_{jup}$ and then it's no longer a planet. This puts a limit on how inclined a planet can be before it becomes a brown dwarf. For planet HD 125612d the limit is $\sim 60°$.
  - If a multiple-planet system ejects a planet it is always the most massive planet that survives.
  - From my simulations I can see that the timescale for the Kozai mechanism is different compared to the timescale for secular oscillations depending on if the outer body is a planet or a binary star. From Ford et al. (2000) we have the period of the oscillations $P \propto m_2^{-1} a_2^3$ where m_2 and a_2 is the mass and the semi-major axis of the outer body. This means that a system could become unstable because of one of the mechanisms before the other has time to change anything.
  - If the initial mutual inclination of two planets is larger than $\sim 39.2°$ the Kozai mechanism kicks in and you get oscillations in eccentricity and inclination.
  - For a system with two planets the Kozai mechanism can make the orbits of the two planets cross. If the orientation of the orbits are random the fraction, η, of orbits that cross can be approximated analytically as a function of the ratio of the semi-major axes of the orbits, $\alpha = \frac{a_1}{a_2} < 1$:

$$\eta(\alpha) \approx \sqrt{\frac{3}{5}\alpha\,(2-\alpha)} \tag{7.1}$$

8 Three-planet systems with unequal separations, $\Delta_{12} \neq \Delta_{23}$

In Section 5 I looked at three-planet systems with equal separations, $\Delta_{12} = \Delta_{23}$. Here I extend that investigation and allow $\Delta_{12} \neq \Delta_{23}$. I do this since it becomes more realistic and can be more easily compared to the observed multiple-planet systems.

8.1 Simulation setup

As in Section 5 I have a large parameter space, especially since I allow different separations between the planets. The simplifications I make are:

- Equal-mass planets (1 M_{Jup}).
- Aligned orbits ($\varpi_1 = \varpi_2 = \varpi_3$ and $\Omega_1 = \Omega_2 = \Omega_3$).
- Small, non-zero, eccentricities ($e_1 = 0.01$, $e_2 = 0.02$ and $e_3 = 0.015$) and inclinations ($I_1 = 0°$, $I_2 = 1.5°$ and $I_3 = 3.0°$).

i.e. the same simplifications as in Section 5 except I have removed the criterion of equal separations.

I pick seven values of Δ (3.9, 4.1, 4.25, 4.5, 4.75, 5.1, 5.25) and look at all 49 possible Δ_{12}-Δ_{23}-combinations. The reason I avoid some values of Δ (e.g. 4.0 and 5.0) is because those systems are close to MMRs which makes them unstable on shorter timescales. I make 30 simulations per combination where the difference in initial conditions between simulations are the initial positions of the outer two planets. With this approach I can use some of my results from Section 5. I run each system until a planet gets ejected or for a maximum of 500 Myr.

Most of the observed three-planet systems (see Figure 7.1) are far from my grid. Either they have larger values on Δ_{12} and Δ_{23} (e.g. HD 40307, HD 69830) or they have Δ_{12} and Δ_{23} that more different than in my grid (e.g. HD 181433, HD 37124). Of the observed systems HD 74156 and 47 UMa are closest to my grid. Other differences are that the observed three-planet systems often have planets with more eccentric orbits, different masses, different distance from star and orbits that are not aligned. This experiment is more to further investigate the dependence of planet separation than to investigate the stability of the actual observed systems. Even if that is the case I get results that can be applied to the observed systems.

8.2 Close encounter timescale

I am again interested in the close encounter timescale $\tau_{CE}(\Delta_{12}, \Delta_{23})$, i.e. the time it takes for two planets to get within one mutual Hill radius (Eq. (2.10)) of each other. As we saw in Section 5 a close encounter eventually leads to the ejection of a planet. I have made two models to estimate the close encounter timescale: The Spine-and-Ribs model and the Minimum-Δ model.

8.2.1 Spine-and-Ribs model

The first model I have developed I call the Spine-and-Ribs model. Its main feature is that you split $\tau_{CE}(\Delta_{12}, \Delta_{23})$ into two parts:

$$\tau_{CE}(\Delta_{12}, \Delta_{23}) = \tau_{CE,eq}(\bar{\Delta}) \cdot f(\varepsilon) \tag{8.1}$$

where $\tau_{CE,eq}$ is the best-fit function for equal separations, Eq. (5.2). $\bar{\Delta} = \frac{\Delta_{12}+\Delta_{23}}{2}$ is the average value of the two separations and $\Delta_{12} = \Delta_{23} = \bar{\Delta}$ is the point on the $\Delta_{12} = \Delta_{23}$-'spine' closest to the actual combination (see Figure 8.1). ε is the perpendicular distance (the 'rib') from $(\bar{\Delta}, \bar{\Delta})$ on the spine to $(\Delta_{12}, \Delta_{23})$ (see Figure 8.1). By definition I set $\varepsilon < 0$ if $\Delta_{12} > \Delta_{23}$, i.e. below the spine. $f(\varepsilon)$ is what I call the rib-function which I fit to my simulations (the median values of the close encounter time).

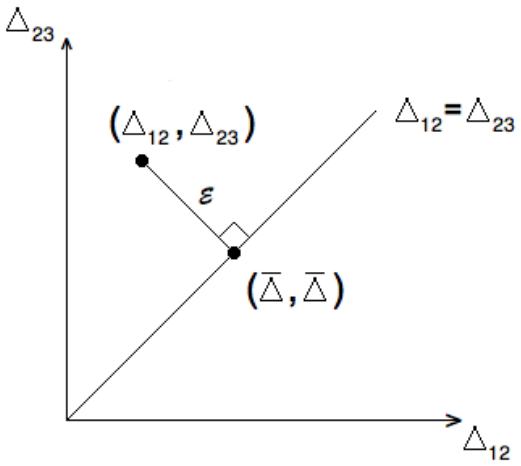

Figure 8.1: Figure showing the $\Delta_{12} = \Delta_{23}$-spine and the ε-rib for the spine-and-ribs approach of the unequal Δ simulations. $\bar{\Delta}$ is the average of Δ_{12} and Δ_{23}.

I run my simulations and find the median values of τ_{CE} for all combinations of Δ_{12} and Δ_{23}. From that I calculate the value on the rib-function, $f(\varepsilon)$, using Eq. (8.1) and Eq. (5.2) and plot it versus the absolute value of ε ($|\varepsilon|$):

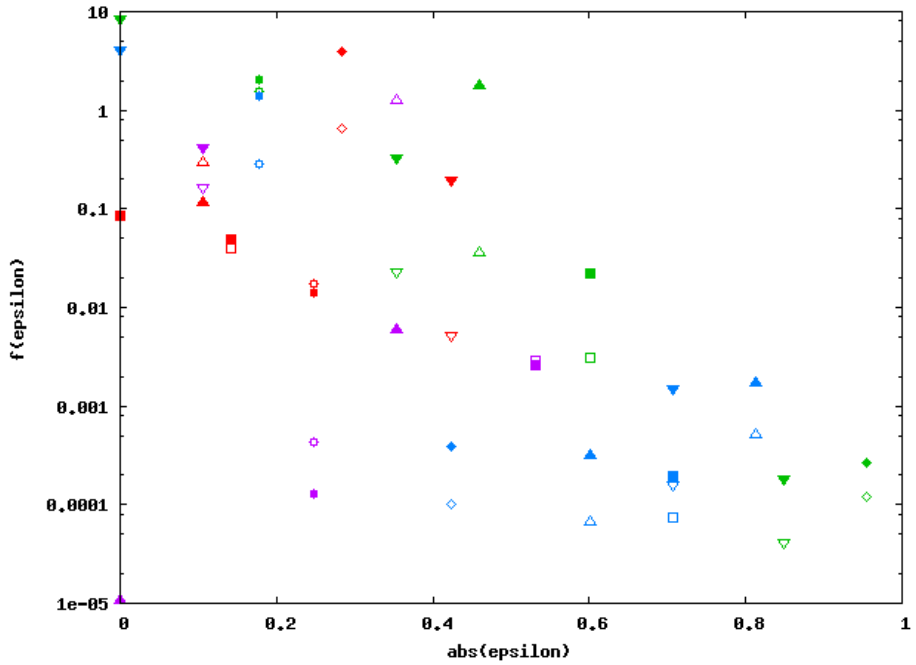

Figure 8.2: Values on the rib-function, $f(\varepsilon)$ as a function of the absolute value of ε for all simulations. Different shapes and colours distinguish different simulations. Filled symbols show simulations with $\varepsilon < 0$ and open symbols show simulations with $\varepsilon > 0$. If the results for certain $\Delta_{12} - \Delta_{23}$-combination is shown with a filled symbol of some colour, the $\Delta_{12} - \Delta_{23}$-combination with exchanged values on Δ_{12} and Δ_{23} is then shown with the same symbol of the same colour but open.

Figure 8.2 shows something that could be a systematic effect. In 16 out of 21 pairs of same two values on Δ the combination with $\Delta_{12} < \Delta_{23}$ (open symbols) has a lower value on $f(\varepsilon)$ (i.e. shorter close encounter timescale) but I have not investigated it further. Many of the simulations with smallest value on $f(\varepsilon)$ have at least one $\Delta_{ij} = 5.1$. Already in Figure 5.1 we saw that $\Delta = 5.1$ gave too low value on the close encounter time. To the data I fit three different kind of rib-functions: $f(\varepsilon) = e^{-a_1|\varepsilon|}$, $f(\varepsilon) = e^{-a_2|\varepsilon|^2}$ and $f(\varepsilon) = e^{-a_3|\varepsilon|^\alpha}$ with the free parameters a_1, a_2, a_3 and α:

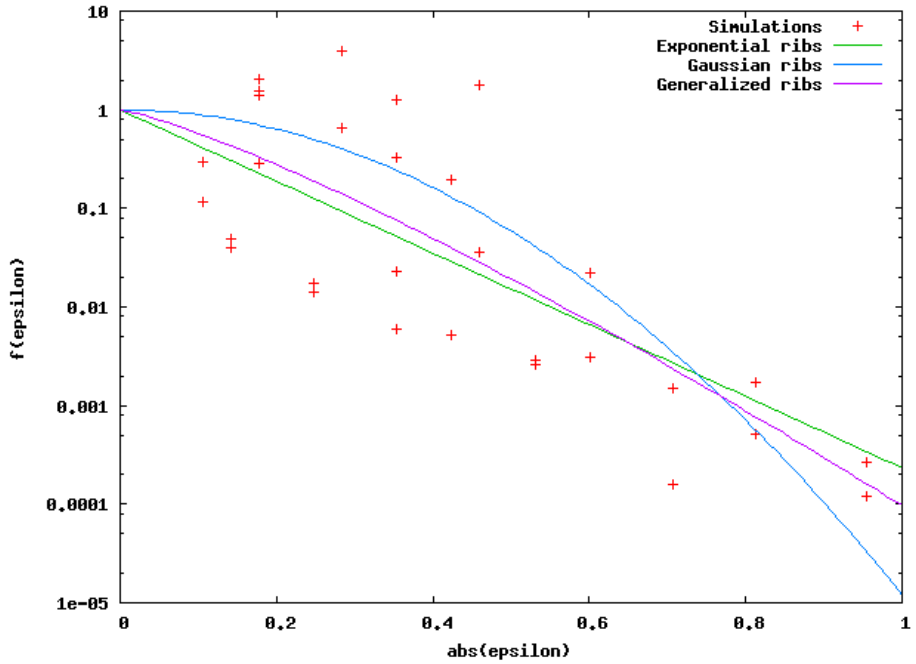

Figure 8.3: Three fits to the rib-function (see Eq. (8.1)): exponential ribs (green line), gaussian ribs (blue line) and generalized ribs (purple line).

My fitted parameters are: $a_1 \sim 8.37$, $a_2 \sim 11.38$, $a_3 \sim 9.25$ and $\alpha \sim 1.23$. As we see in Figure 8.3 neither of the rib-functions fit very well so I move over to another approach. I have tried to fit other functions, $\tau_{CE}(\Delta_{12}, \Delta_{23})$, as well but these were the ones that fitted best.

8.2.2 Minimum-Δ model

My second model to fit the close encounter time to simulations with unequal separations I have called the Minimum-Δ model. The main idea is that the close encounter time, τ_{CE}, is only dependent on one of the separations: the smallest ($\min(\Delta_{12}, \Delta_{23}) = \Delta_{min}$). Intuitively this would be a very reasonable theory if there was one pair of planets that dominated the interactions. However, as we saw in Section 5.4 a three-planet system with equal separations was heated democratically. Does this change in the case of unequal separations and become hierarchical? I plot τ_{CE} in Δ_{12}-Δ_{23}-space as a square where the size of the square is $\propto \log \tau_{CE}$:

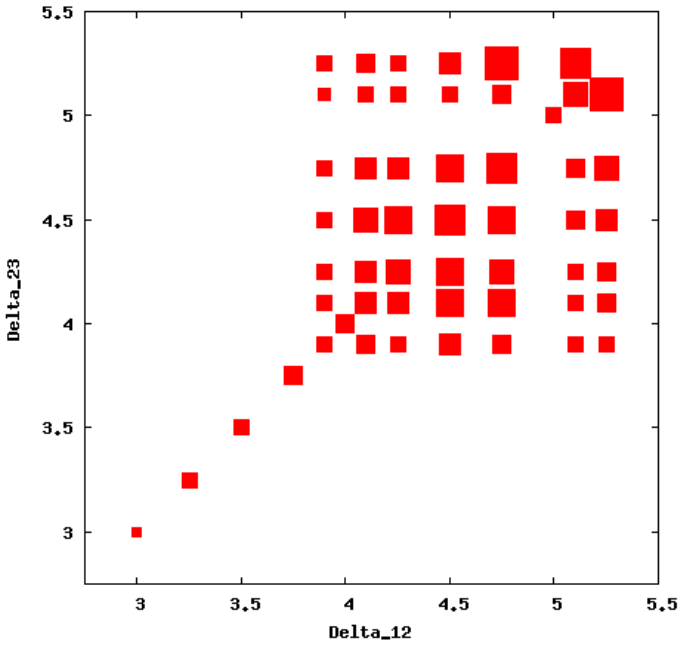

Figure 8.4: Median close encounter times for different combinations of Δ_{12} and Δ_{23}. The size of the square is $\propto \log \tau_{CE}$.

If we look at Figure 8.4 we can see that τ_{CE} increases moving along spine $\Delta_{12} = \Delta_{23}$ (the squares get larger and larger). However, the close encounter time remains relatively constant if you don't change Δ_{min}. As before I exclude simulations with at least one $\Delta_{ij} = 5.1$ in my analysis because of troubles with MMRs. Say you first look at $(\Delta_{12}, \Delta_{23}) = (3.9, 3.9)$ and then increase Δ_{12}. We see that τ_{CE} doesn't change (by much at least). It is the same if you start at, say, $(\Delta_{12}, \Delta_{23}) = (4.1, 4.1)$ and increase Δ_{23}. You can think of it as if Figure 8.4 was built up of L-shapes of with the same τ_{CE} (equally sized squares) and Δ_{min}. Next I plot τ_{CE} vs. Δ_{min}:

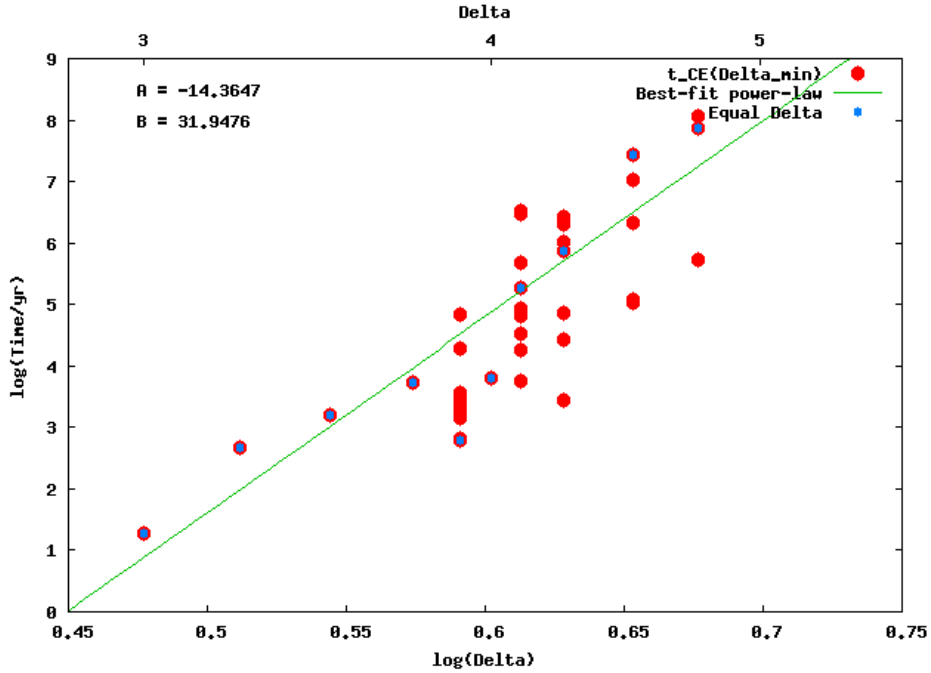

Figure 8.5: Median close encounter times as a function of Δ_{min}. The simulations with $\Delta_{12} = \Delta_{23}$ are marked with a blue dot. The best-fit power-law for equal separations is added for reference: $\log \tau_{CE} = A + B \log \Delta$.

If we compare Figure 8.5 to Figure 8.3 it has a similar goodness-of-fit as the Spine-and-Ribs approach and neither of them fit extremely good.

9 Low-mass planets in a protoplanetary disk

9.1 Description of the problem

One phase of planet formation is you have protoplanets in a protoplanetary disk (PPD). Even though these bodies are less massive than the planets I have studied so far they will still interact with each other and perturb each other's orbits. I have investigated how the close encounter timescale and time between first close encounter and disrupted system changes with mass for an equally separated three-planet system. I have also looked at how these times compare to the lifetime of a PPD and the dampening timescales in a PPD. The mass range of planets I have looked at is 1 to 30 Earth-masses (Earth to ∼Neptune).

One thing that differs between these simulations and those with Jupiter-mass objects is that the disruptive events are collisions between planets rather than ejections of planets. The reason for this is because of the change in the escape speed, v_{esc}, of the planets and how it compares to the orbital speed, v_{orb}. This can be quantified with the Safronov number (Equations (4) and (5) in Ford & Rasio 2008)

$$\theta^2 = \frac{1}{2}\frac{v_{esc}^2}{v_{orb}^2} = \left(\frac{Gm}{R_p}\right)\left(\frac{r}{Gm_c}\right) \tag{9.1}$$

where R_p is the radius of the planet, m is the mass of the planet, m_c is the mass of the star and r is the distance to the star at the final close encounter. If $\theta \gg 1$ the planet is able to eject other planets while if $\theta < 1$ collisions occurs much more often (Ford & Rasio 2008). To get a sense of why this is the case one could imagine that the maximum possible increase in speed for a planet after a close encounter is of the same order as the escape speed of the other planet. The binding energy per unit mass, i.e. the energy required to unbind a planet, of a planet is

$$E = -\frac{Gm_c}{2a} = \frac{v_{orb}^2}{2} - \frac{Gm_c}{r} \tag{9.2}$$

For a circular orbit $a = r$ so the energy required to unbind a planet is $\frac{Gm_c}{2r}$ and by rearranging the terms in the above equation we find that this corresponds to a kick with an energy of order $\frac{v_{orb}^2}{2}$, i.e. a velocity kick of order the orbital speed. If you look at the systems I have investigated all planets have initial semi-major axes around $1-3$ AU which corresponds to a orbital velocity of $v_{orb} \sim 20-30$ km s^{-1}. The escape speed of the Earth is $v_{esc} \sim 11.2$ km s^{-1} which is smaller than the orbital speed. For a 30 $M_\oplus$ object with Earth-density the escape speed is $v_{esc} \sim 35.1$ km s^{-1} which is slightly larger than the orbital speed but still small enough so that collisions dominate. The escape speed of Jupiter is $v_{esc} \sim 59.5$ km s^{-1} which is large enough for ejections to happen. You also have to consider that for a collision to occur the objects need to actually hit each other which has a small cross-section. For ejections, on the other hand, you can do it in steps and increase the semi-major axis with several close encounters further away. This way you don't need a close encounter between two planets where the planets just barely miss each other to gain the maximum possible velocity kick. This drastically increases the cross-section and as we saw in Section 5 this is what actually happens for Jupiter-mass object. They have several hundred close encounters before a planet gets ejected. Another difference is that the the close encounters are gravitationally focused. A close encounter is defined as an event where two planets come within one mutual Hill radius of each other,

Eq. (2.10). The cross-section for two objects to get within r_{min} for a gravitationally focused event is

$$\sigma = \pi r_{min}^2 \underbrace{\left(1 + \frac{v_{esc}(r_{min})^2}{v_\infty^2}\right)}_{focusing factor} \tag{9.3}$$

where r_{min} is the closest approach (in this case 1 r_{mH}), $v_{esc}(r_{min})$ is the escape speed of the object at closest approach and v_∞ is the speed of the object far from the close encounter (in this case the orbital speed). For two Jupiter-mass objects at 1 AU $r_{mH} \sim 0.1$ AU $\sim 200 R_{Jup}$ and for ejection of planets we are interested in a bit stronger scatterings, say within 0.01 AU $\sim 20 R_{Jup}$. From those values we can calculate $v_{esc}(r_{min})$ and see how much the gravitational focusing affects the cross-section. In the case of two Jupiters within $0.1 r_{mH}$ we get the escape speed to be $v_{esc}(0.01 \text{ AU}) \sim 15$ km s^{-1}. The orbital speed is ~ 30 km s^{-1} so gravitational focusing increases the cross-section with a factor $\sim (1 + 0.5^2) = 1.25$. For Earth-mass planets and collisions the focusing factor is ~ 1.11 so it is a bit smaller.

The reason why this is interesting is that planet-planet interactions could potentially disrupt a planetary system undergoing planet formation. If the timescales for close encounters and collisions between planets is shorter than the lifetime of a PPD ($\tau_{PPD} \sim 1 - 10$ Myr, Haisch et al. 2001, Mamajek 2009) planets could have problems to form and accrete gas before the PPD dissipates. One could also compare the timescales to timescales for dampening of eccentricities because of the presence of the gaseous disk. The disk dampens the eccentricities of objects in the disk in several ways as described by Ida et al. (2008): tidal interactions with the disk, aerodynamic gas drag and inelastic collisions. I am only interested in the first two since I am investigating when collisions occur. At 1 AU the dampening timescales are $\tau_{tidal} \sim 300$ yr and $\tau_{drag} \sim 20 e^{-1}$ kyr where e is the eccentricity of the orbit.

What also could be interesting to study is what happens after the collisions? Do the planets merge or do they fragment? If they merge: Could this be a way to increase the sizes of gas giant cores?

9.2 Simulations

9.2.1 Close encounter timescales

For my simulations I use the same setup as in Section 5 except with lower masses on the planets (which changes r_{mH} and hence also the semi-major axes). I have looked at three different masses: 1, 10 and 30 $M_\oplus$. I have run 12 sets of simulations with different Δ for each value on the masses and 30 simulations per set. I run a simulation until I get a collision or for a maximum of 50 Myr ($> \tau_{PPD}$).

I first investigate the close encounter timescale. For 1 $M_\oplus$ planets:

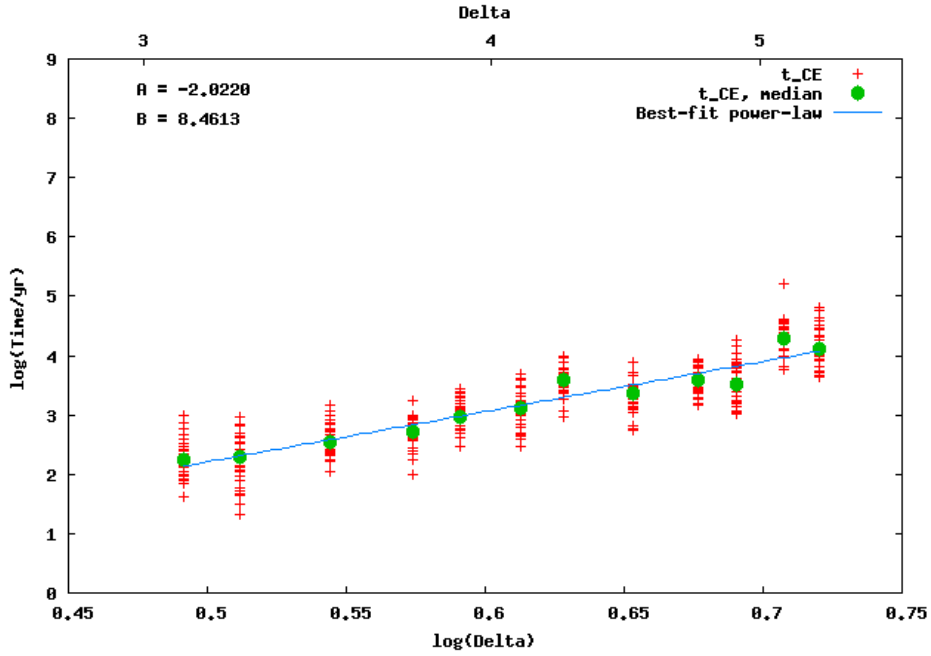

Figure 9.1: Time until first close encounter for three, 1 $M_\oplus$, planets as a function of $\Delta_{12} = \Delta_{23}$. Red crosses are the data for each simulation and green dots are the median values of the time until first close encounter. Best-fit power-law, $\log \tau_{CE} = A + B \log \Delta$ also added (blue line).

for 10 $M_\oplus$ planets:

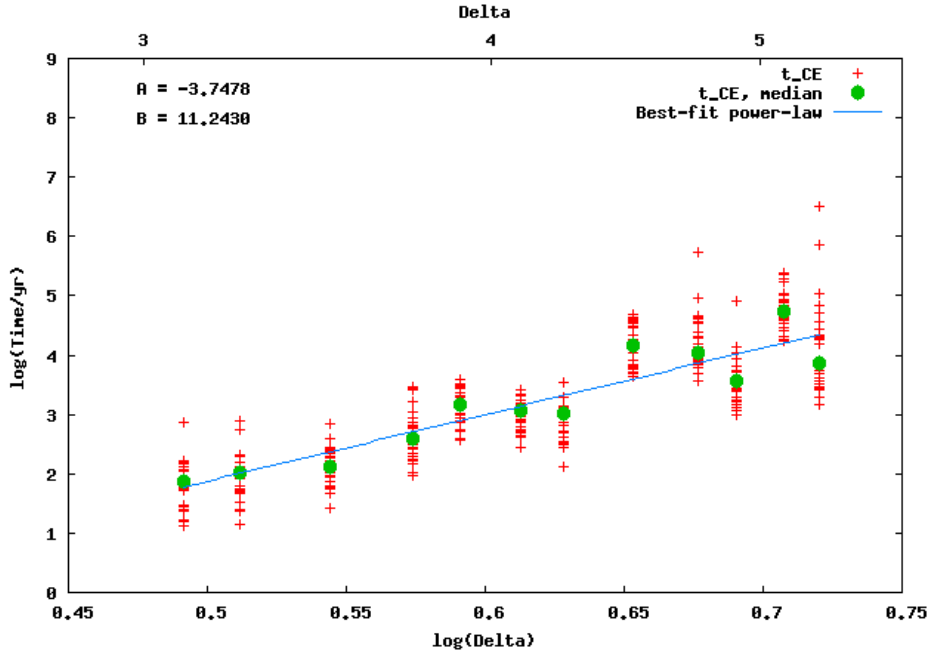

Figure 9.2: Time until first close encounter for three, 10 $M_\oplus$, planets as a function of $\Delta_{12} = \Delta_{23}$. Red crosses are the data for each simulation and green dots are the median values of the time until first close encounter. Best-fit power-law, $\log \tau_{CE} = A + B \log \Delta$ also added (blue line).

and for 30 $M_\oplus$ planets:

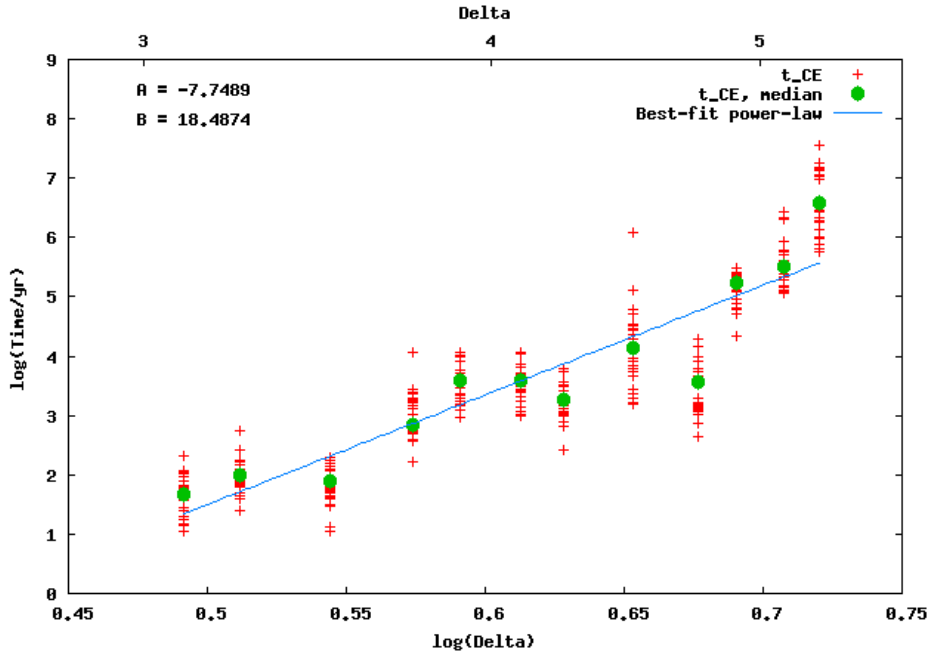

Figure 9.3: Time until first close encounter for three, 30 $M_\oplus$, planets as a function of $\Delta_{12} = \Delta_{23}$. Red crosses are the data for each simulation and green dots are the median values of the time until first close encounter. Best-fit power-law, $\log \tau_{CE} = A + B \log \Delta$ also added (blue line).

We can see that the medians all roughly fit a power-law

$$\log \tau_{CE} = A + B \log \Delta \tag{9.4}$$

as they did for the case with Jupiter-mass objects. I have summarized the results for the simulations for the four different masses in the following table:

	1 $M_\oplus$	10 $M_\oplus$	30 $M_\oplus$	1 M_{Jup}
A	-2.0220	-3.7478	-7.7489	-14.3674
B	8.46127	11.243	18.4874	31.9476
σ_A	0.4544	0.9002	1.44	2.765
σ_B	0.7316	1.449	2.319	4.686

Table 9.1: Best-fit values and errors for A and B in the $\tau_{CE}(\Delta)$ power-law ($\log \tau_{CE} = A + B \log \Delta$) for different planet masses.

If we compare Figures 5.1, 9.1, 9.2 and 9.3 or just look in Table 9.1 we see that B is an increasing function of planet mass. If I plot B vs. planet mass I get:

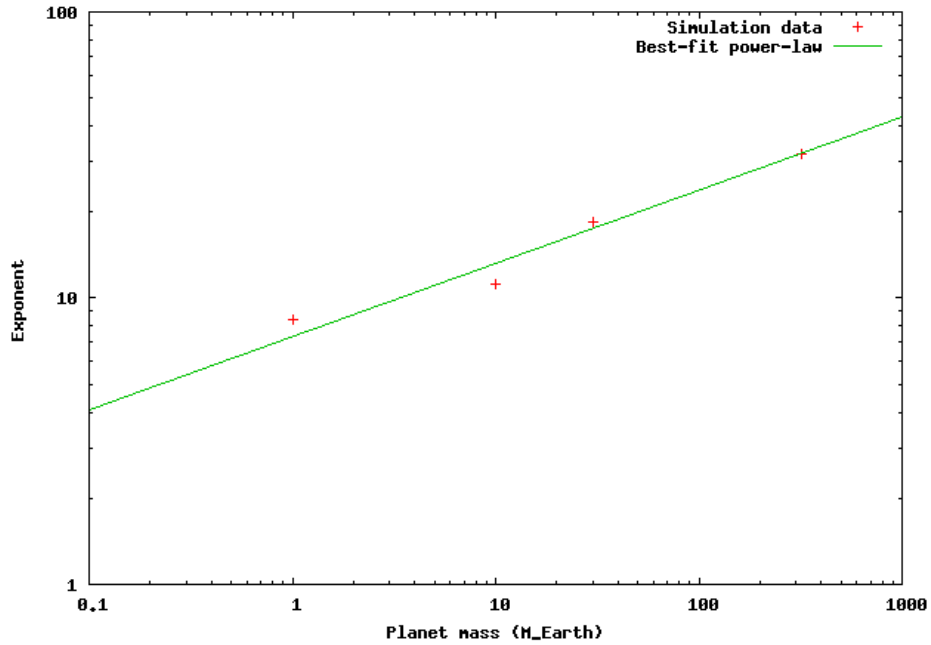

Figure 9.4: Exponent of the $\tau_{CE}(\Delta)$ power-law as a function of the mass of the equal-mass planets. Best-fit power-law also added (green line).

The conclusion is that larger planets avoid close encounters for a longer time. This is a bit contra-intuitive since if we have larger planets we have larger planet-planet interactions but we have to remember that we also get larger absolute distances ($r_{mH} \propto (m_1+m_2)^{1/3}$). The power-law fit is best for the 1 $M_\oplus$ simulations. My explanation for this is that the planets are close enough that they can avoid MMRs which, as we have seen before (e.g. Section 5), can make planet-planet interactions stronger and shorten the time to first close encounter. In Figure 9.4 The points fit surprisingly well to yet another power-law, however, it is only four data points so it might not be very relevant.

As mentioned before the eccentricity of a planet in a disk will be dampened by different mechanisms. The timescale of dampening by tidal interactions with the disk is $\tau_{tidal} \sim 300$ yr and the timescale of dampening by gas drag is $\tau_{drag} \sim 20e^{-1}$ kyr (Ida et al. 2008). The systems with the smallest separation has a τ_{CE} which is smaller than both the dampening timescales. These systems would then, in a real PPD, be able to fight against the dampening. To be able to say more I should compare the dampening timescales to the oscillation periods which you can get from the equations in Section 3.

9.2.2 After the first close encounter

I have also investigated what happens after the first close encounter. I again find, as in Section 5, that all systems with a close encounter eventually become disrupted and have a collision between planets. Again the time between these two events, $\tau_{coll} - \tau_{CE}$, is constant. For systems with 1 $M_\oplus$ planets I get:

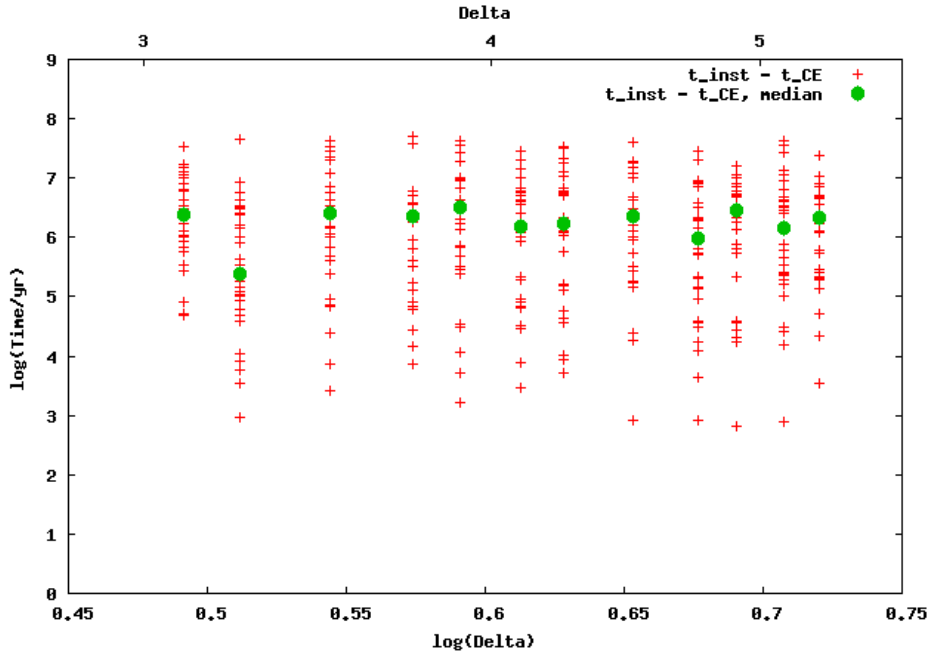

Figure 9.5: Time between first close encounter and instability (collision between two planets) for three, 1 $M_\oplus$, planets as a function of $\Delta_{12} = \Delta_{23}$. Red crosses are the data for each simulation and green dots are the median values.

for 10 $M_\oplus$ planets:

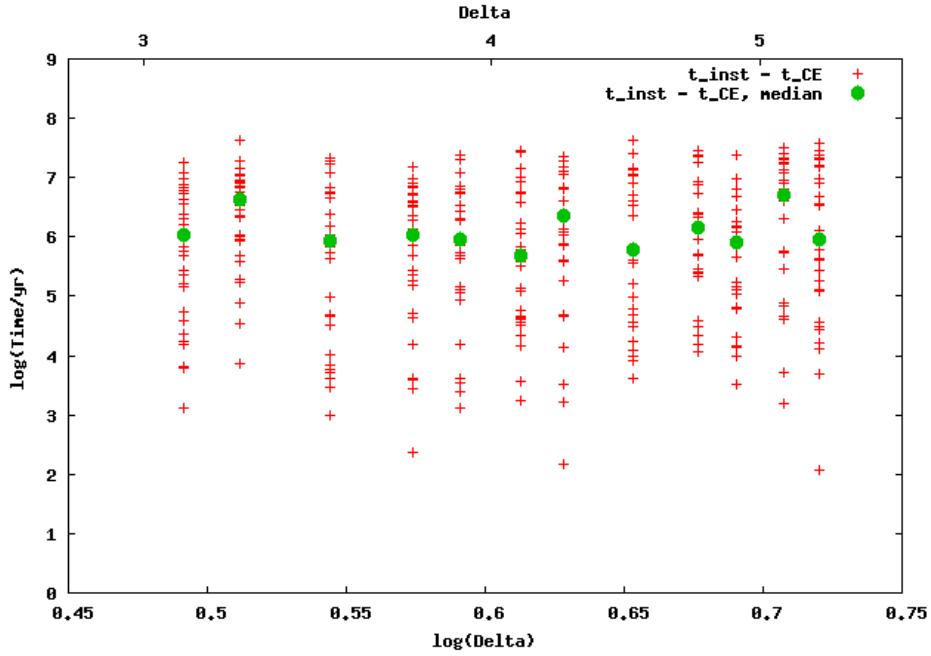

Figure 9.6: Time between first close encounter and instability (collision between two planets) for three, 10 $M_\oplus$, planets as a function of $\Delta_{12} = \Delta_{23}$. Red crosses are the data for each simulation and green dots are the median values.

and for 30 $M_\oplus$ planets:

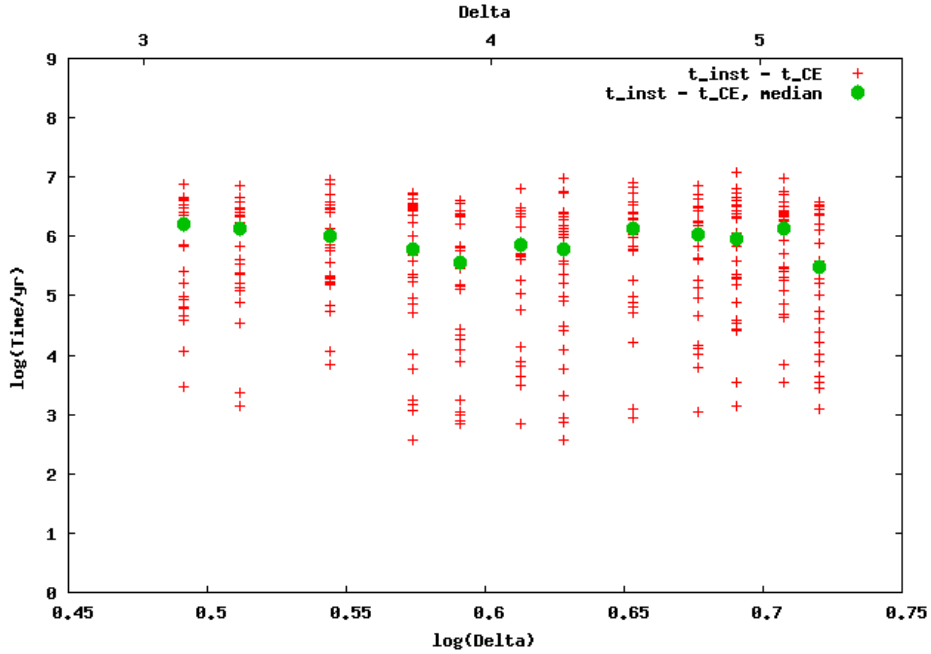

Figure 9.7: Time between first close encounter and instability (collision between two planets) for three, 30 $M_\oplus$, planets as a function of $\Delta_{12} = \Delta_{23}$. Red crosses are the data for each simulation and green dots are the median values.

As stated before, the time is independent on the initial separation and has a value of, for all three masses, $\tau_{coll} - \tau_{CE} \sim 10^{6\pm1}$ yr. If we compare it to the case with Jupiter-mass planets (Figure 5.3) it is a bit different. The time between first close encounter and ejection of a planet for three Jupiter-mass planets was $\tau_{ej} - \tau_{CE} \sim 10^{5\pm1}$ yr (see Figure 5.3), i.e. a bit smaller. The reason why the time between close encounter and collision/ejection is longer for the low-mass systems is that if you have small planets you have small cross-sections and low probability for collisions to occur while if you have high-mass planets the cross-section for close encounters is large and you get many close encounters, build up the eccentricity of planets and eventually eject a planet. The simulations with low-mass planets also shows a larger spread in times. The explanation for this is that the systems with low-mass planets have collisions between planets while systems with high-mass planets eject planets. The spread comes from the fact that a collision is one single event, one collision. For high-mass planets the ejection of a planet is a cumulative effect of many close-encounters, you gradually build up the eccentricities and the semi-major axis of one planet with many close encounters.

From Figures 9.5-9.7 we see that the time between first close encounter and collision between two planets is comparable to the lifetime of a PPD ($\tau_{PPD} \sim 1 - 10$ Myr, Haisch et al. 2001, Mamajek 2009) so this could affect the evolution of gas giant cores. One has to remember, though, that these simulations are made without the gaseous disk and the fact that the mass of those objects increase as they accrete gas.

What I want to say in this section is that the close encounter timescale is a function of both the separations between the planets and the mass of the planets. From the power-

law fits I can get the value of Δ to get close encounters for certain times. I plot curves of isotimes (close encounters in 1, 10, 100, 1000 or 10000 Myr) in m_p-Δ-space:

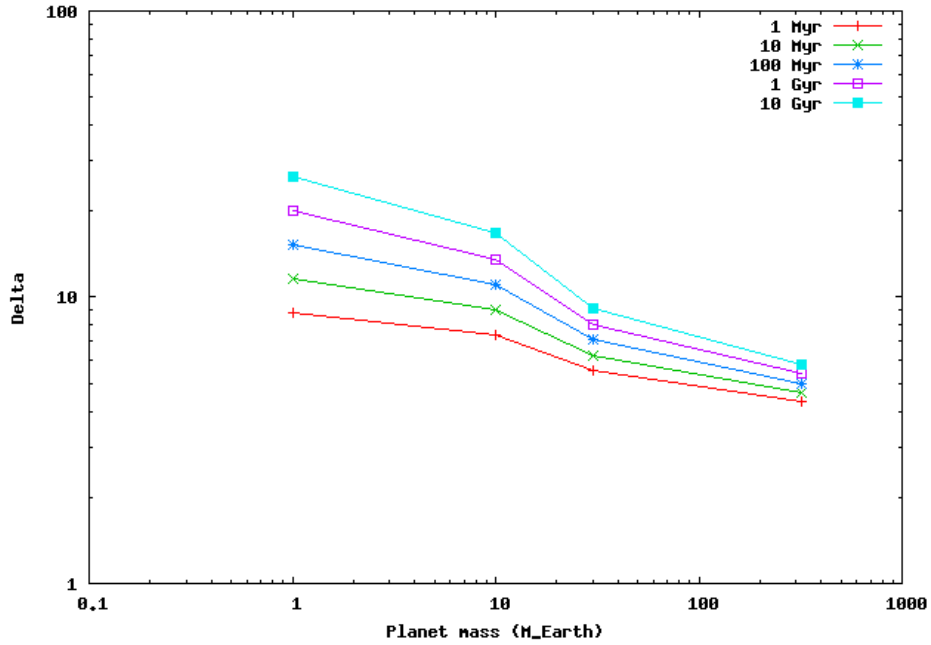

Figure 9.8: Values of Δ required to get a close encounter within a certain time for different values of planet mass. Also plotted is isocurves for five close encounter times. The Δs has been calculated using Eq. (9.4) and Table 9.1.

I calculate the values on Δ using Eq. (9.4) and Table 9.1 to get a close encounter in 1, 10, 100, 1000 or 10000 Myr. In Figure 9.8 we see that smaller planets have to be further away to stay stable (which we knew from Figure 9.4) e.g. if we want a system to have a close encounter after $\tau_{CE} = 1$ Gyr we get the separation for Earth-mass planets to be $\Delta_{1M_\oplus} \sim 20$ and for Jupiter-mass planets to be $\Delta_{1M_{Jup}} \sim 5.4$.

10 Possible future extensions

- One thing that could be interesting is to see how the secular eccentricity oscillations in Section 3 depend on the initial mutual inclination. I would do this by investigating a symmetric system with aligned orbits ($\Omega_1 = \Omega_2$ and $\varpi_1 = \varpi_2$) and with inclinations $I_1 = -I_2$. We can straightforwardly show that the periods of the oscillations wouldn't change with increasing mutual inclination (the frequencies are only dependent on the semi-major axes and the masses since they are the eigenvalues of the $\boldsymbol{A}$- and $\boldsymbol{B}$-matrices, Eqs. (3.4)–(3.5)). The amplitudes on the other hand are functions of the initial conditions. This is exactly the same as for the regular pendulum where the period of the oscillations is independent of the amplitude but equal to $\sqrt{l/g}$, where l is the length of the pendulum and g is the gravitational acceleration of the Earth. By doing this I could find what mutual inclination is needed between two orbits, with certain semi-major axes, to get crossing orbits or orbits that are within one mutual Hill radius. I have all the software needed to do the investigations so I just need to do the simulations

- I would also like to further investigate why the periods of the analytically derived secular oscillations don't match with the N-body simulations in e.g Figures 3.1 and 3.2. Is it just because of the fact that I do a lot of approximations in the derivation of the equations or are there other reasons?

- I also want to further investigate the evolution of a multiple-planet system in the phase between the first close encounter and ejection of a planet (the time between stage B and stage C in Figure 6.1) that I started in Section 5. How does the semi-major axis of the ejected planet evolve as a function of time? Does it increase quickly in beginning and slower in the end since the orbital period is a function of the semi-major axis, $P \propto a^{3/2}$? How quickly is it 'decided' which planet is going to be ejected? Is it set already after a couple of close encounters or not until the end? Before the planet is ejected it has a large semi-major axis (~ 100 AU, Figure 5.6) and a very large eccentricity (~ 1). This means that when it is far away from the star it could maybe be directly imageable. How much time does it spend that far away from the star and how many systems like that should there be? Remember Kepler's second law, Eq. (A.9), which implication is that the planet spends most of its time at apoapsis, far away from the star and the other planets.

- Another thing I want to continue investigating which also is tied to the fact that a multiple-planet system has many (~ 500, Table 5.4) close encounters before a planet is ejected is what those close encounters look like. How much energy, ΔE, is transferred in each close encounter? How many close encounters are there as a function of the amount of energy they transfer?

$$\frac{\mathrm{d}N}{\mathrm{d}(\Delta E)} = f(\Delta E) \tag{10.1}$$

  From this I could find out which types of close encounters contributes the most to the ejection of a planet. Is it many low-energy close encounters or is it few high-energy close encounters?

- One thing I would like to do is continue my investigation of low-mass planets in a protoplanetary disk. I want to compare timescales (i.e. for close encounters, collisions, disk lifetime, eccentricity dampening and eccentricity oscillation periods) in more detail. By doing that I could potentially find out what effect planet-planet interactions have on planet formation. If the dampening timescales are much shorter than the close encounter timescale or eccentricity oscillation period it would not matter at all. However, if it is longer then it is something you have to take into account when you study planet formation.

- In Section 8, Figure 8.2 we saw that it looked like simulations with $\Delta_{12} < \Delta_{23}$ gave smaller τ_{CE} than simulations with $\Delta_{12} > \Delta_{23}$. Is this a systematic effect or just pure chance? In the future I could investigate this further.

References

Bouchy, F., Mayor, M., Lovis, C., Udry, S., Benz, W., Bertaux, J.-L., Delfosse, X., Mordasini, C., Pepe, F., Queloz, D., & Segransan, D. 2009, A&A, 496, 527

Brouwer, D. & Clemence, G. M. 1961, Methods of celestial mechanics (New York: Academic Press)

Chambers, J. E. 1999, MNRAS, 304, 793

Chambers, J. E., Wetherill, G. W., & Boss, A. P. 1996, Icarus, 119, 261

Fischer, D. A., Vogt, S. S., Marcy, G. W., Butler, R. P., Sato, B., Henry, G. W., Robinson, S., Laughlin, G., Ida, S., Toyota, E., Omiya, M., Driscoll, P., Takeda, G., Wright, J. T., & Johnson, J. A. 2007, ApJ, 669, 1336

Ford, E. B., Kozinsky, B., & Rasio, F. A. 2000, ApJ, 535, 385

Ford, E. B. & Rasio, F. A. 2008, ApJ, 686, 621

Gladman, B. 1993, Icarus, 106, 247

Haisch, Jr., K. E., Lada, E. A., & Lada, C. J. 2001, ApJ, 553, L153

Ida, S., Guillot, T., & Morbidelli, A. 2008, ApJ, 686, 1292

Kozai, Y. 1962, AJ, 67, 591

Lovis, C., Ségransan, D., Mayor, M., Udry, S., Benz, W., Bertaux, J.-L., Bouchy, F., Correia, A. C. M., Laskar, J., Lo Curto, G., Mordasini, C., Pepe, F., Queloz, D., & Santos, N. C. 2011, A&A, 528, A112

Malmberg, D., Davies, M. B., & Heggie, D. C. 2011, MNRAS, 411, 859

Mamajek, E. E. 2009, in American Institute of Physics Conference Series, Vol. 1158, American Institute of Physics Conference Series, ed. T. Usuda, M. Tamura, & M. Ishii, 3–10

Mayor, M. & Queloz, D. 1995, Nat, 378, 355

Meschiari, S., Laughlin, G., Vogt, S. S., Butler, R. P., Rivera, E. J., Haghighipour, N., & Jalowiczor, P. 2011, ApJ, 727, 117

Murray, C. D. & Dermott, S. F. 1999, Solar system dynamics (Cambridge Univ. Press, Cambridge, UK)

Quillen, A. C. 2011, MNRAS, 418, 1043

Roy, A. E. 1988, Orbital motion (Bristol, England ; Philadelphia : A. Hilger, 1988. 3rd ed.)

Saffe, C., Gómez, M., & Chavero, C. 2005, A&A, 443, 609

Schneider, J., Dedieu, C., Le Sidaner, P., Savalle, R., & Zolotukhin, I. 2011, A&A, 532, A79

Takeda, G. & Rasio, F. A. 2005, ApJ, 627, 1001

A Derivation of orbital parameters for one planet

In this appendix I derive the orbital parameters for a planet with the help of Murray & Dermott (1999) (I use their convention for variable names). I have produced all the figures in this section myself but with some inspiration from figures in Chapter 2 of Murray & Dermott (1999).

A.1 The two-body problem in two dimensions

A system with two bodies with masses m_c and m_1:

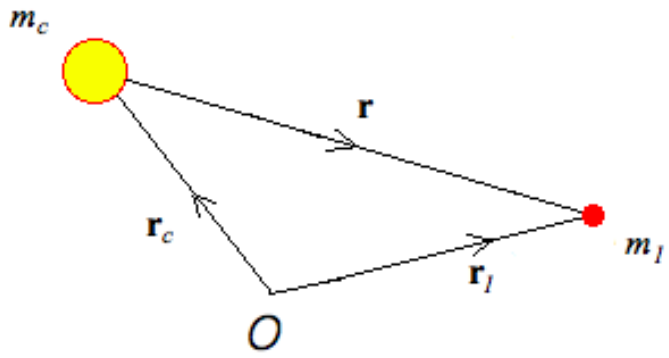

Figure A.1: Structure of a system with two bodies. In the case of a planetary system the yellow dot, m_c, is the star and the red dot, m_1, is the planet. The boldface letters are the position vectors of the masses in an arbitrary frame with origin O. $\mathbf{r}$ is the position of the planet with respect to the star.

The forces between the masses in Figure A.1 can be written as

$$\mathbf{F}_c = m_c\ddot{\mathbf{r}}_c = +G\frac{m_c m_1}{r^3}\mathbf{r} \tag{A.1}$$

$$\mathbf{F}_1 = m_1\ddot{\mathbf{r}}_1 = -G\frac{m_c m_1}{r^3}\mathbf{r} \tag{A.2}$$

where $\mathbf{r} = \mathbf{r}_1 - \mathbf{r}_c$ and $r = |\mathbf{r}|$ is the separation between the planet and the star and two dots represent the second time derivative. We now move over to investigate the planet's, m_1, motion with respect to the star, m_c. We can write the acceleration of the planet as

$$\ddot{\mathbf{r}} = \ddot{\mathbf{r}}_1 - \ddot{\mathbf{r}}_c = -\left[G\frac{m_c}{r^3}\mathbf{r} + G\frac{m_1}{r^3}\mathbf{r}\right] = -\frac{\mu}{r^3}\mathbf{r} \tag{A.3}$$

where $\mu = G(m_c + m_1)$. To continue we need to get a couple of constants of motion to make the calculations a bit easier. First out is the specific angular momentum, $\mathbf{h}$, which we get by taking the vector product between $\mathbf{r}$ and $\dot{\mathbf{r}}$. We can see that this is constant by taking the time derivative

$$\dot{\mathbf{h}} = \frac{\mathrm{d}}{\mathrm{d}t}\left(\mathbf{r} \times \dot{\mathbf{r}}\right) = \dot{\mathbf{r}} \times \dot{\mathbf{r}} + \mathbf{r} \times \ddot{\mathbf{r}} = 0 \tag{A.4}$$

This is zero since $\dot{\mathbf{r}}$ is parallel to itself and $\mathbf{r}$ is parallel to $\ddot{\mathbf{r}}$ (Eq. (A.3)). The fact that $\mathbf{h}$ is constant means that the orbit of m_1 around m_c is confined to a one plane perpendicular to $\mathbf{h}$. To make things easier we now only look at motion in this plane and switch to polar coordinates, (r, θ), centered on $m_c \gg m_1$ in this plane and with an arbitrary reference direction corresponding to $\theta = 0$. Next we denote the unit vectors parallel and perpendicular to $\mathbf{r}$ in the plane of motion with $\hat{\mathbf{r}}$ and $\hat{\boldsymbol{\theta}}$ respectively. Now we can write the position, velocity and acceleration of m_1 as:

$$\mathbf{r} = r\hat{\mathbf{r}} \tag{A.5}$$

$$\dot{\mathbf{r}} = \dot{r}\hat{\mathbf{r}} + r\dot{\theta}\hat{\boldsymbol{\theta}} \tag{A.6}$$

$$\ddot{\mathbf{r}} = \left(\ddot{r} - r\dot{\theta}^2\right)\hat{\mathbf{r}} + \left[\frac{1}{r}\frac{\mathrm{d}}{\mathrm{d}t}\left(r^2\dot{\theta}\right)\right]\hat{\boldsymbol{\theta}} \tag{A.7}$$

From these equations we can get the specific angular momentum

$$\mathbf{h} = \mathbf{r} \times \dot{\mathbf{r}} = (r\hat{\mathbf{r}}) \times \left(\dot{r}\hat{\mathbf{r}} + r\dot{\theta}\hat{\boldsymbol{\theta}}\right) = r^2\dot{\theta}\hat{\mathbf{z}} \Longrightarrow h = |\mathbf{h}| = r^2\dot{\theta} \tag{A.8}$$

where $\hat{\mathbf{z}}$ is the unit vector perpendicular to the orbital plane and it forms a right-handed triad together with $\hat{\mathbf{r}}$ and $\hat{\boldsymbol{\theta}}$. We can look at the motion of the planet over a short time interval. Say the planet has the position (r, θ) at time $t = 0$, at a time $\mathrm{d}t$ later it has the position $(r + \mathrm{d}r, \theta + \mathrm{d}\theta$ (see Figure A.2).

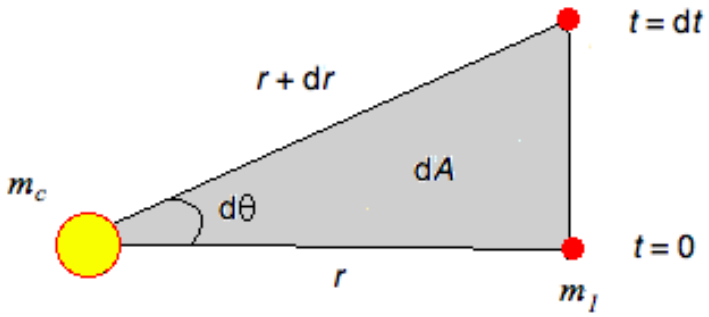

Figure A.2: Kepler's second law: Equal areas are swept out by the radius vector to the planet in equal times.

The area covered by the radius vector of the planet in a time $\mathrm{d}t$ can then be written as

$$\mathrm{d}A = \frac{1}{2}r(r+\mathrm{d}r)\sin\mathrm{d}\theta = \frac{1}{2}r^2\mathrm{d}\theta + \mathcal{O}\left(\text{second order terms}\right) \Longrightarrow$$

$$\frac{\mathrm{d}A}{\mathrm{d}t} = \frac{1}{2}r^2\frac{\mathrm{d}\theta}{\mathrm{d}t} = \frac{1}{2}h \tag{A.9}$$

This is Kepler's second law: Equal areas are swept out in equal times.
Inserting Eq. (A.7) into Eq. (A.3) yields

$$\ddot{r} - r\dot{\theta}^2 = -\frac{\mu}{r^2} \tag{A.10}$$

To solve this equation we make the variable substitution $r = \frac{1}{u}$ we then get

$$\dot{r} = -\frac{1}{u^2}\frac{\mathrm{d}u}{\mathrm{d}\theta}\dot{\theta} = -r^2\dot{\theta}\frac{\mathrm{d}u}{\mathrm{d}\theta} = -h\frac{\mathrm{d}u}{\mathrm{d}\theta} \tag{A.11}$$

$$\ddot{r} = -h\frac{\mathrm{d}^2u}{\mathrm{d}\theta^2}\dot{\theta} = -h\frac{r^2\dot{\theta}}{r^2}\frac{\mathrm{d}^2u}{\mathrm{d}\theta^2} = -h^2u^2\frac{\mathrm{d}^2u}{\mathrm{d}\theta^2} \tag{A.12}$$

Next we insert Eq. (A.12) into Eq. (A.10) and it becomes

$$-h^2u^2\frac{\mathrm{d}^2u}{\mathrm{d}\theta^2} - h^2u^3 = -\mu u^2 \Longrightarrow \frac{\mathrm{d}^2u}{\mathrm{d}\theta^2} + u = \frac{\mu}{h^2} \tag{A.13}$$

This is a second-order differential equation with the general solution (easily solvable by making the substitution $y = u - \frac{\mu}{h^2}$):

$$u = \frac{\mu}{h^2}\left(1 + e\cos(\theta - \varpi)\right) \tag{A.14}$$

where e and ϖ are two constants of integration. From u we can now get r as a function of θ:

$$r = \frac{h^2}{\mu}\frac{1}{1 + e\cos(\theta - \varpi)} \tag{A.15}$$

This is the equation, in polar coordinates, for a conic section, i.e. a circle, an ellipse, a parabola or a hyperbola with eccentricity e. When it comes to planets you are most often interested in bound orbits: ellipses with $e < 1$ so I'm going to focus on that (a circle is an ellipse with $e = 0$). $p = \frac{h^2}{\mu}$ is called the semi-latus rectum and from it one can derive the size, semi-major axis, of the ellipse

$$a = \frac{p}{1 - e^2} = \frac{h^2}{\mu(1 - e^2)} \tag{A.16}$$

We now have enough parameters to describe the shape and orientation of the ellipse in the orbital plane and to get the position of the planet from a given reference direction (see Figure A.3).

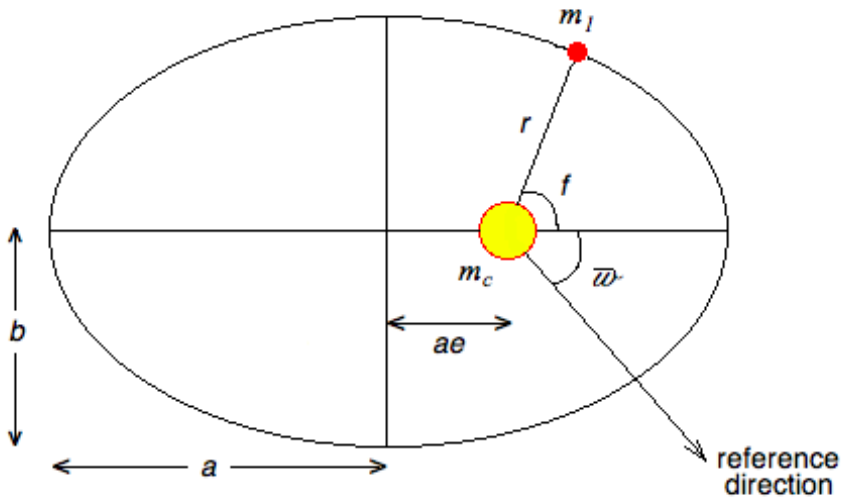

Figure A.3: An ellipse with semi-major axis a, eccentricity e and longitude of periapsis ϖ together with a planet with true anomaly f.

The semi-major axis, a, is the longest diameter of the ellipse: the distance between the periapsis (point in orbit closest to m_c) and the apoapsis (point in orbit furthest away from m_c). The semi-minor axis, b is the smallest diameter of the ellipse and can be calculated from the semi-major axis and the eccentricity, e,

$$b^2 = a^2(1 - e^2) \tag{A.17}$$

The eccentricity describes the elongation of the orbit e.g. the distance between m_c and the centre of the ellipse is ae. The longitude of periapsis, ϖ, is the angle between the reference direction and the periapsis. Finally the true anomaly, $f = \theta - \varpi$, is the angle between the periapsis and radius vector of the planet. With these parameters we can write the distance between m_c and m_1 as

$$r = \frac{a(1 - e^2)}{1 + e\cos(f)} \tag{A.18}$$

The area of an ellipse is $A = \pi ab = \pi a^2\sqrt{1 - e^2}$ which is the same area that the radius vector sweeps out in one orbital period, T. From Eq. (A.9) this area must also be $A = \frac{hT}{2}$ and using Eq. (A.16) we get

$$\pi a^2\sqrt{1 - e^2} = \frac{T\sqrt{a\mu(1 - e^2)}}{2} \Longrightarrow T^2 = \frac{4\pi^2}{\mu}a^3 \tag{A.19}$$

This is Kepler's third law and states that the orbital period squared is proportional to the semi-major axis cubed. In one orbital period the angle f covers 2π radians so we define the mean motion as

$$n = \frac{2\pi}{T} \Longrightarrow \mu = n^2a^3 \Longrightarrow h = na^2\sqrt{1 - e^2} \tag{A.20}$$

The mean motion can be thought of an average angular velocity. The mean motion is constant for the two-body problem but the actual angular velocity $\dot{f}$ is not unless it is a circular orbit.

By taking the dot product of $\dot{\mathbf{r}}$ with Eq. (A.3) and using Eqs. (A.6)–(A.7) we can get another constant of motion

$$\dot{\mathbf{r}} \cdot \ddot{\mathbf{r}} = -\frac{\mu}{r^3}\dot{\mathbf{r}} \cdot \mathbf{r} = -\frac{\mu}{r^3}\left(r\dot{r}\hat{\mathbf{r}} \cdot \hat{\mathbf{r}} + r^2\dot{\theta}\hat{\mathbf{r}} \cdot \hat{\boldsymbol{\theta}}\right) = -\frac{\mu\dot{r}}{r^2} \tag{A.21}$$

By integrating this you get

$$\frac{1}{2}v^2 - \frac{\mu}{r} = E \tag{A.22}$$

where $v^2 = \dot{\mathbf{r}} \cdot \dot{\mathbf{r}}$ and E is an integration constant. This equation shows that the orbital energy per unit mass is conserved. From the definition of f and the fact that ϖ is a constant we get $\dot{f} = \dot{\theta}$. Using this and Eq. (A.6) we can get v^2 as

$$v^2 = \dot{\mathbf{r}} \cdot \dot{\mathbf{r}} = \dot{r}^2 + r^2\dot{f}^2 \tag{A.23}$$

We can get $\dot{r}$ and $r\dot{f}$ by differentiating Eq. (A.18) and using Eq. (A.16)

$$\dot{r} = \frac{\mathrm{d}}{\mathrm{d}t}\left(\frac{a(1-e^2)}{1+e\cos f}\right) = \frac{ae(1-e^2)\dot{f}\sin f}{(1+e\cos f)^2} = \frac{r^2 e\dot{f}\sin f}{a(1-e^2)} = \frac{he\sin f}{a(1-e^2)} \tag{A.24}$$

$$r\dot{f} = \frac{h}{r} = \frac{h\,(1+e\cos f)}{a(1-e)} \tag{A.25}$$

Inserting these two equations in Eq. (A.23) yields

$$\begin{aligned} v^2 &= \frac{h^2}{a^2(1-e^2)^2}\left(e^2\sin^2 f + 1 + 2e\cos f + e^2\cos^2 f\right) = \frac{h^2}{a^2(1-e^2)^2}\left(e^2 + 1 + 2e\cos f\right) \\ &= \frac{h^2}{a^2(1-e^2)^2}\left(2(1+e\cos f) - (1-e^2)\right) = \frac{h^2}{a(1-e^2)}\left(\frac{2}{r} - \frac{1}{a}\right) = \mu\left(\frac{2}{r} - \frac{1}{a}\right) \end{aligned} \tag{A.26}$$

Inserting this in Eq. (A.22) and we find that the orbital energy per unit mass is constant and equal to

$$E = -\frac{\mu}{2a} \tag{A.27}$$

With this and Eq. (A.22) we can find the speed of the planet given the distance to the star. We also get a useful relationship between the energy (E), angular momentum (h) and eccentricity (e) of an orbit by inserting Eq. (A.27) into Eq. (A.16):

$$e = \sqrt{1 - \frac{2Eh^2}{\mu^2}} \tag{A.28}$$

A.2 The position as a function of time

With the previous calculations we can get the position of the planet as a function of the true anomaly, f. However, usually you want the position as a function of time but f can be a rather complicated function of time and it would be nice to have something that increases linearly with time. Therefore we define the mean anomaly, M, as

$$M = n(t - \tau) \tag{A.29}$$

where τ is the time of periapsis passage. M has the dimensions of an angle but is an abstract concept and has no simple geometric interpretation. M has some relation to the true anomaly if we look at Eq. (A.18): when $t = \tau$ (at periapsis) both M and f is zero and at $t = \tau + \frac{T}{2}$ (at apoapsis) $M = f = \pi$. The mean anomaly can be related to an angle with a geometrical interpretation, this angle is the eccentric anomaly, E. Assume we have an ellipse (the orbit) with semi-major axis a and eccentricity e and put it in a circle with radius a. E is defined as the angle between the major axis of the ellipse and the radius from the center O to the intersection point on the circle, see Figure A.4.

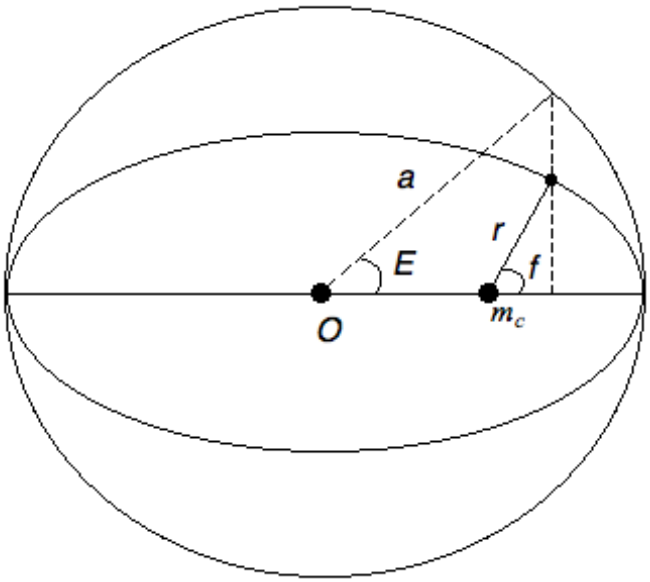

Figure A.4: An ellipse with semi-major axis a and eccentricity e circumscribed by a circle with radius a. Also show the relationship between the eccentric anomaly E and the true anomaly f.

In cartesian coordinates centered in O an ellipse can be described as

$$1 = \left(\frac{\bar{x}}{a}\right)^2 + \left(\frac{\bar{y}}{b}\right)^2 \tag{A.30}$$

From Figure A.4 we can see that we also can write, together with Eq. (A.17),

$$\bar{x} = a\cos E \Longrightarrow \bar{y}^2 = b^2 \sin^2 E \Longrightarrow \tag{A.31}$$

$$\bar{y} = a\sqrt{1 - e^2}\sin E \tag{A.32}$$

changing coordinate system to one centered on m_c (Fig. A.4) instead yields

$$x = a\left(\cos E - e\right) \tag{A.33}$$
$$y = a\sqrt{1-e^2}\sin E \tag{A.34}$$

We can now get r and f as functions of E from above two equations

$$r = \sqrt{x^2+y^2} = a\left(1 - e\cos E\right) \tag{A.35}$$
$$\cos f = \frac{x}{r} = \frac{\cos E - e}{1 - e\cos E} \tag{A.36}$$

which means we can uniquely determine r and f from Eqs. (A.35)–(A.36). Next we need a relationship between M and E to get the position as a function of time. By inserting Eqs. (A.25)–(A.26) in Eq. (A.23) and using Eqs. (A.20) we get

$$\begin{aligned}\dot{r}^2 &= v^2 - \left(r\dot{f}\right)^2 = n^2a^3\left(\frac{2}{r} - \frac{1}{a}\right) - \frac{n^2a^2}{1-e^2}\left(1+\cos f\right)^2 \\ &= n^2a^3\left(\frac{2}{r} - \frac{1}{a}\right) - \frac{n^2a^4(1-e^2)}{r^2} \Longrightarrow \qquad (A.37)\\ \dot{r} &= \frac{na}{r}\sqrt{2ar - r^2 - a^2(1-e^2)} = \frac{na}{r}\sqrt{a^2e^2 - (r-a)^2} \qquad (A.38)\end{aligned}$$

From Eq. (A.35) we get that

$$r - a = -ae\cos E \tag{A.39}$$
$$\dot{r} = ae\dot{E}\sin E \tag{A.40}$$

which means we can write Eq. (A.38)

$$ae\dot{E}\sin E = \frac{na}{a\left(1-e\cos E\right)}\sqrt{a^2e^2 - a^2e^2\cos^2 E} = \frac{nae\sin E}{1-e\cos E} \Longrightarrow \tag{A.41}$$
$$\dot{E} = \frac{n}{1-e\cos E} \Longrightarrow \left(1-e\cos E\right)\mathrm{d}E = n\mathrm{d}t \tag{A.42}$$

Integrating this equation and using the boundary condition that $E = 0$ at periapsis passage, $t = \tau$, gives us

$$E - e\sin E = n(t-\tau) = M \tag{A.43}$$

This equation is transcendental in E i.e. it contains both an E-term and a $\sin E$-term. This means that E cannot be expressed as a simple function of M and you have to resort to approximations if you want to solve it e.g. numerical methods such as the Newton-Raphson method. In any case we can now get the position of the planet as a function of time with the following procedure:

i) First we need to get the mean anomaly from Eq. (A.29). We can get the mean motion from the semi-major axis using Eq. (A.20).

ii) Next we solve Eq. (A.43) to get E by using some approximation.

iii) Finally we can get the position (r and f) from Eqs. (A.35)–(A.36).

A.3 The two-body problem in three dimensions

In previous sections we found that the orbit of a single planet always lies in one plane perpendicular to the angular momentum. We also found that the orbit and the position of the planet in the orbit could be described with four different parameters:

- The semi-major axis a which describes the size (largest diameter) of the orbit. It can be obtained from the orbital energy of the planet (Eq. (A.26)).
- The eccentricity e which describes how elongated, non-circular the orbit is. It can be obtained from the angular momentum through Eqs. (A.8) and (A.20).
- The longitude of periapsis ϖ which is the angle between an arbitrary reference direction and the direction to periapsis (the point in the orbit closest to the star).
- The true anomaly f which is the angle between the direction to periapsis and the current position of the planet as seen from the star. It can be obtained from the mean and eccentric anomaly (Eqs. (A.29), (A.36) and (A.43))

The first three parameters are constants describing the shape and orientation of the orbit while the fourth varies with time and determines the planet's position in the orbit.

To extend this to three dimensions we need to add two more parameters: the inclination, I, and the longitude of ascending node, Ω, (see Figure A.5).

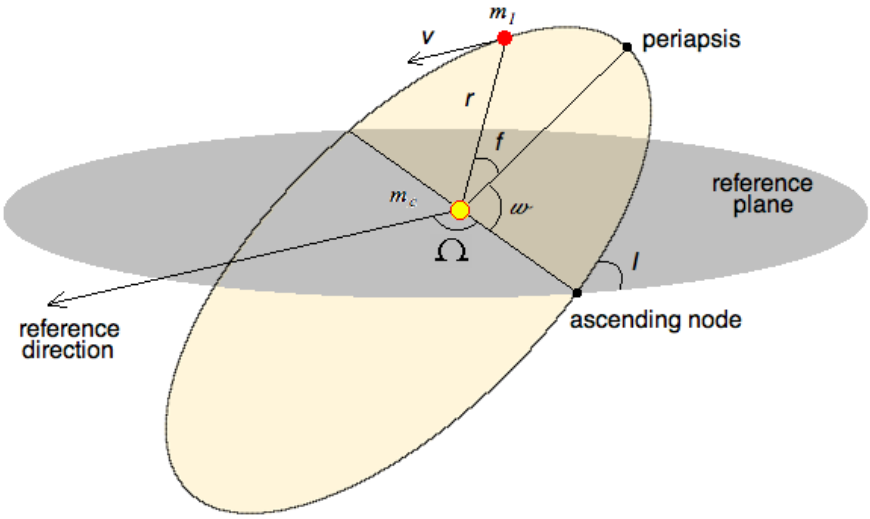

Figure A.5: Orbit of a planet in three dimensions with respect to an arbitrary reference plane showing the definitions of the inclination I and the longitude of ascending node Ω.

The inclination is defined as the angle between the reference plane and the orbital plane. The inclination is also the angle between the normal to the reference plane and the angular momentum vector of the orbit. The line created by the intersection between the orbital plane and the reference plane is called the line of nodes and the point where the orbit crosses the reference plane from south to north is called the ascending node. The longitude of ascending node is then defined as the angle between the reference direction and radius vector to the ascending node. In Figure A.5 there is one more angle, the

argument of periapsis, ω, which is the angle between the ascending node and periapsis. When $I = 0$ we can get the longitude of periapsis, ϖ, from Ω and ω

$$\varpi = \Omega + \omega \tag{A.44}$$

This definition is also used when $I \neq 0$ even though Ω and ω lie in different planes, ϖ then becomes a so called 'dogleg' angle.

B Derivation of the secular oscillation equations

A two-planet system in Cartesian coordinates looks like:

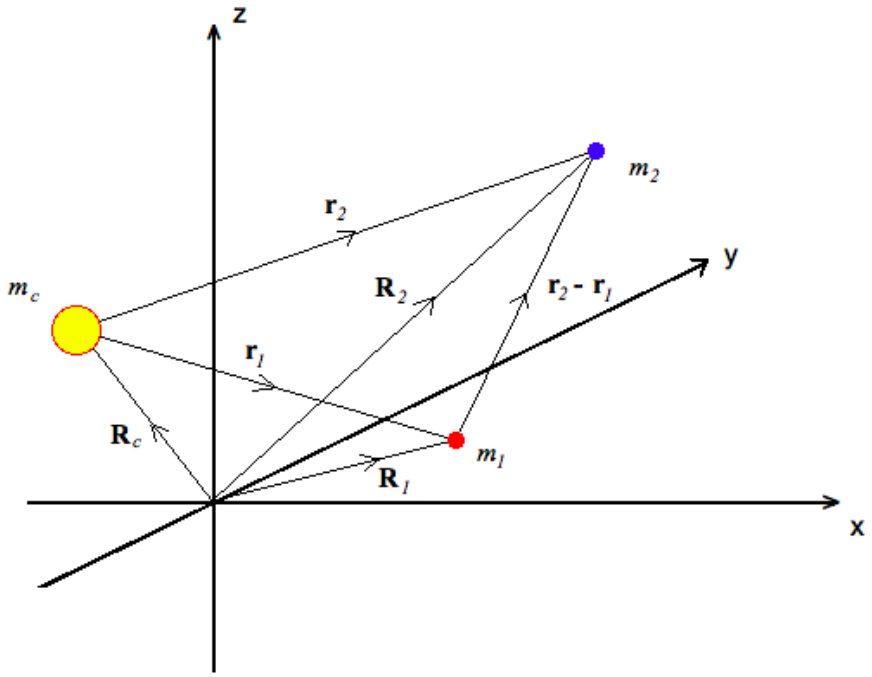

Figure B.1: Structure of a system with three bodies. In the case of a two-planet system the yellow dot, m_c, is the star, the red dot, m_1, is the inner planet and the blue dot, m_2, is the outer planet. The boldface letters are the position vectors of the masses: capital letters for the positions in an arbitrary frame of reference and lower case letters for the positions of the planets with respect to the star.

With perturbation theory you can derive an approximation to the secular oscillations of a two-planet system. This has been done by e.g. Murray & Dermott (1999) but I have redone it to understand the dependence on orbital parameters for the secular oscillations. m_1 and m_2 are the masses of the planets, subscript 1 for the inner planet and 2 for the outer planet. m_c is the mass of the star. Use the approximation that $m_1 \ll m_c$ and $m_2 \ll m_c$. Another approximation we make is that there is no MMR so we remove any dependence on the mean longitudes (position of the planet in its orbit). For these derivations we need the disturbing functions of the planets. The disturbing function of a planet is a function that arises in the equation of motion because of the third body. The equation of motion of the inner planet can be written as (vectors relative to the central mass)

$$\ddot{\boldsymbol{r}}_1 = \nabla \left(U_1 + \mathcal{R}_1 \right) \tag{B.1}$$

where

$$U_1 = G\frac{(m_c + m_1)}{r_1} \tag{B.2}$$

is the normal two-body potential and

$$\mathcal{R}_1 = \frac{Gm_2}{|\boldsymbol{r}_2 - \boldsymbol{r}_1|} - Gm_2\frac{\boldsymbol{r}_1 \cdot \boldsymbol{r}_2}{r_2^3} \tag{B.3}$$

is the disturbing function arising because of the other planet (Murray & Dermott 1999). You get similar equations for the outer planet by changing subscripts 1 to 2 and vice versa

$$\mathcal{R}_2 = \frac{Gm_1}{|\boldsymbol{r}_1 - \boldsymbol{r}_2|} - Gm_1\frac{\boldsymbol{r}_2 \cdot \boldsymbol{r}_1}{r_1^3} \tag{B.4}$$

Express in reference orbital parameters: a, e, I, Ω, ϖ and λ (semi-major axis, eccentricity, inclination, longitude of ascending node, longitude of periapsis and mean longitude). Then keep terms to first order in mass, second order in eccentricity and inclination and independent of the mean longitudes (secular). Left with, (Murray & Dermott 1999),

$$\begin{aligned}
\mathcal{R}_D^{(sec)} = & \frac{1}{8}\left[2\alpha\frac{\mathrm{d}}{\mathrm{d}\alpha} + \alpha^2\frac{\mathrm{d}^2}{\mathrm{d}\alpha^2}\right] b_{1/2}^{(0)}\left(e_1^2 + e_2^2\right) \\
& - \frac{1}{2}\alpha b_{3/2}^{(1)}\left(\sin^2\left(\frac{1}{2}I_1\right) + \sin^2\left(\frac{1}{2}I_2\right)\right) \\
& + \frac{1}{4}\left[2 - 2\alpha\frac{\mathrm{d}}{\mathrm{d}\alpha} - \frac{\mathrm{d}^2}{\mathrm{d}\alpha^2}\right] b_{1/2}^{(1)} e_1 e_2 \cos\left(\varpi_1 - \varpi_2\right) \\
& + \alpha b_{3/2}^{(1)} \sin\left(\frac{1}{2}I_1\right)\sin\left(\frac{1}{2}I_2\right)\cos\left(\Omega_1 - \Omega_2\right)
\end{aligned} \tag{B.5}$$

where $\alpha = a_1/a_2$, $a_1 < a_2$, $b_{1/2}^{(0)}, b_{1/2}^{(1)}$ and $b_{3/2}^{(1)}$ are Laplace coefficients of α defined as

$$b_x^{(y)}(\alpha) = \frac{1}{\pi}\int_0^{2\pi} \frac{\cos\left(y\psi\right)\mathrm{d}\psi}{\left(1 - 2\alpha\cos\psi + \alpha^2\right)^x} \tag{B.6}$$

with x being half integers ($x = 1/2, 3/2, 5/2, ...$) and y being integers. Write the disturbing function for the planets as

$$\begin{aligned}
\mathcal{R}_1 &= \frac{Gm_2}{a_2}\mathcal{R}_D^{(sec)} = \frac{Gm_2}{a_1}\alpha\mathcal{R}_D^{(sec)} \\
\mathcal{R}_2 &= \frac{Gm_1}{a_1}\alpha\mathcal{R}_D^{(sec)} = \frac{Gm_1}{a_2}\mathcal{R}_D^{(sec)}
\end{aligned} \tag{B.7}$$

For small inclinations we have $\sin\left(\frac{1}{2}I_i\right) \sim \frac{1}{2}I_i$. For small masses of the planets and small perturbations we get $Gm_c \sim n_1^2 a_1^3 \sim n_2^2 a_2^3$ where $n = \frac{2\pi}{P}$ is the mean motion. Useful relations between Laplace coefficients are

$$2\alpha\frac{\mathrm{d}b_{1/2}^{(0)}}{\mathrm{d}\alpha}+\alpha^2\frac{\mathrm{d}^2b_{1/2}^{(0)}}{\mathrm{d}\alpha^2}=\alpha b_{3/2}^{(1)} \tag{B.8}$$

$$2b_{1/2}^{(1)}-2\alpha\frac{\mathrm{d}b_{1/2}^{(1)}}{\mathrm{d}\alpha}-\alpha^2\frac{\mathrm{d}^2b_{1/2}^{(1)}}{\mathrm{d}\alpha^2}=-\alpha b_{3/2}^{(2)} \tag{B.9}$$

which means we get

$$\begin{aligned}\mathcal{R}_1=n_1^2a_1^2\frac{m_2}{m_c+m_1}\Bigg[&\frac{1}{8}\alpha^2b_{3/2}^{(1)}e_1^2-\frac{1}{8}\alpha^2b_{3/2}^{(1)}I_1^2\\&-\frac{1}{4}\alpha^2b_{3/2}^{(2)}e_1e_2\cos\left(\varpi_1-\varpi_2\right)\\&+\frac{1}{4}\alpha^2b_{3/2}^{(1)}I_1I_2\cos\left(\Omega_1-\Omega_2\right)\Bigg]\end{aligned} \tag{B.10}$$

$$\begin{aligned}\mathcal{R}_2=n_2^2a_2^2\frac{m_1}{m_c+m_2}\Bigg[&\frac{1}{8}\alpha^2b_{3/2}^{(1)}e_2^2-\frac{1}{8}\alpha^2b_{3/2}^{(1)}I_2^2\\&-\frac{1}{4}\alpha^2b_{3/2}^{(2)}e_1e_2\cos\left(\varpi_1-\varpi_2\right)\\&+\frac{1}{4}\alpha^2b_{3/2}^{(1)}I_1I_2\cos\left(\Omega_1-\Omega_2\right)\Bigg]\end{aligned} \tag{B.11}$$

combine these two equations to get

$$\begin{aligned}\mathcal{R}_j=n_ja_j^2\Bigg[&\frac{1}{2}A_{jj}e_j^2+A_{jk}e_1e_2\cos\left(\varpi_1-\varpi_2\right)\\&+\frac{1}{2}B_{jj}I_j^2+B_{jk}I_1I_2\cos\left(\Omega_1-\Omega_2\right)\Bigg]\end{aligned} \tag{B.12}$$

where $j=1,2$; $k=2,1$ $(k\neq j)$ and

$$A_{jj}=+n_j\frac{1}{4}\frac{m_k}{m_c+m_j}\alpha\bar{\alpha}b_{3/2}^{(1)}(\alpha) \tag{B.13}$$

$$A_{jk}=-n_j\frac{1}{4}\frac{m_k}{m_c+m_j}\alpha\bar{\alpha}b_{3/2}^{(2)}(\alpha) \tag{B.14}$$

$$B_{jj}=-n_j\frac{1}{4}\frac{m_k}{m_c+m_j}\alpha\bar{\alpha}b_{3/2}^{(1)}(\alpha) \tag{B.15}$$

$$B_{jk}=+n_j\frac{1}{4}\frac{m_k}{m_c+m_j}\alpha\bar{\alpha}b_{3/2}^{(1)}(\alpha) \tag{B.16}$$

where $\bar{\alpha}=\alpha$ if external perturber $(j=1)$ and $\bar{\alpha}=1$ if internal perturber $(j=2)$. Put into two matrices:

$$\boldsymbol{A}=\begin{pmatrix}A_{11}&A_{12}\\A_{21}&A_{22}\end{pmatrix}\quad\text{and}\quad\boldsymbol{B}=\begin{pmatrix}B_{11}&B_{12}\\B_{21}&B_{22}\end{pmatrix} \tag{B.17}$$

$\boldsymbol{B}$ is not linearly independent. $B_{11} = -B_{12}$ and $B_{21} = -B_{22}$. This is because it is only the mutual inclination of the two orbits that is relevant, not the individual values of the two inclinations. Matrices only function of the masses and the semi-major axes (taken to be constant).

Next we need Lagrange's planetary equations describing evolution of orbital parameters (Brouwer & Clemence (1961) and Roy (1988)):

$$\frac{\mathrm{d}a}{\mathrm{d}t} = \frac{2}{na}\frac{\partial \mathcal{R}}{\partial \epsilon} \tag{B.18}$$

$$\frac{\mathrm{d}e}{\mathrm{d}t} = -\frac{\sqrt{1-e^2}}{na^2 e}\left(1-\sqrt{1-e^2}\right)\frac{\partial \mathcal{R}}{\partial \epsilon} - \frac{\sqrt{1-e^2}}{na^2 e}\frac{\partial \mathcal{R}}{\partial \varpi} \tag{B.19}$$

$$\frac{\mathrm{d}\epsilon}{\mathrm{d}t} = -\frac{2}{na}\frac{\partial \mathcal{R}}{\partial a} + \frac{\sqrt{1-e^2}\left(1-\sqrt{1-e^2}\right)}{na^2 e}\frac{\partial \mathcal{R}}{\partial e} + \frac{\tan\frac{1}{2}I}{na^2\sqrt{1-e^2}}\frac{\partial \mathcal{R}}{\partial I} \tag{B.20}$$

$$\frac{\mathrm{d}\Omega}{\mathrm{d}t} = \frac{1}{na^2\sqrt{1-e^2}\sin I}\frac{\partial \mathcal{R}}{\partial I} \tag{B.21}$$

$$\frac{\mathrm{d}\varpi}{\mathrm{d}t} = \frac{\sqrt{1-e^2}}{na^2 e}\frac{\partial \mathcal{R}}{\partial e} + \frac{\tan\frac{1}{2}I}{na^2\sqrt{1-e^2}}\frac{\partial \mathcal{R}}{\partial I} \tag{B.22}$$

$$\frac{\mathrm{d}I}{\mathrm{d}t} = -\frac{\tan\frac{1}{2}I}{na^2\sqrt{1-e^2}}\left(\frac{\partial \mathcal{R}}{\partial \epsilon} + \frac{\partial \mathcal{R}}{\partial \varpi}\right) - \frac{1}{na^2\sqrt{1-e^2}\sin I}\frac{\partial \mathcal{R}}{\partial \Omega} \tag{B.23}$$

where $\epsilon = \lambda - nt$ is the mean longitude at epoch (mean longitude at $t = 0$). With no MMRs $\mathcal{R}$ is independent of λ and ϵ leading to constant semi-major axes (no energy transfer). Hence we are not interested in the first and third equations and terms with $\frac{\partial \mathcal{R}}{\partial \epsilon}$ or $\frac{\partial \mathcal{R}}{\partial a}$. Then we get Lagrange's planetary equations to lowest order in e and I:

$$\dot{e}_j = -\frac{1+\mathcal{O}(e_j^2)}{n_j a_j^2 e_j}\frac{\partial \mathcal{R}_j}{\partial \varpi_j} \approx -\frac{1}{n_j a_j^2 e_j}\frac{\partial \mathcal{R}_j}{\partial \varpi_j} \tag{B.24}$$

$$\begin{aligned}\dot{\varpi}_j &= \frac{1+\mathcal{O}(e_j^2)}{n_j a_j^2 e_j}\frac{\partial \mathcal{R}_j}{\partial e_j} + \frac{\left(1+\mathcal{O}(e_j^2)\right)\left(\frac{I_j}{2}+\mathcal{O}(I_j^3)\right)}{n_j a_j^2}\frac{\partial \mathcal{R}_j}{\partial I_j} \approx \\ &\approx \frac{1}{n_j a_j^2 e_j}\frac{\partial \mathcal{R}_j}{\partial e_j}\end{aligned} \tag{B.25}$$

$$\begin{aligned}\dot{I}_j = &-\frac{\left(1+\mathcal{O}(e_j^2)\right)\left(\frac{I_j}{2}+\mathcal{O}(I_j^3)\right)}{n_j a_j^2}\frac{\partial \mathcal{R}_j}{\partial \varpi_j} \\ &-\frac{\left(1+\mathcal{O}(e_j^2)\right)\left(\frac{1}{I_j}+\mathcal{O}(I_j)\right)}{n_j a_j^2}\frac{\partial \mathcal{R}_j}{\partial \Omega_j} \approx -\frac{1}{n_j a_j^2 I_j}\frac{\partial \mathcal{R}_j}{\partial \Omega_j}\end{aligned} \tag{B.26}$$

$$\dot{\Omega}_j = \frac{\left(1+\mathcal{O}(e_j^2)\right)\left(\frac{1}{I_j}+\mathcal{O}(I_j)\right)}{n_j a_j^2}\frac{\partial \mathcal{R}_j}{\partial I_j} \approx \frac{1}{n_j a_j^2 I_j}\frac{\partial \mathcal{R}_j}{\partial I_j} \tag{B.27}$$

At this point it is convenient to define eccentricity and inclination 'vectors' with components:

$$h_j = e_j \sin\varpi_j, \quad k_j = e_j\cos\varpi_j \tag{B.28}$$

$$p_j = I_j \sin\Omega_j, \quad q_j = I_j\cos\Omega_j \tag{B.29}$$

$$\boldsymbol{h} = \begin{pmatrix} h_1 \\ h_2 \end{pmatrix}, \quad \boldsymbol{k} = \begin{pmatrix} k_1 \\ k_2 \end{pmatrix} \tag{B.30}$$

$$\boldsymbol{p} = \begin{pmatrix} p_1 \\ p_2 \end{pmatrix}, \quad \boldsymbol{q} = \begin{pmatrix} q_1 \\ q_2 \end{pmatrix} \tag{B.31}$$

Now the disturbing function becomes

$$\begin{aligned} \mathcal{R}_j = n_j a_j^2 \Bigg[& \frac{1}{2} A_{jj} \left(h_j^2 + k_j^2 \right) + A_{jk} \left(h_j h_k + k_j k_k \right) \\ & + \frac{1}{2} B_{jj} \left(p_j^2 + q_j^2 \right) + B_{jk} \left(p_j p_k + q_j q_k \right) \Bigg] \end{aligned} \tag{B.32}$$

where k as subscript is not the same as the 'horizontal' part of the eccentricity vector. Write the time derivatives of the eccentricity and inclination vectors as:

$$\begin{aligned} \frac{\mathrm{d}h_j}{\mathrm{d}t} &= \frac{\partial h_j}{\partial e_j}\frac{\mathrm{d}e_j}{\mathrm{d}t} + \frac{\partial h_j}{\partial \varpi_j}\frac{\mathrm{d}\varpi_j}{\mathrm{d}t} = \sin\varpi_j \frac{\mathrm{d}e_j}{\mathrm{d}t} + e_j \cos\varpi_j \frac{\mathrm{d}\varpi_j}{\mathrm{d}t} = \\ &= \frac{h_j}{e_j}\frac{\mathrm{d}e_j}{\mathrm{d}t} + k_j \frac{\mathrm{d}\varpi_j}{\mathrm{d}t} \end{aligned} \tag{B.33}$$

$$\begin{aligned} \frac{\mathrm{d}k_j}{\mathrm{d}t} &= \frac{\partial k_j}{\partial e_j}\frac{\mathrm{d}e_j}{\mathrm{d}t} + \frac{\partial k_j}{\partial \varpi_j}\frac{\mathrm{d}\varpi_j}{\mathrm{d}t} = \cos\varpi_j \frac{\mathrm{d}e_j}{\mathrm{d}t} - e_j \sin\varpi_j \frac{\mathrm{d}\varpi_j}{\mathrm{d}t} = \\ &= \frac{k_j}{e_j}\frac{\mathrm{d}e_j}{\mathrm{d}t} - h_j \frac{\mathrm{d}\varpi_j}{\mathrm{d}t} \end{aligned} \tag{B.34}$$

$$\begin{aligned} \frac{\mathrm{d}p_j}{\mathrm{d}t} &= \frac{\partial p_j}{\partial I_j}\frac{\mathrm{d}I_j}{\mathrm{d}t} + \frac{\partial p_j}{\partial \Omega_j}\frac{\mathrm{d}\Omega_j}{\mathrm{d}t} = \sin\Omega_j \frac{\mathrm{d}I_j}{\mathrm{d}t} + I_j \cos\Omega_j \frac{\mathrm{d}\Omega_j}{\mathrm{d}t} = \\ &= \frac{p_j}{I_j}\frac{\mathrm{d}I_j}{\mathrm{d}t} + q_j \frac{\mathrm{d}\Omega_j}{\mathrm{d}t} \end{aligned} \tag{B.35}$$

$$\begin{aligned} \frac{\mathrm{d}q_j}{\mathrm{d}t} &= \frac{\partial q_j}{\partial I_j}\frac{\mathrm{d}I_j}{\mathrm{d}t} + \frac{\partial q_j}{\partial \Omega_j}\frac{\mathrm{d}\Omega_j}{\mathrm{d}t} = \cos\Omega_j \frac{\mathrm{d}I_j}{\mathrm{d}t} - I_j \sin\Omega_j \frac{\mathrm{d}\Omega_j}{\mathrm{d}t} = \\ &= \frac{q_j}{I_j}\frac{\mathrm{d}I_j}{\mathrm{d}t} - p_j \frac{\mathrm{d}\Omega_j}{\mathrm{d}t} \end{aligned} \tag{B.36}$$

Insert Lagrange's planetary equations and use the chain rule a couple of more times e.g. $\frac{\partial \mathcal{R}_j}{\partial e_j} = \frac{\partial \mathcal{R}_j}{\partial k_j}\frac{\partial k_j}{\partial e_j} = \frac{k_j}{e_j}\frac{\partial \mathcal{R}_j}{\partial k_j}$ and similarly for the derivative of the disturbing function with respect to other variables.

$$\frac{\mathrm{d}h_j}{\mathrm{d}t} = \frac{1}{n_j a_j^2 e_j}\left(k_j\frac{\partial \mathcal{R}_j}{\partial e_j} - \frac{h_j}{e_j}\frac{\partial \mathcal{R}_j}{\partial \varpi_j}\right) = \frac{1}{n_j a_j^2}\underbrace{\left(\frac{k_j^2}{e_j^2} + \frac{h_j^2}{e_j^2}\right)}_{=1}\frac{\partial \mathcal{R}}{\partial k_j} =$$

$$= \frac{1}{n_j a_j^2}\frac{\partial \mathcal{R}}{\partial k_j} \tag{B.37}$$

$$\frac{\mathrm{d}k_j}{\mathrm{d}t} = \frac{1}{n_j a_j^2 e_j}\left(-\frac{k_j}{e_j}\frac{\partial \mathcal{R}}{\partial \varpi_j} - h_j\frac{\partial \mathcal{R}}{\partial e_j}\right) = \frac{1}{n_j a_j^2}\left(-\frac{k_j^2}{e_j^2} - \frac{h_j^2}{e_j^2}\right)\frac{\partial \mathcal{R}}{\partial h_j} =$$

$$= -\frac{1}{n_j a_j^2}\frac{\partial \mathcal{R}}{\partial h_j} \tag{B.38}$$

$$\frac{\mathrm{d}p_j}{\mathrm{d}t} = \frac{1}{n_j a_j^2 I_j}\left(q_j\frac{\partial \mathcal{R}_j}{\partial I_j} - \frac{p_j}{I_j}\frac{\partial \mathcal{R}_j}{\partial \Omega_j}\right) = \frac{1}{n_j a_j^2}\underbrace{\left(\frac{q_j^2}{I_j^2} + \frac{p_j^2}{I_j^2}\right)}_{=1}\frac{\partial \mathcal{R}}{\partial q_j} =$$

$$= \frac{1}{n_j a_j^2}\frac{\partial \mathcal{R}}{\partial q_j} \tag{B.39}$$

$$\frac{\mathrm{d}q_j}{\mathrm{d}t} = \frac{1}{n_j a_j^2 I_j}\left(-\frac{q_j}{I_j}\frac{\partial \mathcal{R}}{\partial \Omega_j} - p_j\frac{\partial \mathcal{R}}{\partial I_j}\right) = \frac{1}{n_j a_j^2}\left(-\frac{q_j^2}{I_j^2} - \frac{p_j^2}{I_j^2}\right)\frac{\partial \mathcal{R}}{\partial p_j} =$$

$$= -\frac{1}{n_j a_j^2}\frac{\partial \mathcal{R}}{\partial p_j} \tag{B.40}$$

$$\tag{B.41}$$

The derivatives of the disturbing function with respect to h_j, k_j, p_j and q_j becomes

$$\frac{\partial \mathcal{R}}{\partial h_j} = n_j a_j^2\left(A_{jj}h_j + A_{jk}h_k\right) \tag{B.42}$$

$$\frac{\partial \mathcal{R}}{\partial k_j} = n_j a_j^2\left(A_{jj}k_j + A_{jk}k_k\right) \tag{B.43}$$

$$\frac{\partial \mathcal{R}}{\partial p_j} = n_j a_j^2\left(B_{jj}p_j + B_{jk}p_k\right) \tag{B.44}$$

$$\frac{\partial \mathcal{R}}{\partial q_j} = n_j a_j^2\left(B_{jj}q_j + B_{jk}q_k\right) \tag{B.45}$$

and the differential equations for h_j, k_j, p_j and q_j become

$$\dot{h}_j = A_{jj}k_j + A_{jk}k_k \tag{B.46}$$

$$\dot{k}_j = A_{jj}h_j + A_{jk}h_k \tag{B.47}$$

$$\dot{p}_j = B_{jj}q_j + B_{jk}q_k \tag{B.48}$$

$$\dot{q}_j = B_{jj}p_j + B_{jk}p_k \tag{B.49}$$

From the above equations we see that h_j and k_j are decoupled from p_j and q_j. Write in matrix form

$$\dot{\boldsymbol{h}} = \boldsymbol{A}\boldsymbol{k}, \quad \dot{\boldsymbol{k}} = -\boldsymbol{A}\boldsymbol{h} \tag{B.50}$$

$$\dot{\boldsymbol{p}} = \boldsymbol{B}\boldsymbol{q}, \quad \dot{\boldsymbol{q}} = -\boldsymbol{B}\boldsymbol{p} \tag{B.51}$$

Differentiating with respect to time once more gives the following equation (for $\boldsymbol{h}$)

$$\ddot{\boldsymbol{h}} = \boldsymbol{A}\dot{\boldsymbol{k}} = -\boldsymbol{A}^2\boldsymbol{h} \Longrightarrow \ddot{\boldsymbol{h}} + \boldsymbol{A}^2\boldsymbol{h} = 0 \tag{B.52}$$

and similarly for $\boldsymbol{k}$, $\boldsymbol{p}$ and $\boldsymbol{q}$. This is an eigenvalue problem with solutions

$$h_j = \sum_{i=1}^{2} e_{ij} \sin\left(g_i t + \beta_i\right), \quad k_j = \sum_{i=1}^{2} e_{ij} \cos\left(g_i t + \beta_i\right) \tag{B.53}$$

$$p_j = \sum_{i=1}^{2} I_{ij} \sin\left(f_i t + \gamma_i\right), \quad q_j = \sum_{i=1}^{2} I_{ij} \cos\left(f_i t + \gamma_i\right) \tag{B.54}$$

subscript j determines which planet and subscript i determines the mode of oscillation. Frequencies g_i and f_i are eigenvalues to $\boldsymbol{A}$ and $\boldsymbol{B}$ respectively. The initial conditions of the system determine the amplitudes (e_{ji} and I_{ji} which are components of the eigenvectors) and phases (β_i and γ_i). From the definition of $\boldsymbol{B}$ we have that $B_{11}B_{22} - B_{12}B_{21} = 0$ so the characteristic equation for $\boldsymbol{B}$ becomes

$$\begin{aligned} 0 = \begin{vmatrix} B_{11} - f & B_{12} \\ B_{21} & B_{22} - f \end{vmatrix} = B_{11}B_{22} - f\left(B_{11} + B_{22}\right) + f^2 - B_{12}B_{21} = \\ = f\left(f - \left(B_{11} + B_{22}\right)\right) \end{aligned} \tag{B.55}$$

i.e. one of the eigenvalues is $f_1 = 0$. This degeneracy arises because it is only the mutual inclination that is important not the individual inclinations. This is only dependent on the orbital parameters and not on the positions in the orbits. The results holds when:

i) There is no mean motion resonance

ii) $\boldsymbol{r}_1 < \boldsymbol{r}_2$, i.e. the orbit of the inner planet stays inside the orbit of the outer planet.

iii) The eccentricities and inclinations are small enough so that a second order approximation is enough.